GEOCHRONOLOGY OF THE PAI AEOCLIMATIC EVENTS OF THE LATE CENOZOIC PERIOD IN THE KASHMIR VALLEY

by

Sheela Kusumgar
Physical Research Laboratory
Ahmedabad 380009

and

Tata Institute of Fundamental Research
Bombay 400 005

A thesis
submitted for the degree of

DOCTOR OF PHILOSOPHY

of the

UNIVERSITY OF BOMBAY

March 1980

C O N T E N T S

S Y N O P S I S

The present study was carried out to provide a chronology to the palaeoclimatic and palaeoenvironmental events of the late Cenozoic period in the Kashmir valley using radioactive and magnetic polarity dating methods.

The Kashmir valley (Lat. 33° 30' to 34° 30' N., Long. 74° to 75° 30' E.) has a continuous and easily accessible record of the late Cenozoic lake sediments of about 3000m thickness. This relict lake bed which was drained out due to tectonic uplift provides suitably exposed sections with well preserved signatures of the various glacial and interglacial events, marking palaeoclimatic fluctuations. The lake sediments rest on the Palaeozoic and Triassic basal rocks.

The deposits of the basin can be divided into three members: Loess, Upper Karewa and Lower Karewa. As the drained out lake bed presents plateau like surfaces, they have been termed Karewa in the local dialect. This term has now been accepted in the geological literature. The Lower Karewa deposits comprise tilted and folded beds of boulder conglomerate, lignite with an alternation of clay, silt and sand layers. Their total thickness is estimated to be about 2500m. The Upper Karewa formation, on the other hand, consists of horizontal beds of gravel, calcareous clays, marl-bands etc.

and has a total thickness of about 100m. Various glacial moraines and out-washes intrude into the Karewa formations and provide stratigraphic markers. According to de Terra and Paterson, the lake finally drained out during the II inter-glacial, thus exposing the lake beds on the Himalayan north-east side also. The Pir Panjals were continuously rising and the lake beds on that side were already exposed when the Karewa lake shrank and shifted towards the Himalayan side. It appears that the last(?) glacial period is marked by loessic deposition which is thicker on the Pir Panjal side, as it was exposed earlier, and thinner on the Himalayan side.

This continuous record of the Late Cenozoic palaeoenvironmental events has been a subject of great interest to geologists for over 100 years. The classical methods of geomorphology, palaeontology, and palynology have been applied to these deposits but not yet in a comprehensive and systematic manner. So far no physical methods were available to the earlier workers and therefore many controversies remained unresolved. For example, the beginning of the Karewa lake has been variously dated from Miocene to Pleistocene times.

The Kashmir basin attracted our attention as it provided a unique sediment profile of ~3000m thickness in a continental

situation. So far the long palaeoclimatic records were provided only by the sea-cores and the lake profiles (for example, lake Biwa or lake Van) have been so far bored only upto a maximum depth of 200m or so. But since in the case of Kashmir we could go back to perhaps 5 m.y. and sample 3000m 'deep' sediment without recourse to boring, I took up the problem of dating the Karewa lake sediments by using radioactive and palaeomagnetic techniques.

The results of these studies are presented in six chapters, the first being introductory and the last summarising the conclusions.

In CHAPTER TWO, I have provided an outline of the geomorphological features and their stratigraphic correlations in the valley. I have described the physiography and geological formations including the present day ecology. I have also tried to define the problem of Plio-Pleistocene boundary. The drainage pattern and glacial manifestations have been described in detail as they provide geomorphological markers for dating the events. The role played by tectonics has also been explained.

In short, the available evidence on geomorphology, palynology, and palaeontology has been summarised to provide a backdrop for the problems to be tackled. Though the available palaeontological and palynological evidence is not yet adequate, it does

provide broad chronological pegs on which a time-frame can be hung. It must be emphasized that it is a continuous and unique record so it is an ideal location for magnetic stratigraphy.

I have also shown that the loess represented the last depositional episode in the valley and probably marks the last glacial aridity. In the body of the loess there are several palaeosols which should represent the relatively wetter and warmer episodes in an otherwise arid and cold phase.

CHAPTER THREE deals with radioactivity dating in which I include radiocarbon and uranium/thorium methods. I have described the theory and technique of both the methods and their limitations in the context of the samples collected by me. I have also described the methane reactor that was developed by me for preparing radiocarbon samples.

The upper part of the "Loess" deposit has been dated with the ^{14}C method; both organic and inorganic fractions were extracted and their radioactivity determined to check on the validity of the "dates". It is gratifying to note that in general there was a good concordance between the ^{14}C dates based on organic and inorganic fractions.

Since the Karewas cannot be dated with the ^{14}C method, I have attempted to obtain approximate "ages" using the Ionium method. There are many marl beds and calcareous layers in the Upper Karewa deposits which I thought could be dated with the Ionium dating, following Kaufman and Broecker's attempt at the lakes Lahontan and Bonneville. Although we examined several samples, we have not been successful largely because of the high clay content of these samples ($\backsim$50%). Further experiments to obtain purer carbonate samples are being made.

The top palaeosol, on the Himalayan margin of the lake, gives c.18,000 $\pm$ 1000 B.P. date and probably represents the last deglaciation in the valley. These sites are generally located at about c.1600m altitude. This result is in accord with the evidence from ^{14}C dated pollen profile from a bog at c.3120m altitude that the deglaciation was in progress there at c.15,000 B.P. Thus I find that the last deglaciation in the Central Asian context had started around c.18,000 $\pm$ 1000 B.P., which is now in keeping with the latest global evidence as reported by the Climatic Committee report on the Australian Academy of Sciences. The lower palaeosols are older than 30,000 B.P. About 10 sites have been sampled for palaeosol-dating.

In CHAPTER FOUR, I discuss the problems and results of the magnetic measurements made on the Karewa profile. We have taken the Hirpur section as the typical representative formation of the Lower Karewa and for the Upper Karewa, Saki Paparian and Olchibagh have been chosen. The results have been verified by sampling few other sites. As the Upper Karewa deposit has a thickness of only about 100m, I could do an intensive sampling by covering all the clay bands present. Thus about 80 samples were measured for the Upper Karewa. The Lower Karewa samples presented formidable problems of extensive field-work and accessibility of the exposed sections because of their sheer steepness. I have satisfactorily covered only about a 10km long section in the Rimbiara valley, near Hirpur. As it was essential to cover the whole Lower Karewa section to detect all the magnetic epochs, I decided upon an extensive sampling and collected about 80 samples at broad intervals. Thus my palaeomagnetic stratigraphy is based upon 150-160 magnetic samples.

In this Chapter, I have also dealt with the principles and technique besides giving the sampling procedure adopted by me. The measurements were made with the help of an astatic magnetometer mounted with Helmholtz coils to neutralize the earth's ambient magnetic field; this instrument which was made available for my work was housed at a field station far away from the city for higher sensitivity measurements.

The magnetic measurement results have been stratigraphically correlated to the different exposed sections available in the valley. All the Upper Karewa samples show normal polarity. Near the top of the Hirpur section (Lower Karewa) I have some samples depicting a reversed polarity covering a 10m thick segment of the section. The lower sections exhibit normal polarity. Keeping in view the geological stratigraphy, radioactive dates and the climatic events, I find that the magnetic measurements provide a consistent chronological framework. Our results thus show that the Karewa lake sediments probably cover the Brunhes (< 0.72 m.y.), Matuyama (0.72-2.47 m.y.) and Gauss (2.47-3.41 m.y.) magnetic epochs.

CHAPTER FIVE makes use or the chronology determined in the present work using the radioactive and palaeomagnetic techniques, to locate various palaeoclimatic and palaeoenvironmental events in the valley in a time-sequence.

CHAPTER SIX summarizes the results of the present work which clearly points to the availability of a complete palaeoclimatic sequence covering the late Cenozoic. It would be important to check by sampling several sites in the Lower Karewas to determine the oldest available sequence.

Three conclusions could be drawn from the present work:

(1) The top-most palaeosol in the loessic deposit represents the last deglaciation which started at 1600m at 34° N. Lat. at about c.1800 ± 1000 B.P.

(2) The Upper Karewa represents Brunhes Epoch (<0.72 m.y.).

(3) There is good indication that the top-most section of the Lower Karewa represents the Matuyama Epoch (0.72-2.47 m.y.) and the section below probably indicates the Gauss (2.47-3.41 m.y.) magnetic normal Epoch.

These investigations have made available a chronologic sedimentary sequence covering the late Cenozoic in the Kashmir valley which can now be more extensively studied using conventional techniques to delineate palaeoclimatic changes in this period.

It should be emphasized that this work provides the first dates on the Karewas based on physical dating methods.

STATEMENT REQUIRED UNDER ORDINANCE O.770

I hereby state that the work described in this thesis has not been submitted to this or any other University for Ph.D. or any other degree.

STATEMENT REQUIRED UNDER ORDINANCE O.771

a) Statement regarding the discovery and important new facts

Absolute chronologies have been provided to the palaeo-climatic and palaeoenvironmental events of the Late Cenozoic period in the Kashmir valley. For the first time, I have used physical dating methods for providing chronologies to exposed 'Karewas' (the relict lake beds) in the Kashmir valley. So far only classical methods were used to date the Karewas.

The radioactive dating methods were used for dating the palaeosols within the topmost loessic deposit and the Upper Karewas. The magnetic polarity dating was employed for the Upper and the Lower Karewa deposits.

The top-most palaeosol within the loessic deposits dates to $\underline{c}$.18,000 $\pm$ 1000 years before present, thus dating the last deglaciation in Kashmir. The Upper Karewa is ascribable to the Brunhes Epoch ($<$ 0.72 m.y.). The topmost sediment below the gravel bed in the Hirpur section probably belongs to the Matuyama Epoch (0.72-2.47 m.y.) and the section below this probably the Gauss (2.47-3.41 m.y.) magnetic normal epoch.

b) Statement regarding contribution of the author

The large number of samples of soils (palaeosols) for radiocarbon dating and samples of clay for palaeomagnetic studies were collected at several sites in the Kashmir valley and were measured by the author. Assistance was provided in the field work by Dr. D.P. Agrawal, Mr. R.V. Krishnamurthy, Mr. V. Nautiyal and Dr. R.K. Pant.

The preparation of counting gas for radiocarbon dating and the extractions of uranium and thorium were done by the author with occasional help from Mr. R.V. Krishnamurthy, Dr. S. Krishnaswami, Dr. R.K. Pant and Dr. B.L.K. Somayajulu.

The low background, gas proportional counters were used for radiocarbon dating. The procedure of preparing contamination free counting gas in a closed reaction vessel was developed by the author.

The palaeomagnetic measurements were carried out using an astatic magnetometer housed at Tata Institute of Fundamental Research (Khandala) and at the National Geophysical Research Institute (Hyderabad) in collaboration with Dr. S.D. Likhite and Mr. S. Rao.

The planning of sampling procedures and sampling regions, was done in consultation and collaboration with my guide Dr. D. Lal and Dr. D.P. Agrawal

The interpretation of experimental results have been carried out by the author in consultation with my guide Dr. D. Lal, Dr. D.P. Agrawal and Dr. C.R.K. Murthy.

In all these phases of investigations the author carried out a significant share of work.

A list of publications of the author together with a copy each of the papers supporting the thesis are attached at the end of the thesis.

(Sheela Kusumgar)

I certify that the above statements are correct

D. Lal
(Guiding Teacher)

LIST OF FIGURES

LIST OF TABLES

ACKNOWLEDGEMENTS

I am beholden to Prof. D. Lal for his valuable guidance and inspiration during the course of this work. I would also like to record my gratitude to Prof. S.P. Pandya for his help and encouragement. Gratitude is also due to Prof. D.P. Agrawal and Prof. C. Radhakrishnamurthy for their multiple help, both in the field and in the lab and for their guidance

My senior colleagues, both of the old Tata Institute of Fundamental Research, Bombay, and PRL, especially, Profs. N. Bhandari, S. Krishnaswami, B.L.K. Somayajulu and Drs. R.N. Athavale, R.K. Pant, S.K. Bhattacharya, extended multifarious help. Among younger colleagues, considerable help was received from Ss. R.V. Krishnamurthy and Vinod Nautiyal. Dr. Someshwar Rao of National Geophysical Research Institute, Hyderabad, helped me to make a few palaeomagnetic measurements at their lab. Most of the other palaeomagnetic measurements were made at TIFR's lab at Khandala, with the valuable help of Prof. C. Radhakrishnamurthy and Sri S.D. Likhite. For assistance received for making U/Th measurements, thanks are due to Ss. D.V. Borole, N. Hussain, M.M. Sarin and Pankaj Sharma. I record my sincere thanks to all these seniors and colleagues.

I sincerely appreciate the excellent typing work done by Sri P. Pillai and the willing co-operation extended to me in documentation by Ss S.C. Bhavsar, S.K. Bhavsar, Ranpura, S. Vora

and Ghanshyam Patel. Sri N.B. Vaghela rendered significant laboratory help in the course of the thesis work. To all these I am thankful.

Without the affectionate help and inspiration from Aparna and Vibha, I could not have completed this work. Ila also spared her busy time for checking the typescript.

I would also like to record my thanks to the Department of Science & Technology, for their financial assistance for field work.

CHAPTER I

INTRODUCTION

This thesis tries to derive an absolute chronological framework for the palaeoenvironmental and palaeoclimatic events as recorded in the sediments of the Karewa lake in the Kashmir valley. Though geologists and palaeontologists have been working in this area for over a century, yet the physical methods of dating employed by me have been used for the first time in the valley; and, in fact, palaeomagnetic dating for the Cenozoic formations in the valley is being attempted for the first time in India.

Several important considerations influenced my decision to select the Kashmir valley:

(1) The basin provided a unique record of about 3000 m of a sediment profile.

(2) Tectonic uplifts and a 5000 sq. km. areal spread of the relict lake allowed me to pick, choose and correlate different sections for sampling of the complete profile, without getting into the formidable logistics of deep-drilling.

(3) From the continental situation, the basin provided a unique palaeoclimatic record going back to the Cenozoic period. Such deep records are hardly accessible elsewhere, excepting from

the sea-cores.

(4) For field-work and stratigraphic correlation in the Kashmir basin, I could get expert help and guidance from other workers.

The valley of Kashmir (Lat. 33° 30'-34° 30' N., Long. 74°-75° 30' E.) is flanked by the Himalayas on the northeast and the Pir Panjals on the southwest. The lake was formed by the uplift of the Pir Panjals which impounded the extant Himalayan drainage. The depositional processes have been influenced by both climatic and tectonic factors. The valley sediments provided a plateau like surface which in the local dialect is called 'Karewa', a term now used in the geological literature for the relict basin sediments. The sedimentary profile is divided into three members: the Lower Karewa (also called, Hirpur Formation); the Upper Karewa (also called, Nagum Formation); and the Loess. The first two are of lacustrine and the uppermost is of aeolian origin. As stated above, these deposits have an overall depth of 3000 m and 5000 sq. km. areal extent.

The valley has attracted the attention of geologists and palaeontologists for more than a century (Godwin-Austen, 1859; Lydekker, 1883; de Terra and Paterson, 1939; Wadia, 1941; Farooqi and Desai, 1974; and Bhatt, 1976). The considerable

previous geological work alone makes it possible for one to grasp the problems and plan sampling strategies. Though there are still unresolved geological problems, yet it's only the hard work of geologists and palaeontologists from Lydekker's (1883) and Godwin-Austen's (1859) times onwards, that the basin sediments are understood well-enough for the application of finer precision of the physical methods.

Through geomorphological and palaeontological studies, which will be discussed in detail in the next chapter, various age estimates were given for the beginnings of the lake which varied from Miocene to Pleistocene periods. Though there still is a difference of greater than 12 m.y. about the age of the Karewa lake, yet even this information is valuable in the planning of the sampling and the amount of work involved in any such effort.

In this study, I have used mainly three techniques of dating: the radiocarbon, the uranium series and the palaeomagnetic dating methods.

Radiocarbon, an isotope of carbon, was first used by Libby (1955) for dating organic remains. It is produced in the atmosphere by the interaction of slow neutrons with nitrogen nuclei and has a half-life of 5730 years (Godwin, 1962). The

radiocarbon method is now a well established method (for details, see Chapter III) and was used to date the palaeosols within the loessic deposits as also the archaeological deposits overlying the loess. The ^{14}C dating method has a range only upto 40,000 years and we therefore tried the uranium series dating method to be able to extend the dating limit further.

The disequilibrium features of the radioactive uranium in natural waters provide quite a few possibilities of using them as dating methods (Chapter III). We have tried to use here $^{234}U/^{238}U$ ratio changes with depth as also ^{230}Th deficiency method. Both these methods have been tried by me carefully. However, the results did not turn out to be very satisfactory, because of a high percentage of clay fractions in the samples.

The palaeomagnetic polarity reversal method, however, proved more useful and allowed us to date the whole sedimentary profile of the Karewas (Chapter IV). Since it is only a relative method of dating, we had to ensure the relative completeness of the sedimentary record, as also define some independent chronological markers in the profile. Pleistocene fossils and absolute dating of the upper portions of the profile allowed us to put the magnetic polarity scale in an absolute time-frame.

Since this thesis was mainly aimed at dating the sedimentary profile and the events recorded in it, we bring out the relevance

of our dating efforts towards this aim in Chapter V. It is obvious that one is dating only the various manifestations of the climatic change as recorded by variations in flora, fauna, sedimentology etc. of the Karewas. It may be mentioned that since our dating applied to definite lithozones, even if the climatic interpretations of fossil and sedimentological data subsequently change, our chronology will continue to hold good as it is directly related to the lithozones which are fixed points of the sedimentary profile.

The last chapter summarizes the conclusions.

CHAPTER II

II. GEOMORPHOLOGY AND STRATIGRAPHY OF THE SEDIMENTARY DEPOSITS IN THE KASHMIR VALLEY

II.1. General features

II.1.A. Geomorphology and geology
II.1.B. The Karewas and their origins
II.1.C. Chronological controversies
II.1.D. Glacial features

II.2. Palaeontological data

II.3. Our approach and sampling

II.1. General features

This chapter provides the essential backdrop to the problems of stratigraphy, recognition of palaeoclimatic events, chronology and terminology of the Cenozoic formations in the valley. The importance, validity and meaning of our chronologic data depends a great deal on the geomorphologic and sedimentologic framework delineated here.

I also attempt to explain in this chapter the need for physical dating of the Karewa events, as chronological discrepancies of $\geq$10 million years exist between different estimates.

II.1.A. Geomorphology and geology

The Kashmir valley (Lat. 33° 30' N. to 34° 30' N., Long. 74° E. to 75° 30' E.) lies in the northwestern part of the Himalayan mountain chain within India. Geographically it forms part of the Himalayan region.

The valley (Fig. II.1) has an area of nearly 5000 sq. km. and is ellipsoidal in shape. The longer axis (140 km) roughly trends northwest to southeast (general trend of the Himalayan chain). The width varies greatly but the maximum is reached in the central part (40 km).

Fig. II.1. Map of Kashmir valley (after de Terra and Paterson, 1939), showing sampling locations and Karewa sediment distribution.

(1) Burzahom; (2) Saki Paparian; (3) Olchibagh; (4) Pakharpura; (5) Tsrar Sharif; (6) Puthkhah; (7) Hirpur

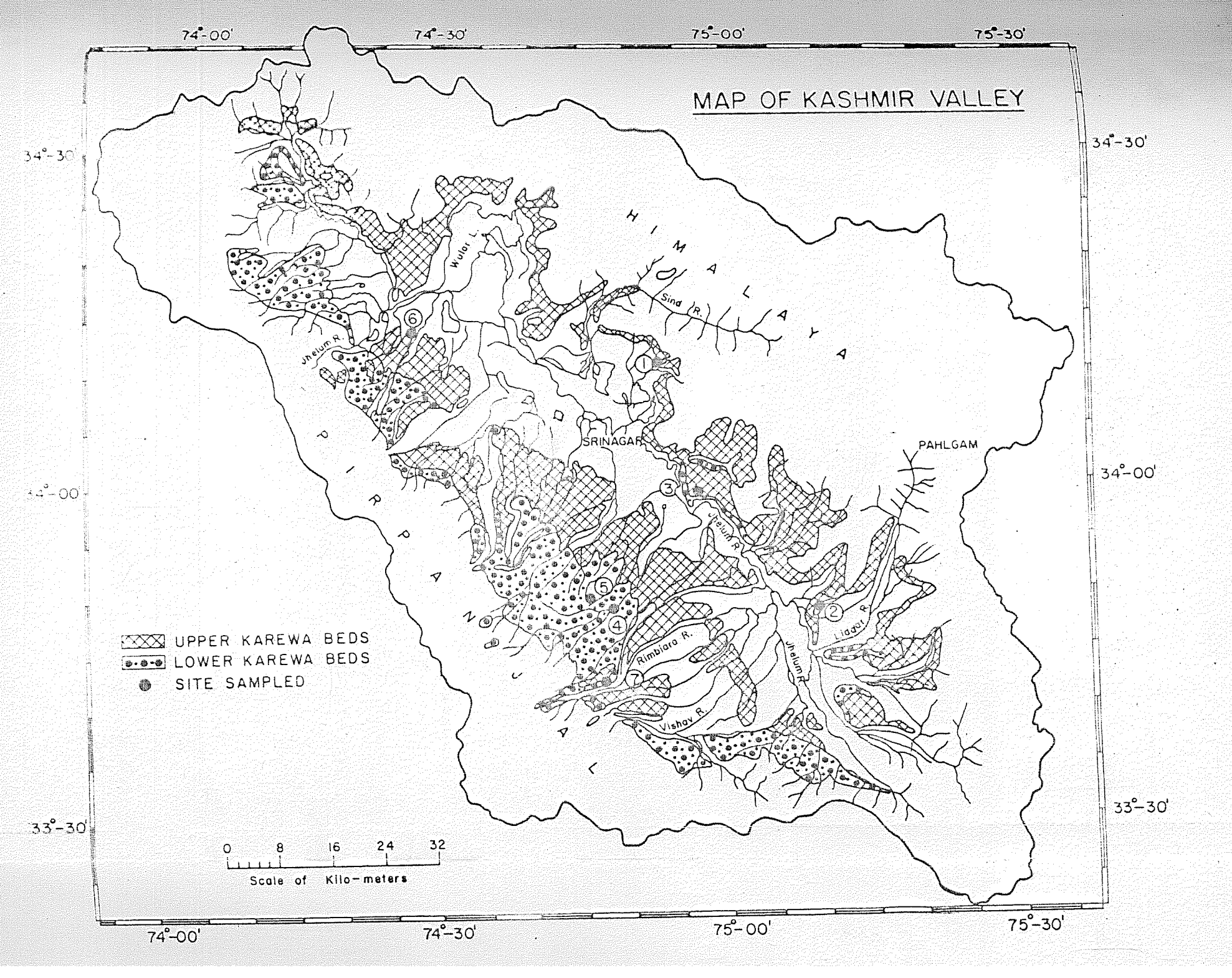
MAP OF KASHMIR VALLEY
74°-00'
74°-30'
75°-00'
75°-30'
34°-30'
34°-00'
33°-30'
HIMALAYA
PIR PANJAL
SRINAGAR
PAHLGAM
Wular L.
Sind R.
Jhelum R.
Lidder R.
Rimbiara R.
Vishav R.
UPPER KAREWA BEDS
LOWER KAREWA BEDS
SITE SAMPLED
0 8 16 24 32
Scale of Kilo-meters

The valley is intermontane fault basin with a sinking tendency and the mountain belt has a rising propensity - these are the main factors responsible for the palaeogeography of the region (de Terra & Paterson, 1939).

The Kashmir valley lies between the Pir Panjal and the Great Himalayan ranges. In this region the Pir Panjal range reaches an elevation of about 4000 m and the Great Himalayan Range of about 6000 m. The maximum and minimum elevations, of the valley proper, are 2200 m and 1500 m respectively. The elevation difference of 700 m is evenly distributed through the numerous 'Karewa' terraces. The term Karewa, adopted from the Kashmiri language meaning flat-topped plateau like natural features, was introduced into the geological literature by Lydekker (1878) and is used to designate the soft sedimentary fill of the valley.

A transverse section of the Karewa sediments shows a slant of 640 m over a distance of 40 km from the Pir Panjal to the Himalayan slope. Its deepest portion lies along the Jhelum river whose course runs through the rocky spurs of the north-eastern flank. The entire Pir Panjal drainage, except for the Jhelum, enters the basin at about 2100 m, whereas the Himalayan streams enter the valley at about 1600 m elevation (de Terra and Paterson, 1939).

Lakes and swamps occupy much of the northwestern part of the valley. The lakes Wular, Manasbal, Ankar and Dal lie in the flood plain of the Jhelum, whose broad meanders have cut swampy lowlands out of the Karewa terraces (de Terra and Paterson, 1939). The occurrence of the sub-recent/recent alluvium is restricted in general to the more central portions of the Kashmir valley. Along the major drainage lines the alluvial tract extends deep into the Pir Panjal and the Great Himalayan ranges (Bhatt, 1975).

The periphery of the Karewa basin indicates that Panjal trap and Triassic limestone are the most widely distributed rock units of the basement, particularly in the central and southwestern parts of the Kashmir valley (Bhatt, 1975). It is likely that in the valleys of Liddar, Sind, Pohru and Mawar, the Lower Palaeozoic rocks form the base for the Karewa sediments. Occasionally, in the central parts of the Kashmir valley basement rocks, consisting mostly of Triassic limestone and some of Panjal trap, crop out in the form of small inliers, such as at Biru, Tral Kham, Sombur, Anantnag, Baba Rafiuddin etc. Such inliers are, however, more numerous along the peripheral ranges, where they represent valleyward extension of the mountain spurs. The position of Kashmir within the Himalayan mountains is determined by two important geologic features: its location on

the margin of a young mobile mountain belt and its proximity to a structural syntaxis. The first feature characterizes it from the very outset as unstable ground, liable to profound crustal disturbances and geographic changes. The second feature is partly due to the orographic outlines of the Kashmir valley basin.

Low anticlinal ridges and intermediate synclines give this area the aspect of a fold belt in the process of formation (de Terra and Paterson, 1939).

II.1.B. The Karewas and their origins

The studies on the Karewas go back to the nineteenth century when Lydekker (1878) investigated the lithology and stratigraphy of these deposits. Middlemiss (1911, 1924) followed up these studies with special reference to structure and tectonics. The most detailed and multipronged study was made by de Terra & Paterson (1939). In recent years several other workers have continued such investigations (Chatterjee and Bhatt, 1969; Bhatt, 1976; Farooqui and Desai, 1974; Roy, 1975; Pant et al, 1978; Agrawal et al, 1978).

Below we will discuss the problems related to the definition, origins, distribution and terminology of the Karewas.

The Karewa deposits have been designated as the Karewa group (Farooqi and Desai, 1974; Bhatt, 1976), which is divided into two parts. The Lower and the Upper Karewas have been defined respectively as 'Pakharpura Formation' and 'Shopian Formation' by Farooqi and Desai (1974). Bhatt (1976) does not agree with their terminology and argues that especially for the Upper Karewa, the stratigraphic definition is based upon only localised geomorphic features. Accordingly, Bhatt (1976) has redefined them under the stratigraphic terms 'Hirpur Formation' for the Lower Karewa and 'Nagum Formation' for the Upper Karewa, and relies upon different type sections. The Hirpur Formation is essentially a lacustrine sequence with minor valley-fill, deltaic and lagoonal deposits in the marginal areas of the basin, while the Nagum Formation represents glacio-fluvial and loessic deposits (Bhatt, 1976).

Lower Karewa (Hirpur Formation): The Hirpurs consist of a sequence of dark bluish-grey clays, light-grey clays, grey sandy clays, laminated varve clays, green sands with sporadic abundance of sand beds intercalated with lignite beds in the marginal areas of the basin. It may be noted that exposures of lignite beds are restricted to the southwestern margin. In the flank of the Pir Panjal range (along the southwestern margin of the Karewa basin) a prominent and persistent conglomerate

horizon is exposed in the lower part (Fig. II.2). The varve clay sequence probably indicates a lacustrine origin of the Hirpur sediments.

In addition to the lacustrine features, fresh water gastropod shells in some clay beds such as at Gulmarg, Trapa sp. at Liddermarg and Guripur provide further evidence for lacustrine origin of the Hirpurs. Krynine (in de Terra and Paterson, 1939, p.235) also holds similar views based upon his sedimentalogical studies. The conglomerate horizon was so far considered to form the base of the Karewa sequence (de Terra and Paterson, 1939; Vishnu Mittre, 1964; Farooqi and Desai, 1974). Bhatt's (1976) study in the upper Rembiara valley has, however, revealed the presence of a 250 m thick deposit of sands, clays and lignites underlying the conglomerate horizon near Dubjan (Lat. 33° 40' N., Long. 74° 38' E.). We have also observed these underlying deposits. Significantly enough, the constituent gravels of all the layers show a preferred orientation towards the northeast which is the regional dip direction of the Hirpur Formation. Bhatt (1975) therefore infers that the conglomerate sequence represents a post-tectonic molasse, formed by a tectonic agency related to the Pir Panjal range rather than its being a glacial outwash deposit as suggested by de Terra and Paterson (1939). The total thickness of the Basal Conglomerate being 200 m, it is hardly possible that a mild glaciation (I Glaciation of Pleistocene)

Fig. II.2. Hirpur Section-A showing Basal Conglomerate near Dubjan. It has a thickness upto 200 m.

Fig. II.3. Schematic sections across the Kashmir basin, showing the stages of the Karewa lake formation as a result of tectonic movements (after de Terra and Paterson, 1939).

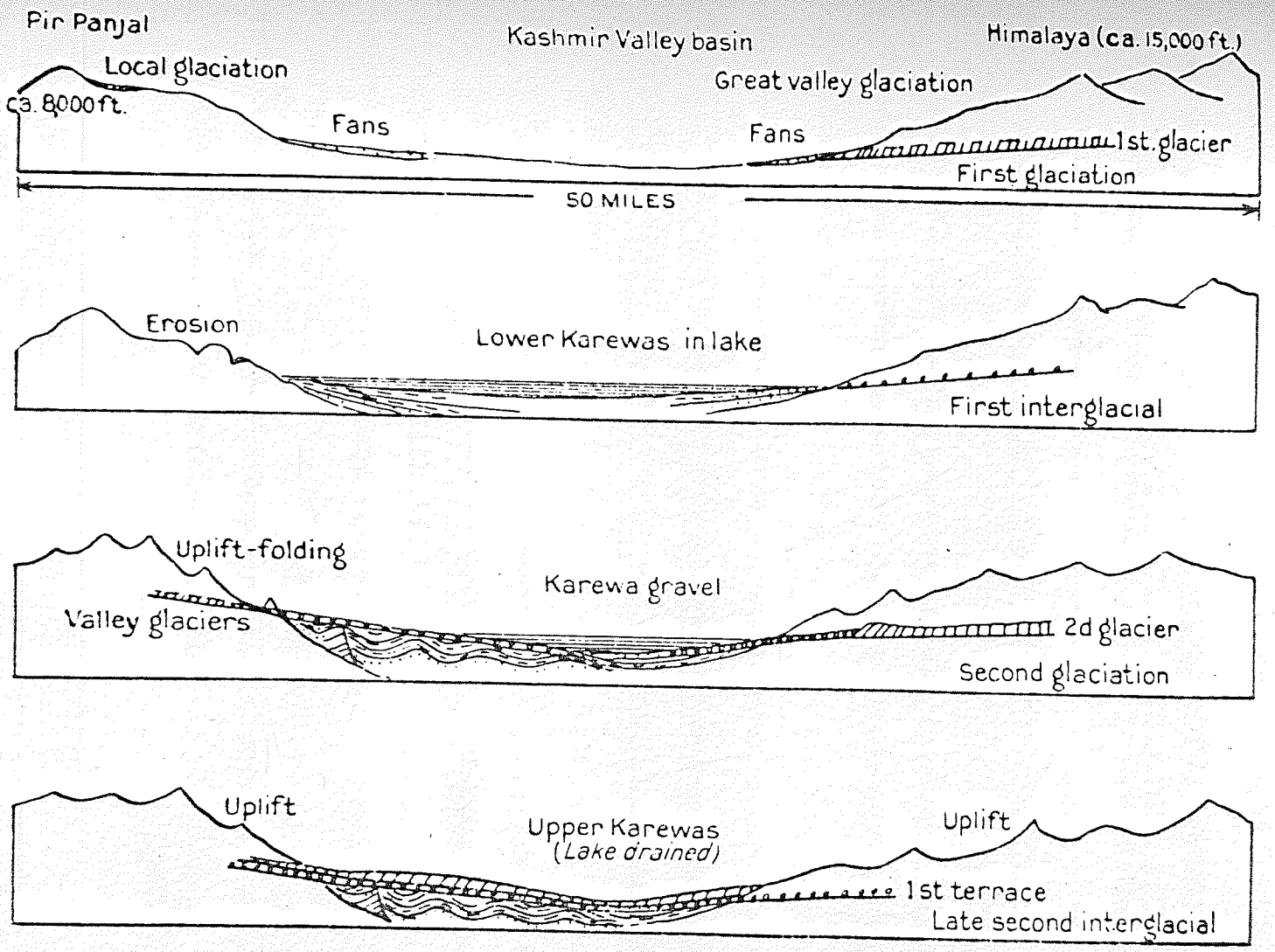
Pir Panjal
Kashmir Valley basin
Himalaya (ca. 15,000 ft.)
Local glaciation
ca. 8,000 ft.
Great valley glaciation
Fans
Fans
1st. glacier
First glaciation
50 MILES
Erosion
Lower Karewas in lake
First interglacial
Uplift-folding
Karewa gravel
Valley glaciers
2d glacier
Second glaciation
Uplift
Upper Karewas
(Lake drained)
Uplift
1st terrace
Late second interglacial

could have given rise to such a thickness of deposits. The presence of the conglomerate mostly along the major drainage lines in the Pir Panjal further suggests that its deposition in the basin took place through a fluvial agency (Bhatt, 1975).

Upper Karewa (Nagum Formation): The Nagum Formation includes in its sequence three lithofacies which are described below, as described by Bhatt (1976).

The basal part is represented by glacio-fluvial gravel fan and gravel bed of re-sorted glacial moraines, made up mostly of fragments of Panjal volcanics, with a minor component of quartzite and limestone. In the central part of the Kashmir valley the gravel fragments are rounded to sub-rounded. South-westwardly towards the source in the Pir Panjal range, however, the clasts become angular to subangular. Along a cross-section across the Kashmir valley, the thickness of glacio-fluvial facies of the Nagum Formation is highly variable; it is about 130 m on the Pir Panjal flank but only about 10-15 m on the Himalayan side. de Terra and Paterson (1939), however, referred to this deposit as Karewa gravel and considered it to represent re-sorted glacial debris belonging to the II Glacial stage of Pleistocene, a view with which Wadia (1961) also agreed.

The lacustrine lithofacies above the gravel of the Nagum formation restricted to northeastern part and about 100 m thick at Sombur (Lat. 34° 57' N., Long. 74° 56' E.), consist of pale yellow laminated marls and silt with marlekar bands, and layers of interbedded medium to coarse grained greenish sands, marlstone, calcareous grits and varved clays. These lithological characteristics unmistakably point to their being lake sediments. Preponderance of marls indicates alkaline environment of deposition. Bhatia (1968) has reported from this lithofacies a prolific fresh water ostracode assemblage, indicating a large permanent, cool, slightly alkaline lake environment of deposition, comparable to that of the present day Wular lake.

Loessic deposits: The topmost member of the Karewa sequence is represented by a brown, granular, non-stratified silty deposit, with carbonaceous bands in between. These carbonaceous bands represent palaeosols, indicating temporary periods of non-deposition and also indicating probably humid and warm climate (Embleton and King, 1969; Kusumgar et al, 1979). The loessic deposit invariably caps the Karewa sequence everywhere.

In the southwestern (Pir Panjal) side of the Kashmir valley these deposits have two, three or more distinct palaeosols within them. In the northeastern part one comes across only two to three palaeosols within the loessic deposits. On the

pir Panjal side there are some sites with 90 m thick loessic deposits just above the gravel bed, whereas on the Himalayan side the loessic thickness is only about 10 m and the deposits overly the lacustrine beds of the Upper Karewa.

The top loessic deposits apparently formed during the last glacial period which was marked by low temperatures and general aridity. But the palaeosols within the loess probably represent warmer/wetter conditions (Embleton and King, 1969; Grootes, 1977).

The loessic deposits possess the property to remain stable even in a vertical cutting (Bhatt, 1976) and do not show any depositional structure. They are well-graded and have a maximum size ranging from 10 μ to 50 μ. The aeolian origin of these deposits has now been confirmed on the basis of sedimentalogical and SEM studies (Pant et al, 1978; Agrawal et al, 1978).

Origin of the Karewas: Godwin-Austin (1864) and Lydekker (1883) had proposed that the original Karewa lake was formed by the uplift of the Pir Panjal. All the earlier investigators have agreed that it was the Jhelum Gorge through which the lake was drained out but none visualized the damming process (de Terra and Paterson, 1939; Fig. II.3).

The key region to the solution of the problem lies between Baramula and Rampur. In this portion the river cuts through

a high spur at Shir Narwao, where its course is still deflected. This spur is part of the ancient divide through which the ancestral Jhelum cut backward, finally to capture the drainage of the Kashmir basin. The ancient divide is a fault-line scarp on the Kashmir side, characterized by seismic disturbances. The river was nearly graded when the uplift must have carried the old divide to such a height that the river was deflected and prevented from pursuing its course. The Jhelum gradient was fairly established and there was no deep transverse gorge such as exists today, which means that a slight initial uplift would have been sufficient to first block the stream and then turn it backward to the basin. A landslide may have dislodged the fan deposits on the now steepened slope and helped to bar the stream. After this, flooding of the basin must have been instantaneous, as indeed the sudden change from coarse sandy to clay beds in the Lower Karewa indicates. The lake probably established its spillway at an early period, but as its channel had been dislodged through uplift, it could not cut into its old bed but was forced to flow across a convenient gap in the rocky divide. This retarded the outflow of the lake, the bottom of which undoubtedly subsided further in adjustment to the Pir Panjal uplift. This sinking of the lake basin led in turn to new displacements along the mountain front, the faulting carried the old Jhelum to even greater height. The spillway now entrenched

itself more vigorously in the bedrock, which may have caused the first draining of the Karewa lake at the first interglacial period. This is the phase of the green-sand deposition along with Himalayan slope and of the upper lignite bearing sandy beds on the Pir Panjal side. The lake was at a low level and considerably reduced in size when the second glaciation set in. The Lower Karewa beds were already tilted, and the spillway was unquestionably firmly established in the bed rock, but from now on the existence of the lake was no longer so dependent on the ratio of uplift to erosion but rather on lowering of the spillway and water supply in the basin. The relative scarcity of glacial-lake deposits indicates that during the second glacial the inflow slackened and the spillway presumably remained stationary. At the beginning of the following interglacial period, however, the lake deepened again, and it must for a time have been well sealed off, as the sediments prove (marl-bearing beds). Once more the uplift temporarily interrupted the outflow, and in this process subsidence of the lake floor, which caused lowering of the lake level, must have played a dominant part. Presumably, this deepening of the lake was short-lived, because not only the rainfall decreased but the amount of the ice in the valleys as well. Once the lake had regained the spillway it emptied quickly, and with continued uplift the new Jhelum valley deepened, thus leading to complete spilling of the lake (de Terra and Paterson, 1939).

II.1.C. Chronological controversies

The main reason for this research was to resolve the widely divergent chronologies for the sedimentation in the Karewa lake. In fact, the discrepancies between the different estimates for the beginnings of the Karewas are more than 12 million years (Tables II.1, 2, 3 & 4). Since the Karewas preserve a valuable palaeoclimatic record, I thought that the application of physical methods of dating would help a great deal in providing better chronology to these events.

Below we discuss the various age estimates for the Karewa events.

Lydekker for the first time used the term 'Karewa' and divided it into the Upper and Lower parts, assigning the Upper Siwalik or Pliocene age (Lydekker, 1883). Dianelli (in de Terra and Paterson, 1939) made extensive observations on the glacial sequence and recognised four main glaciations in the Pleistocene. Middlemiss (1911, 1924) also assigned Plio-Pleistocene age to the Karewas.

A more systematic study was carried out by de Terra and Paterson (1939). The presence of Elephas hysudricus helped de Terra and Paterson (1939) in assigning a definite Pleistocene age to the Lower Karewa and thus correlating it with the Pinjor

Table II.1. de Terra's Stratigraphic succession of the Karewas (after de Terra and Paterson, 1939)

PLEISTOCENE	UPPER KAREWA 300 m	II INTERGLACIAL II GLACIAL
	LOWER KAREWA 600 m	I INTERGLACIAL I GLACIAL
Older rocks (Triassic limestones, Panjal Volcanics, etc)		

Table II.2. Wadia's stratigraphic succession of the Karewas (Wadia, 1948)

PLEISTOCENE PLIOCENE	UPPER KAREWA 300-500 m	Well bedded sands and clays with boulders and erratics, varve clays Basal boulder bed II Glacial
	LOWER KAREWA 1,550-1,675 m	Blue buff and blue grey shales, sands and gravel, crossbedded varve clays I Glacial Dark, often carbonaceous shales, sandstones with thick conglomerate beds and lignite seams Pre-Glacial
		Pre-Tertiary

Table II.3. Roy's stratigraphic succession of the Karewas (Roy, 1975)

PLEISTOCENE	UPPER KAREWA 300 m	Horizontally bedded sands and silts, sandy and granular clays, boulders and erratics, also tillites, loamy materials, conglomerates and gravels Glacial
MIO PLIOCENE	LOWER KAREWA 600 m	Folded and faulted soft, dark grey, tough clays, shales and sands with seams of lignite and well bedded pebble beds
Pre-Tertiary		

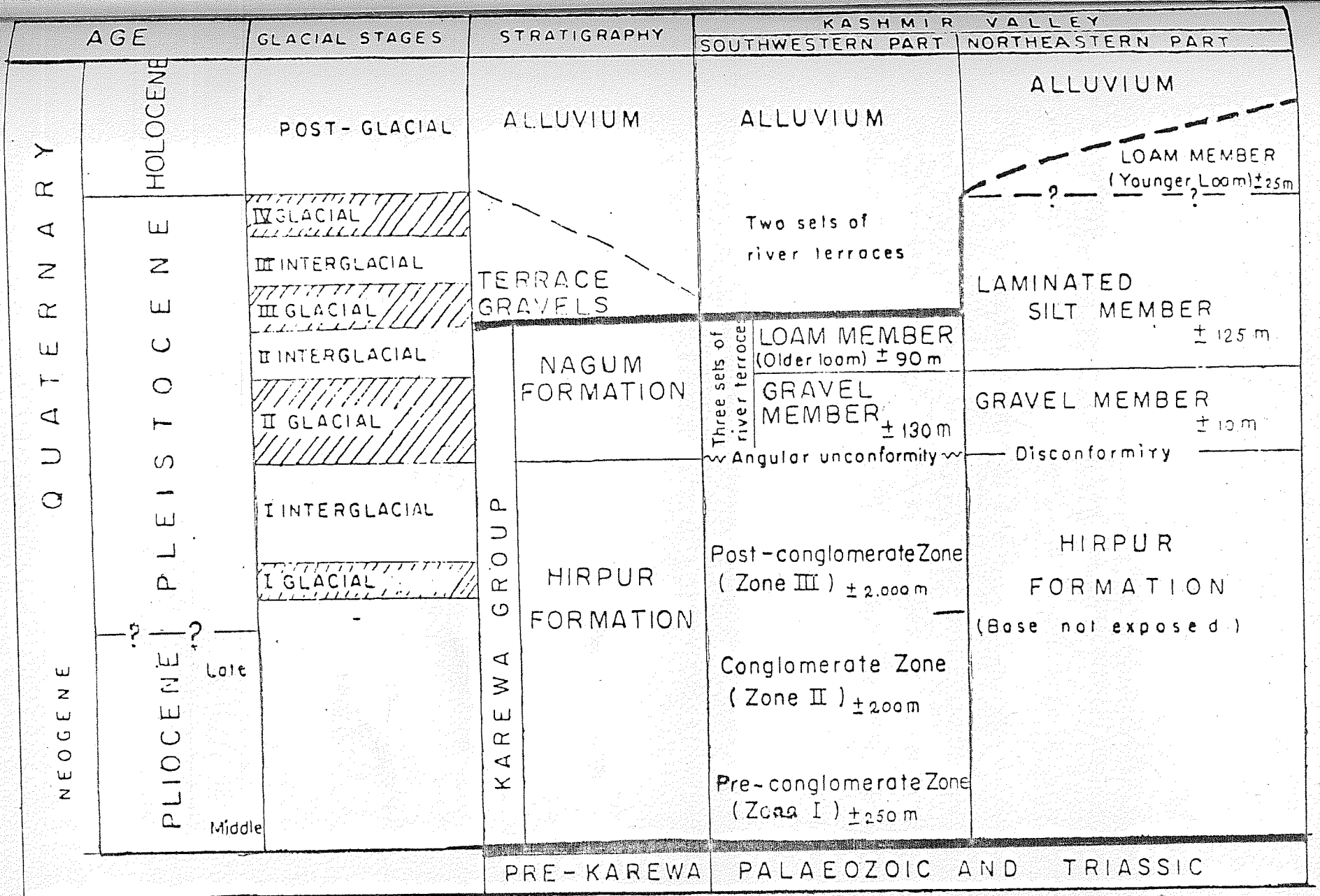
AGE
GLACIAL STAGES
STRATIGRAPHY
KASHMIR VALLEY
SOUTHWESTERN PART
NORTHEASTERN PART
QUATERNARY
HOLOCENE
POST-GLACIAL
ALLUVIUM
ALLUVIUM
ALLUVIUM
LOAM MEMBER
(Younger Loam) ± 25m
Two sets of river terraces
IV GLACIAL
III INTERGLACIAL
TERRACE GRAVELS
III GLACIAL
II INTERGLACIAL
NAGUM FORMATION
LOAM MEMBER
(Older loam) ± 90 m
Three sets of river terrace
GRAVEL MEMBER ± 130 m
LAMINATED SILT MEMBER ± 125 m
GRAVEL MEMBER ± 10 m
II GLACIAL
Angular unconformity
Disconformity
I INTERGLACIAL
KAREWA GROUP
HIRPUR FORMATION
Post-conglomerate Zone (Zone III) ± 2,000 m
HIRPUR FORMATION
(Base not exposed)
I GLACIAL
Conglomerate Zone (Zone II) ± 200 m
NEOGENE
PLIOCENE
PLEISTOCENE
Late
Middle
Pre-conglomerate Zone (Zone I) ± 250 m
PRE-KAREWA
PALAEOZOIC AND TRIASSIC

stage of the Upper Siwaliks (Table II.1). Wadia (1941, 1948) also investigated the major glaciations, their bearing on the Karewa deposits, Plio-Pleistocene boundary and the advent of Early man. He assigned a pre-glacial (Pliocene) age (Table II.2) to the lower units of the Lower Karewa, overlain by beds containing moraines of the earliest glaciations, followed by those of the successive glaciations. The diatom evidence in Lower Karewa can be sub-divided bio-stratigraphically into two bio-zones, the lower part being characterised predominantly by Centrales, the upper one by Pennales (Roy, 1975; Table II.3). The Upper Karewa is devoid of diatoms. As regards the lower age limit of the Karewas, Roy (1975) while agreeing with Middlemiss (1924) and Wadia (1948) that it extends into Pliocene, suggests that it may even extend into Miocene. Further he thinks that the Sombur bone bed belongs to the Upper Karewa though de Terra and Paterson (1939) ascribed it to the Lower Karewa. The Pleistocene age assigned to the Sombur deposit on the vertebrate fossil evidence thus may be used only to date the upper part of the Lower Karewa. Of course at Sombur the Lower Karewa sediments are very poorly preserved.

II.1.D. Glacial features and terraces

Three interglacial and four Pleistocene glacial features have been recognised by de Terra in Kashmir, following the Alpine sequence, along the valleys of Liddar and Sind on the Himalayan side. From the glacial relicts the intensity of different glaciations could be determined. The first two glacial advances were much more extensive than the rest and the II glacial period was the most extensive and came down upto the 1500 m contour. From the size of moraines the extent and the intensity have been estimated. At Mangon, the terminal moraines came as far down as 1680 m in the Sind valley. From the extents of erosion and deposition, the duration of the interglacial periods have also been determined. It appears that the glacial periods were much shorter than the interglacial periods (de Terra and Paterson, 1939).

The terraces on the tributaries of the Jhelum can be correlated with various glacial advances and retreats. Krishnaswamy, who was a member of the Yale-Cambridge team, describes (Krishnaswamy, 1947) the processes as follows:

> Terraces are found mainly in the transverse valleys of the flaking mountains and are well preserved along the Vishav river (a tributary of the Jhelum), south of Srinagar and east of Shupian. The first terrace was cut into the Karewa formation by the river by dissecting the soft silt until it reached the underlying more resistant gravel fans. This must have happened before

the third glacial advance, because its moraines are found at a much lower level, 30 m beneath the surface of the fans of the second glaciation. Evidently the streams could have dissected the Upper Karewa beds of the lake only after it had been drained out. And there is evidence of this in the tributary valley west of Srinagar and elsewhere in the form of a ledge referable to Terrace 1 between the two slopes, the upper one of which belongs to the Upper Karewas. Below the lower slope, the moraines of the third glaciation occur. The lower slope thus belongs to the latter half of the second interglacial and the ledge (Terrace 1) must therefore belong to the earlier half of the second interglacial period.

Terrace 2 is encountered below a prominent slope and in general is not well preserved. However, in three instances its correlation with the terminal moraines of the third glaciation was clear. Terrace 3 is conspicuous by its great width. Up-stream this terrace cuts into the third glacial moraine, as in the Pir Panjal mountains, and therefore is erosional in origin and has to be placed in the third interglacial.

The fourth glaciation was less effective in Kashmir than the preceding ones and the glacial outwash resulting from it is therefore generally thinner. The corresponding terrace (Terrace 4) lies for the most part 12 m to 15 m above the present stream-levels and carries a veneer of loamy silt probably derived from the weathered loess.

The fifth and lowest terrace concludes the system and is encountered in most valleys of the Kashmir basin 6 m to 10 m below an erosional slope cut into Terrace 4. It is composed chiefly of a brown loamy silt, corresponding clearly to the Late post-glacial advance, which in turn relates itself clearly to the youngest and freshest set of the small, thin moraines at the highest valley level on either flanks of this basin.

Thus the Quaternary terraces 1 to 5 in the glacial portion of the Kashmir Himalayas have been due to alternating aggradations of stream-level corresponding to glacial stages (Terrace 2, 4 & 5) and degradation in the interglacial stages (Terrace 1 and 3), aided by interpolated diastrophic uplifts. The terraces therefore begin from the later half of the second interglacial.

II.2. Palaeontology of the Karewas

The Karewas are quite rich in a variety of faunal and floral remains which provide significant chronological and palaeo-ecological markers. As I am using palaeomagnetic dating, which is only a relative method, such fossil markers provide vital bio-stratigraphic clues. For example, the Villafranchian fauna, which marks the Pleistocene, cannot occur beyond the Matuyama Reversed Epoch.

I have tried to tabulate the fossil evidences under separate categories: plant megafossils (Table II.5); spores and pollen (Table II.6); diatoms (Table II.7); invertebrates (Table II.8); and vertebrates (Table II.9).

Though we have a large number of fossils, their stratigraphic locations are known only in a very broad sense. We have therefore depended on absolute dating methods to define the uppermost part of the Karewa stratigraphic column. Through personal enquiries from the various workers we have, however, checked that the Villafranchian fauna occurs only in upper parts of the Lower Karewa.

Table II.5. Plant remains from the Karewas

Location	Horizon	Type of plant remains (megafossils)	Reference
Ninglenala, Bota Pathri, Lidder Marg, Laredura, Dangarpur etc.	Lower Karewa	Woody plants: Ranunculaceae, Berberidaceae, Aceraceae, Hippocastanaceae, Sabiaceae, Papilionaceae, Rhamnaceae, Rosaceae, Araliaceae, Cornaceae, Caprifoliaceae, Oleaceae, Cupuliferae, Junglandaceae, Ulmaceae, Salicaceae, Coniferae Herbaceous plants: Nymphaeaceae, Hydrocaryaceae, Typhaceae Fern: Adiantum pinnule(?), Dryopteris, Selaginella(?)	de Terra and Paterson (1939)
Hirpur	"	Acer, Quercus, equisetaceuous plant	Tripathi and Chandra (1962)
Rosulu	"	Acer, Quercus, equisetaceuous, plant, willow leaves	"
-	"	Acer, Quercus, Alnus, Berberis, Betula, Boxes, Cotoneaster, Hedera, Parrotia, Pittiosporum, Pyrus, Rhamnus, Rosa, Rubns, Ulmus etc.	"
Raithan	"	Trapa bispinosa, Trapa natans	"
Ninglenala	"	Quercus sp., Trapa sp.	Roy (1975)

Table II.6. Spores and pollen remains from the Karewas

Location	Horizon	Name of fossil, spores and pollen	Reference
Not known	Lower Karewa	Pinus, Cedrus, Picea, Abies, Betula, Carpinus, Corylus, Alnus, Salix, Plantago, Fuglans, Fraxinus, Maryophyllum, Artsemisia, Cupressaceae, Graminacae, Ephedra, Maclura, Ulmus and Persicaria, Chenopodiaceae, Compositae, Maoutia	Woodhouse and de Terra (1935)
"	"	Grassy plants	"
"	"	Aquatic vegetation - Typha. Forest vegetation - Alnus, Plantago, Chenopods etc.	Nair, (1960)
"	"	Prominent oak phase	Vishnu-Mittre, Singh and Saxena (1962)

Table II.7. Diatom types from the Karewas

Location	Horizon	Diatom types	Reference
-	Upper Karewa	Devoid of diatoms	Roy (1975)
Sombur	Lower Karewa?	Devoid of diatoms	"
Botapathri, Sochalpathri, Hakarpathri	"	Cyclotella, Melosira, Cocconeis, Stephanodiscus, Coscinodiscus, Eunotia, Fragilaria, Stauroneis, Epithemia, Pinnularia, Caloneis, Cymbella, Achnenthes, Rhaponeis, Gomphonema, Synedra, Amphora, Hantzschia, Tetracyclus, Tabellaria, Navicula, Rhopalodia and Mastagloia	Roy (1975), Iyengar and Subrahmanyan (1943)
Handwor	Lower Karewa	Cymbella, Cocconeis, Cyclotella, Cymatopleura, Epithemia, Navicula, Rhoicosphenia, Stephanodiscus, Synedra, Gomphenema, Nitzschia, Rhopalodia, Amphora, Fragilaria, Stauroneis and Pleurosigma	Conger (in de Terra and Paterson, 1939)
Nichahom	"	Melosira, Cyclotella, Cocconeis, Diploneis, Synedra, Cymbella, Gomphonema, Hantzschia, Rhopalodia, Navicula, Achnenthes, Eunotia, Pinnularia, Stephanodiscus etc.	Roy (1975)
Taundus	"	Melosira, Stephanodiscus, Cyclotella, with very few Gomphonema, Diploneis, Cymbella, Synedra, Fragilaria, Nitzschia, Eunotia and Rhoicosphenia	"

Table II.7 (continued)

Location	Horizon	Diatom types	Reference
Baramula	Lower Karewa	Cyclotella, Melosira, Cocconeis, Diploneis, Cymbella, Fragilaria, Synedra, Navicula, Achnenthes, Epithemia, Galoneis, Amphora, Nitzschia, Gomphenema, Stephanodiscus, Stauroneis, Pinnularia etc.	Roy (1975)
Fagirbagh	"	Fragilaria, Cymbella, Gomphonema, Diploneis, Pinnularia, Synedra, Cyclotella and Melosira	"
Wogur	"	Fragilaria, Melosira, Cyclotella and Synedra	"
Hakriaj nar	"	Cyclotella, Melosira, Stephanodiscus with few Fragilaria and Epithemis	"
Sukhnag	"	Cyclotella, Melosira, Coscinodiscus, with a few Cocconeis, Eunotia, Cymbella, Diploneis, Epithemia, Gomphonema, Fragilaria, Synedra, and Caloneis	"
Raithan	"	Cyclotella, Melosira, Stephanodiscus, Cocconeis, Fragilaria, Synedra, Stauroneis, Cymbella, Eunotia, Pinnularia, Epithemia, Diploneis, Caloneis, Tetracyclus, Achenenthes, Navicula, Frustulia, Licmophora, Nitzschia, Hantzschia, Gomphonema, Amphora, Rhoicosphenia, Rhopalodia etc.	"
Badrish nala	"	Diploneis, Navicula, Melosira, Fragilaria, Stephanodiscus, Gomphonema and Cyclotella	"

Table II.7 (continued)

Location	Horizon	Diatom types	Reference
Laradura	Lower Karewa	Cyclotella, Melosira and Coscinodiscus, Cocconeis, Synedra, Fragilaria, Pinnularia, Srauroneis, Cymbella, Eunotia, Surirella, Navicula, Diploneis, Amphora and Gomphonema	Rao and Awashthi (1962); Roy (1975)
Tsanam	"	Milosira, Cyclotella and Stephanodiscus	Roy (1975)
Liddermarg	"	Cyclotella, Melosira, Stephanodiscus and Coscinodiscus with a few Fragilaria, Caloneis, Stauroneis, Cymbella, Eunotia, Epithemia and Amphora	"
Dainzeb	"	Cyclotella, Melosira, and Coscinodiscus with very few Epithemia, Fragilaria, Stauroneis and Cymbella	"
Danider	"	Cocconeis, Fragilaria, Pinnularia, Cymbella, Eunotia, Stauroneis, Navicula, Diploneis, Amphora with few Cyclotella and Melosira	"

Table II.8. Fossil invertebrate (Ostracodes) from the Karewas

Location	Horizon	Invertebrate fossils (Ostracodes)	Reference
Near Naugam Highway	Upper Karewa	Darwinula Stevensoni (A), Potamocypris minuta Patriciae (R), c. sp. of c-angulate (R), c. Candida (F), c. latea (A), c. neglecta (C), c. sp. of c. detecta (R), Candonopsis sp. of c. Kingsleyi (R), Cypria opthelmica (R), Ilyocypris bradyi (A), I. Shawneetownesis (F), Ilyocypris sp. (R), Limnocythere Staplini (F), Limnocythere sp. (F), Cyprinotus Salinus (R), Cypris Subglobosa (A), Cypridopsis Vidua (F), c. Compressa (R), I. Kashmirensis (F)	Bhatia (1968)
"	"	Darwinula Stevensoni (R), Cypris Subglobosa (A), Cypridopsis vidua (F), c. lactea (R), c. neglecta (F), Ilyocypris bradyi (A), I. Shawneetownensis (R)	"
Khrew	"	Cypridopsis Vidua (C), c. lactee (R), Ilyocypris bradyi (A), Ilyocypris sp. (R) Liminocythere sp. (R)	

Table II.9. Fossil invertebrates (fresh water and land molluscan) from the Karewas

Location	Horizon	Invertebrate fossils (fresh water and land molluscan)	Reference
Not known	Lower and Upper Karewas	Bensonia, Bithynia, Valvata, Estheria, Gyraulus, Corbicula, Lamellidens, Planorbis, Lymnaea, Psidium etc.	Roy (1975)
Nichahom	Lower Karewa	Fossil anthropods with Esthernia, a locust, a mosquito scorpion and fly, Fossaria sp. indet A and B (R), Planorbis Planorbis tangitarensis (A), Menetus sp. of M. Pearletti (R)	Tripathi and Chandra (1962); Bhatia (1974)
Raithan	"	Planorbis Planorbis tangitarenis (A), Vallonia Pulchella (F), Vertigo Ovata (A), Cochalicopalubrica (A), Succinea indica (A), Operculum Type A and B (A) P. (E.?) mitchelli (A)	
Gulmarg	Upper Karewa	Lymnae (Galba) andersoniana forma simulans (R), L. (Pseudosuccinea) acuminata forma hians (R), Indoplanorbis exustus (A), Planorbis Planorbis tangitarensis (A), Anisus gulmargensis (F), Armiger Annandalei (R), Cochlicopalubrica (F), Succinea indica (A), Pisidium (Eupisidium), hydaspicola (R), P. (E.?) mitchelli (A)	Bhatia (1974)
Bijbihara	Upper Karewa	Planorbis Planorbis tangitarensis (F), Gyraulus convexiusculus (F), Pisidium hydaspicola (R), P. (E.?) mitchelli (F)	

Table II.10. Fossil vertebrate remains from the Karewas

Location	Horizon	Vertebrate fossil	Reference
Baramula	Lower Karewa	*Sivatherium giganteum*	Badam (1972)
Sombur	"	*Sus. sp.*	Badam (1972)
"	"	*Elephas hysudricus* number of bones of artiodactyle mammals and birds	de Terra and Paterson (1939)
Anantnag	"	*Equus Sivalensis*	Badam (1972)
Zangam	"	*Giraffa sp.*, *Elephas sp.*, *Elephas hysudricus*	Badam (1972)
Badgam	"	*Cervus sp.*	de Terra and Paterson (1939)
Pampur	Upper Karewa	*Bos. sp.*	?
"	Karewa	*Hypselephas hysudricus*	Tripathi and Chandra (1962)
Nichahom	Lower Karewa	Fish and bird bones	"
Hatwer	"	*Palaeoloxodon anticuus* (*namadicus*)	"
Tsrar Sharif	"	Proboscidean tusk, artiodactyle limb bones and bird bones	"
Gojipather	Karewa	*Boselelephas tragocamelus*	"

Table II.10 (continued)

Location	Horizon	Vertebrate fossil	Reference
Marahom	Karewa	Fish remain	Tripathi and Chandra (1962)
Pattan	Upper Karewa	Rhinocerous	Badam (1968, 1972)
Shupian Tehsil	Lower Karewa (upper part of Lower Karewa	Equus sivalensis	Tiwari and Kachroo (1979)

II.3. Our approach and sampling

Our aim was to date the climatic events witnessed by the Kashmir valley. We therefore had to try to date the various manifestations of the climatic change, like floral and faunal variations; advances and retreats of glaciers; terrace systems; loess formations and their palaeosols; sedimentary cycles in the Karewa basin etc. Since we chose the sediments of the Karewa basin for our study, our sediment profile starts from the formation of the Karewa lake to the recent archaeological deposits that overly the loessic deposits.

Since we have used relative dating methods like magnetic polarity reversals besides absolute methods, we have to ensure two things before sampling: (i) completeness of the sediment record sampled; and (ii) absolute chronological markers to place the magnetic polarity scale in an absolute time-frame.

For the stratigraphic scheme we have relied upon the earlier work by de Terra and Paterson (1939) and Bhatt (1976). Essentially there are three main members in the depositional formations of the Kashmir basin: the Lower Karewa, the Upper Karewa and the Loess.

The Hirpur (Lower Karewa) lake was formed by the rise of the Pir Panjals. Further uplift on the Pir Panjal side raised the Hirpur lake sediments, thus tilting and shifting the lake

to the Himalayan side. The loess now had exposed Hirpur sediments to be deposited upon, but on the Himalayan side, the Nagum Lake (Upper Karewa) was alive. As a result, the loess of the Pir Panjal side is partly coeval with the Upper Karewas of the Himalayas. When finally even the Nagum Lake was drained off, loess deposited all over the exposed lake sediments of both the north-eastern and south-western sides. Thus, to complete the sedimentary record one has to cover all these depositional members.

We have, therefore, sampled the Upper Karewa (lacustrine) and the Loess (aeolian) from the Himalayan side and the Hirpur Lower Karewa sequence on the Pir Panjal flank. Thus we have ensured that the complete sedimentary record of the basin is covered by our sampling. For example, at Saki Paparian a complete Upper Karewa sequence is probably sitting over a Lower Karewa deposit marked by cross-bedded sands and bluish clay. The two are separated by a thin gravel sheet which is a continuation of the gravel bed separating the Upper from the Lower Karewas (Fig. II.4).

For absolute chronological markers we have made use of both fossils and absolute dating methods. For example, Burzahom is one of our representative sections (Fig. II.5) where we have dated the archaeological deposits to c.4500-3500 B.P. (Agrawal and Kusumgar, 1974). Below the archaeological deposits is the

Fig. II.4. A view of the lowest part of the Saki Paparian section showing the horizontal lacustrine strata of the Upper Karewa overlying the tilted cross-bedded sands and bluish clays, probably belonging to the Lower Karewa. The two are separated by a thin sheet of gravel here.

loess with three palaeosol bands which have also been ^{14}C dated. For dating the next underlying member (lacustrine Upper Karewa) we tried to date the marlekar bands by U-series method. This stratigraphically controlled dating not only ensured that we had a complete sequence upto the late Holocene but we could also roughly extrapolate the age of the Upper Karewas on the basis of the available absolute dates.

For the Lower Karewas, we had three stratigraphic controls: the Boulder Conglomerate; the Gravel 2; and the Gravel 3; the last separates the Upper from the Lower Karewas. These markers provide adequate stratigraphic controls to divide the Hirpur sedment profile into several sub-sections for palaeomagnetic stratigraphy. This approach would also help in correlating the various Hirpur formation sections at different sites with each other.

We have tabulated (Tables II.5 to II.10) the fossil evidence from the Karewas, but very few fossils are really useful as chronological markers. Diatoms show a distinctive bio-stratigraphic distribution. The Centrales are confined to the lower part and the Pennales to upper part of the Lower Karewas; the Upper Karewas, however, are bereft of them (Roy, 1975). Though a large number of vertebrate fossils are known (Badam, 1979) from the Karewas, yet stratigraphically controlled samples

Fig. II.5. Schematic section at Burzahom, near Srinagar. It shows, from top bottomwards, an archaeological (Neolithic) deposit; followed by a loessic deposit, along with its three palaeosols; at the bottom is the beginning of the lacustrine Upper Karewa sediments. Radiocarbon dates are marked against the deposits.

BURZAHOM
Section looking East

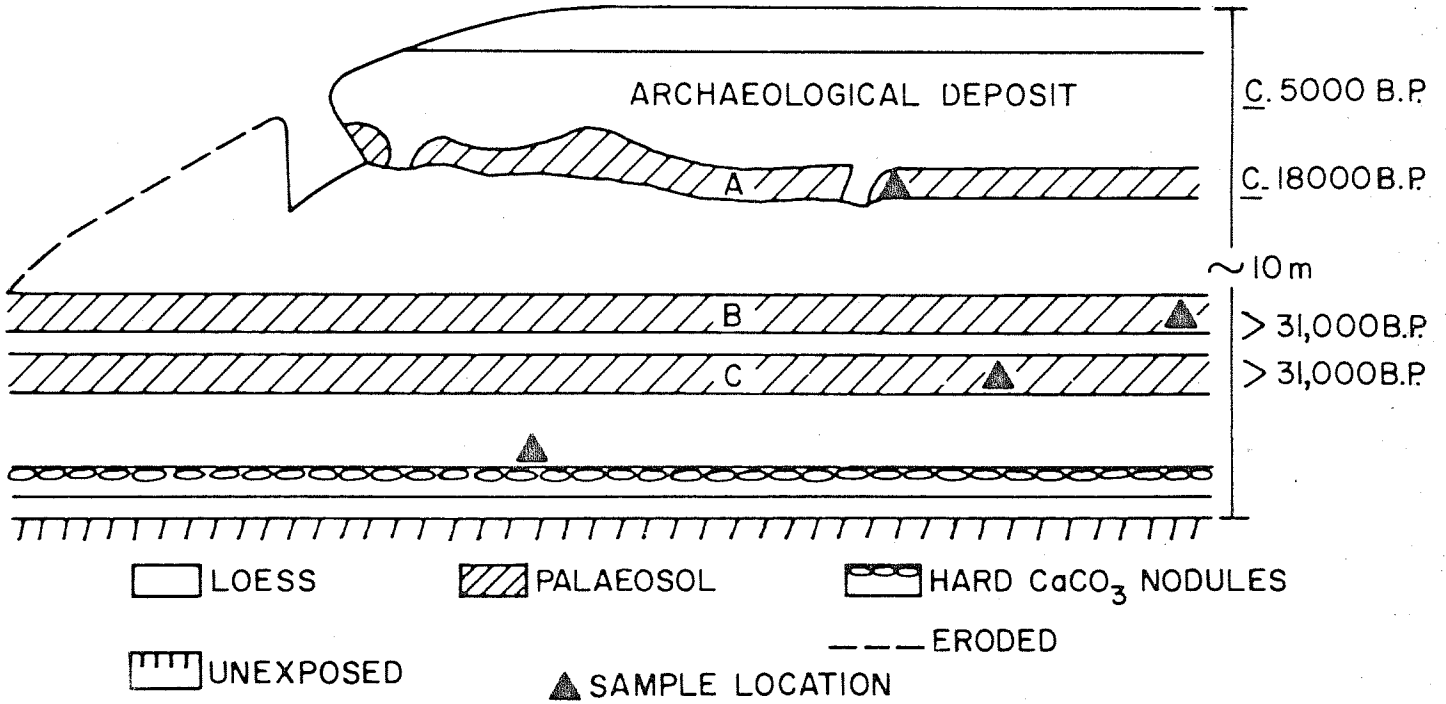

are few. Elephas hysudricus, Equus sivalensis etc. are confined to the upper-most part of the Hirpur sequence viz., above Gravel 2 in our scheme. It is, therefore, obvious that the Plio-Pleistocene boundary (Olduvai event on the magnetic scale) has to be located between Gravel 2 and 3, as indeed the magnetic measurements indicate (Chapter IV).

Our litho- and magneto-stratigraphic scheme has the potential to provide a framework in which all the fossil data can be put at its proper place and a bio-stratigraphy is evolved for each type of fossil evidence. Of course, such a correlation can be brought about only through a big project in which the original palaeontologists who have worked in the area coordinate their efforts following the stratigraphic scheme suggested here.

In the present state of field-information, there is no better preserved or more complete section of the Lower Karewas than the one exposed by the River Rembiara between Dubjan and Shopian. It has all the virtues of being selected as the key type section for the Lower Karewas. We have also made this as our index section.

For the Upper Karewa sections, we found Saki Paparian and Olchibagh as the best preserved ones. We have therefore used them, especially, Saki Paparian, as the type section for the Upper Karewas.

A detailed discussion of the dating of the climatic events will be given in Chapter V.

CHAPTER III

III. RADIOACTIVE DATING

III.1. Introduction

III.2. Radiocarbon dating

III.2.A. Principles
III.2.B. Techniques

III.2.B.1. Chemical procedure
III.2.B.2. Assaying techniques and detection limits
III.2.B.3. Calculation of ages

III.2.C. Dating material and sample collection
III.2.D. Results and discussion

III.3. Uranium series dating

III.3.A. Principle
III.3.B. Techniques

III.3.B.1. Extraction and radiochemical purification
III.3.B.2. Assay of uranium and thorium isotopes

III.3.C. Sample collection
III.3.D. Results and discussion

III.1. Introduction

Several radioactive isotopes produced by cosmic rays in the earth's atmosphere were discovered during 1948-1960 (Libby, 1955; Lal and Peters, 1962); out of these ^{14}C and possibly ^{10}Be are suitable for dating the Karewas. Several radioactive isotopes belonging to the U/Th series can also be used for dating the Karewas. We have attempted to make use of the two radioactive methods for dating (besides palaeomagnetic dating, Chapter IV) the Loess and the Upper Karewa formations in Kashmir.

In this Chapter we will discuss the dating techniques based on the radioactive isotopes ^{14}C, ^{234}U, ^{238}U and ^{230}Th which were used in the present work.

III.2. Radiocarbon dating

Amongst the physical methods, the radiocarbon dating technique for dating organic remains is still unsurpassed in accuracy. Normally its dating range is 40,000 years; the range can, however, be extended to 75,000 years by an enrichment technique (Grootes, 1977) and possibly upto 100,000 years using the recently developed accelerator atom counting technique (Muller et al, 1978; Bennett et al, 1978). The principle and the techniques involved in radiocarbon dating are given below.

III.2.A. Principles

The technique of determining the chronology of ancient civilizations by measuring the radiocarbon content of organic remains was developed by Libby and collaborators (Anderson, Arnold and Libby, 1949; Libby, 1955, 1970). The method is based on the fact that radiocarbon (^{14}C) atoms are continuously produced in the atmosphere as a result of (n, p) reaction induced by slow neutrons on atmospheric nitrogen nuclei (^{14}N). A lesser amount ($\lesssim$10%) is also produced as a result of the interaction of fast neutrons with nitrogen and oxygen nuclei of the atmosphere (Lal and Peters, 1962). The newly formed carbon is oxidized to $^{14}CO_2$ and rapidly mixes with atmospheric carbondioxide ($^{12}CO_2$). Part of the atmospheric $^{14}CO_2$ and $^{12}CO_2$ enter plant tissue as a result of photosynthesis. Animals partake of carbon through the consumption of vegetable matter. The larger part of the $^{14}CO_2$ (and $^{12}CO_2$) goes to the ocean where it gets incorporated in the marine carbonates (CO_2, HCO_3^-, CO_3^-) through the exchange processes occurring at the air-sea interface. Thus the marine biosphere also receives a supply of radiocarbon. From the atmosphere, which is its birth place, ^{14}C is distributed globally through the 'carbon cycle'. A steady-state equilibrium is maintained by the production of ^{14}C in the atmosphere and its radioactive decay. All living matter on earth is thus labelled by radiocarbon atoms at a constant level (activity per gm of

carbon). It is this large-scale labelling which gives the radiocarbon method a very wide scope of applicability (Libby, 1955; Olsson, 1970).

The basic assumptions for 'dating' with radiocarbon can be summarised as follows:

(1) The production rate of ^{14}C has been essentially constant over a period of the order of several half-lives of the isotope (10^5 years) and its activity is well mixed in the atmosphere.

(2) The size of the dynamic carbon reservoirs (atmosphere, biosphere and the ocean) has not changed appreciably in size.

(3) After the removal of a carbon containing substance from the dynamic carbon reservoir, there is no fresh supply of carbon and the loss is due only to radioactive decay of ^{14}C atoms with a half-life of 5730 years. In other words, the system to be dated becomes isolated and ceases to exchange carbon with the environment.

If these assumptions are valid, the age of a sample bearing organic carbon is given by:

$$A = A_o e^{-\lambda t} \qquad \ldots\ \text{III.1.}$$

where A is the measured activity due to ^{14}C in units of disintegrations per minute (dpm) per gm of carbon, A_o is the equilibrium concentration and λ is the disintegration constant (yr^{-1})

$$\lambda = \frac{0.693}{t_{\frac{1}{2}}} \quad \text{.... III.2.}$$

where $t_{\frac{1}{2}}$ = half life of ^{14}C (5730 years).

A great deal of work has been done in order to find out to what extent these assumptions are realistic. In view of the expansion of the routine dating range to approximately 75,000 years one has to check carefully on the validity of the assumptions(1) and (3). A brief review of these studies is given below.

Measurement of wood samples whose age had been independently determined by tree ring counting and of organic material associated with annual layers of varves (Stuiver, 1970; Yang and Fairhall, 1972) showed that both short and long term variations of the initial ^{14}C content did occur. It has been established that a slow decrease in ^{14}C concentration of about 10% occurred during the period 8000 B.P. to the present (Suess, 1970; Ferguson, 1970; Michael and Ralph, 1972; Damon et al, 1972).

This variation has been ascribed to the fluctuations in the cosmic ray flux penetrating the earth's atmosphere due to changes in the level of modulation of cosmic rays by solar wind or in the intensity of the earth's magnetic field. Evidence for the latter is strongly suggested from the observed correlation of ^{14}C variation with the intensity of earth's magnetic field during the Holocene (Bucha, 1970).

In view of the above, we have made the plausible assumption that ^{14}C production over the last 10^5 years did not change by more than 25%; correspondingly, the oldest samples will have uncertainties of $\pm$ 2000 years.

The closed system assumption (No. 3) has turned out to be only partially valid in the case of materials containing exclusively inorganic carbon. Organic materials, on the contrary, do not exchange carbon with the surroundings. They occur, however, mixed both with inorganic and organic matter of different ages, referred to as contaminants. In practice it is often possible to eliminate contamination and to develop criteria which can be used to decide that this has been accomplished.

With the above considerations in mind, one can calculate the age of a sample by measuring A in equation III.1 and substituting the values of A_o and λ. In practice, both A and A_o are measured where A_o refers to activity of an international

standard prepared in the same way and measured in the same counting system as A. This method avoids various possible complications so that the results of different laboratories are comparable. At the Fourth Radiocarbon Conference at Groningen (Godwin, 1959) the standard for modern activity of A.D. 1950 has been defined to be 95% of the ^{14}C activity of a certain batch of oxalic acid prepared by the U.S. National Bureau of Standard (NBS). This was subsequently specified to apply to counting gas prepared from the NBS oxalic acid, having $\delta^{13}C$ PDB = -19‰ (Flint and Deevey, 1961).

The unknown activity of a sample is usually measured in a gas proportional or liquid scintillation counter under the same standard conditions as the activity, A_o, of the standard sample. For long the internationally accepted value for the half-life of ^{14}C has been 5568 $\pm$ 30 years. According to some subsequent careful measurements, however, the value of 5730 $\pm$ 40 years seemed to be a better working value (Godwin, 1962). As can be seen from the relation (III.1), the calculated age is directly proportional to the value of $t_{\frac{1}{2}}$ used. Therefore the percentage systematic error in a date arising from the use of an incorrect value of half-life is equal to the percentage error in the value of $t_{\frac{1}{2}}$.

The use of a more current value of the ^{14}C half-life, $t_{\frac{1}{2}}$ = 5730 years, instead of the conventional value of 5568 years, would lead to an expansion of the complete time scale by a

constant factor (1.03). In both the cases the relative position of measured samples on the ^{14}C time scale remains unaffected.

III.2.B. Techniques

In this section we will discuss the methods adopted for the preparation of the samples, the counting of ^{14}C activity and the derivation of age from the measured activities.

III.2.B.1. Chemical procedure

The first step is to convert organic carbon and carbonate to carbondioxide in a glass vacuum system (Fig. III.1). Carbonate samples were treated with A.R. grade concentrated phosphoric acid in an evacuated flask. Evolved carbondioxide was then passed through a moisture retaining trap (carbon tetrachloride plus trichloroethylene taken in equal volume and slush was made with liquid nitrogen to get -80°C) and a silica-gel-cum-activated charcoal tube and collected in traps cooled by liquid nitrogen. In the case of organic carbon the sample was burned by heating it in a stream of oxygen. The gases evolved were passed through heated CuO (at 800°C), a moisture trap, acidified $KMnO_4$, heated AgO (at 350°C), and finally through two moisture collecting traps cooled at -80°C. The purified carbondioxide, free from H_2S, NO_2, N_2O_5, etc. was collected in traps at liquid nitrogen

Fig. III.1. Combustion train for preparing CO_2 for radiocarbon dating. Sample is burnt in a quartz tube which is heated by burners and heaters (F1 and F2) and CO_2 thus evolved is passed through a heated CuO tube; acidified $KMnO_4$ (T_2, T_3) and through heated AgO (F_3). The purified CO_2 is finally collected in traps T_5 to T_7 at -195°C.

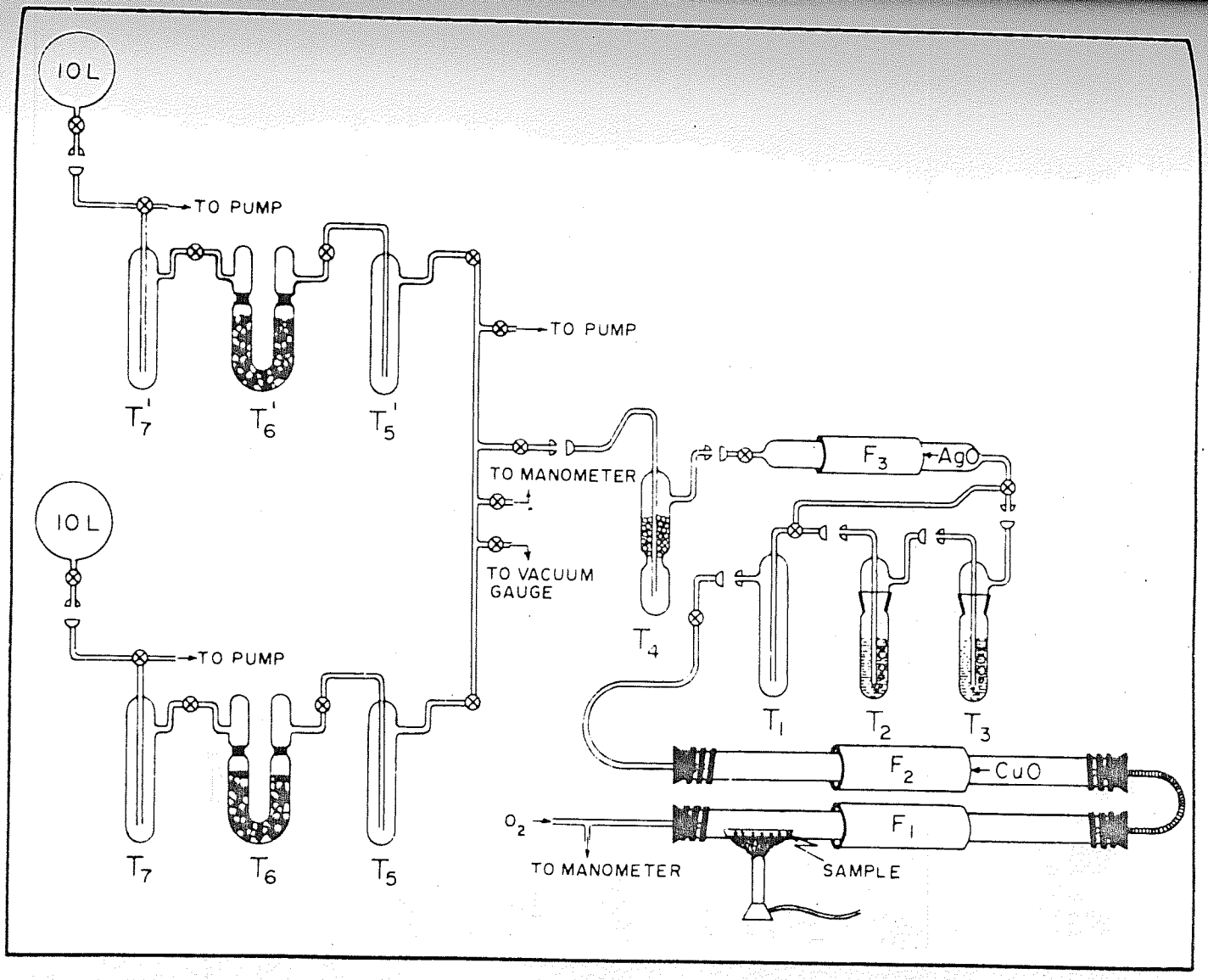
10 L
TO PUMP
T_7'
T_6'
T_5'
TO PUMP
TO MANOMETER
TO VACUUM GAUGE
10 L
TO PUMP
T_7
T_6
T_5
T_4
F_3
AgO
T_1
T_2
T_3
F_2
CuO
F_1
O_2
TO MANOMETER
SAMPLE

temperature. Unutilised oxygen was pumped away (Fig. III.1).

In the next step the prepared CO_2 gas was converted to methane (Fig. III.2, 3) for counting in a proportional counter. This method contrasts with the practice adopted by some other laboratories where CO_2 gas itself is counted. The advantages in using the method of methane counting are: (i) rapid synthesis; (ii) preparation of radon free gas; (iii) the non-explosive nature of methane. In addition, methane behaves as a good counting gas even with a purity level of 99% in contrast to CO_2 which requires still higher purity.

Methane was synthesised from the carbondioxide gas produced from the sample carbon in a reaction vessel according to the following reaction:

$$CO_2 + 4H_2 \longrightarrow CH_4 + 2H_2O \quad \ldots\ldots \text{III.3.}$$

The reaction was successfully used for the first time by Fairhall et al (1961) for radiocarbon measurement. For using this method, the hydrogen gas should be free of any ^3H activity and was obtained from Messrs Griesheim GMBH, Dusseldorf, and Indian Oxygen Ltd., Calcutta. The reaction vessel designed by us has a volume of 26 litres, and is made of hemispherical stainless steel vessels with flanges on their rims. At the bottom is a stainless steel finger (Fig. III.3). The stainless steel finger is covered with an external heater connected to an automatic

Fig. III.2. Methane purification system for radiocarbon samples. Traps N, O and P are cooled to about -80°C and Q, R and S are cooled to -195°C. The mixture of gases enter the system at N are finally pure CH_4 is collected in a 10 L. flask. N, O and P retain all moisture and Q and R any traces of unconverted CO_2. Pure methane distills over to S and hydrogen is pumped off.

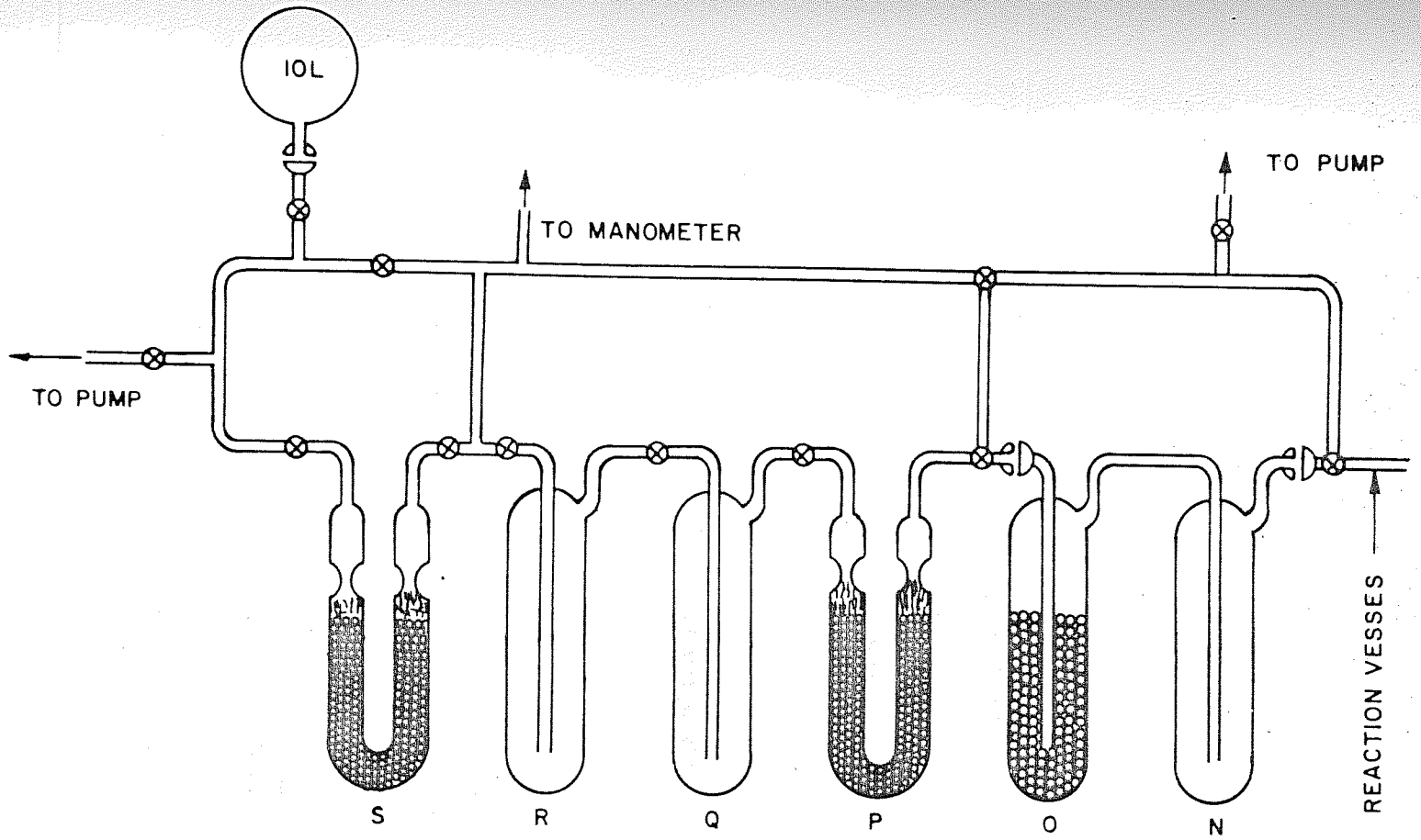
10L
TO MANOMETER
TO PUMP
TO PUMP
REACTION VESSES
S
R
Q
P
O
N

Fig. III.3. Reaction vessel to reduce carbondioxide to methane. The lower thimble contains the catalyst (X) and is heated to about 500°C. Total CO_2 is converted to methane in about 4 to 5 hours. The reaction vessel is cooled by a water tank (W) or by a fan on the top.

C – COOLING COILS

F – FLANGES

G – TEFLON O-RING

P PRESSURE GAUGE

W WATER JACKET

S – SILVER TUBE

H – HOLES

X – CATALYST PELLETS

R – FURNACE

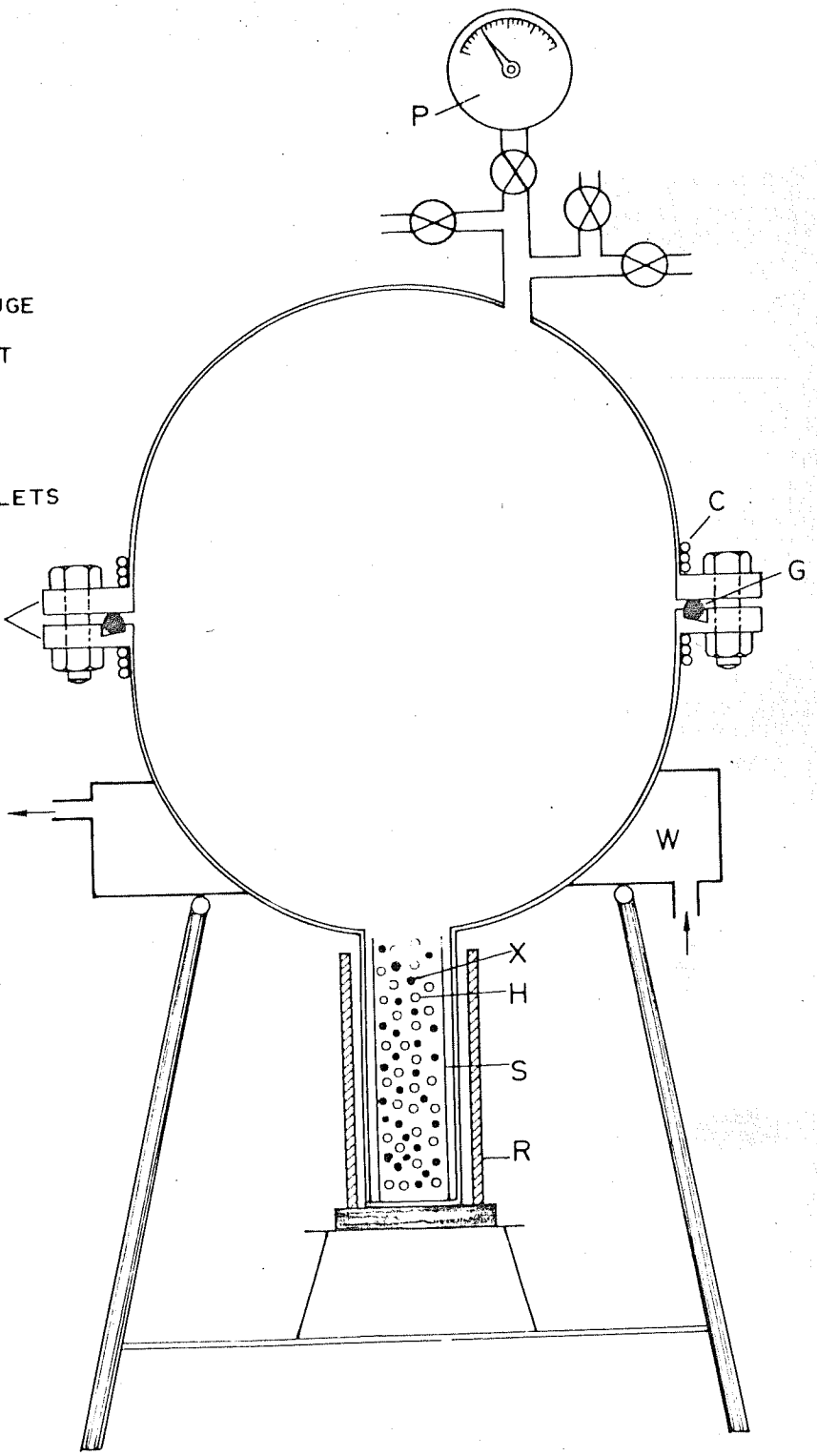

switch and pyrometer to maintain the temperature at ~ 500°C. The catalyst used is 0.5% Ru on Al_2O_3 pellets and is housed in the finger (thimble). The two reactor parts are closed with a teflon O-ring, placed in the groove on the flanges. For synthesis, CO_2 and H_2, corresponding to 20% excess over the stoichiometric requirement, were let into the reactor and the catalyst thimble heated to 500°C. The reaction took about four to five hours to complete.

After completion of the reaction, CH_4 was separated from H_2O, excess of unconverted H_2 and also from CO_2 (in case the reaction was not complete). The reaction products were let through three dry-ice cooled traps to remove all traces of H_2O and subsequently through two liquid nitrogen cooled traps to remove CO_2, if any. In liquid nitrogen cooled traps, CH_4 was also partly trapped with 1.5 cm Hg pressure. Finally all CH_4 was distilled in liquid nitrogen cooled silica-gel (12-28 mesh) kept in a U-tube trap. The reactor was emptied and hydrogen was removed, by gentle pumping for 20 to 30 minutes with rotary pump, on the leading end of S (Fig. III.2). No methane was lost from S provided the quantity of silica-gel exceeds 7 g per litre of CH_4. All CH_4 got distilled in silica-gel trap within an hour or so, with pumping on the outlet end of S, alternating at every 15 minutes with the help of a liquid nitrogen cooled activated charcoal trap. The methane so purified was then

expanded into flasks. The analysis by gas chromotography of a purified CH_4 sample showed $<$0.2% of hydrogen and 0.1% of carbondioxide. The above procedure enabled complete synthesis of even large samples. This trouble-free high efficiency synthesis rests on the fact that we use hydrogen in excess of stoichiometric requirements. The excess of 20% used is an optimum amount corresponding to conversion yields close to 100%. But the reaction results in incomplete synthesis with yields of 95%, if 30% excess H_2 is used. In such cases, purification of CH_4 from excess H_2 becomes quite problematic.

Before filling the methane gas in the counter a further purification of the sample gas was carried out. Methane was first trapped in a liquid-nitrogen-cooled charcoal-silica-gel (in the ratio of 1:5 by volume) U tube trap and then allowed to distil to a liquid air cooled trap by warming up the charcoal-silica-gel trap to room temperature. This methane trap was pumped for 10-15 seconds to remove any residual hydrogen.

III.2.B.2. Assaying techniques

The upper limit of dating by the normal radiocarbon method depends on the sensitivity of the techniques used for the measurement of the ^{14}C activity of the sample. With most of the sensitive techniques available at present one can measure ^{14}C concentration upto a factor of 150 smaller compared to that of modern carbon,

corresponding to an age of ~40,000 years i.e. 7 half-lives of ^{14}C. In older samples, it becomes necessary to make an enrichment of ^{14}C in the sample and this pushes back the limit of the ^{14}C method to c.70,000 years (Haring et al, 1958; Vogel and Zagwijin, 1967).

The recently developed direct counting technique for radiocarbon atoms has extended the range of radiocarbon dating upto 100,000 years. Here one measures the relative number of ^{14}C atoms in a sample. Recently, data obtained by the normal counting method and by the electrostatic accelerators have been compared. The dates determined by the two methods are concordant with each other (Bennett et al, 1978).

Although a number of methods are available for the measurement of residual radiocarbon activity in a given sample, in the present work the methane gas proportional counting method (Fairhall et al, 1961; Agrawal et al, 1965) has been used. Two counters were used for this purpose. The counters and associated electronics were sensitive and stable enough to measure activities corresponding to (30-35) x 10^3 years.

^{14}C measurement was done in a low background gas proportional counting system shown in Fig. III.4. The vital components of the system are counter, shield, cathode follower, a three channel analyser, high voltage power supply and auxiliary power supply.

Fig. III.4. A schematic diagram of the "housing" of the Houterman's-Oschger counter and the electronics selection and recording system.

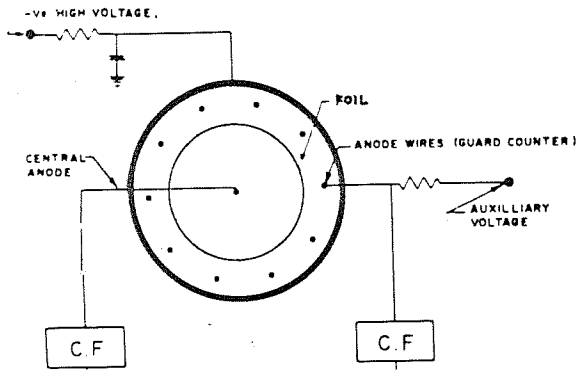

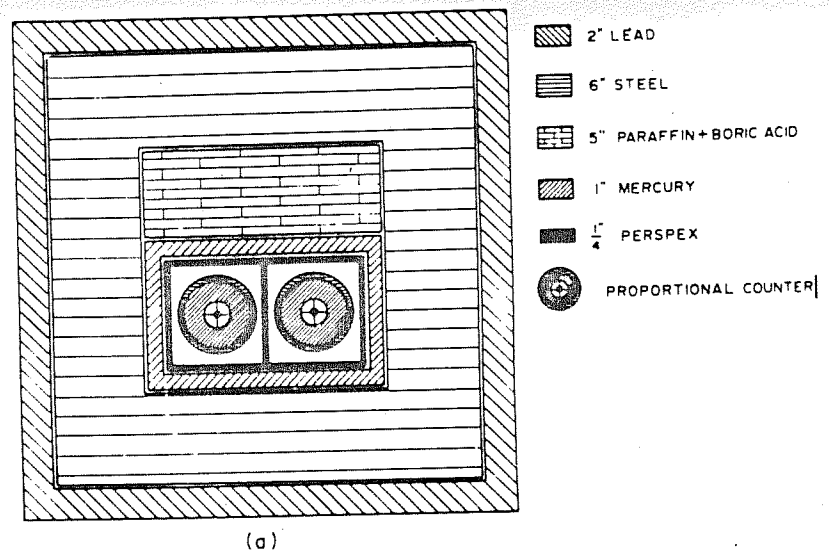

(a)

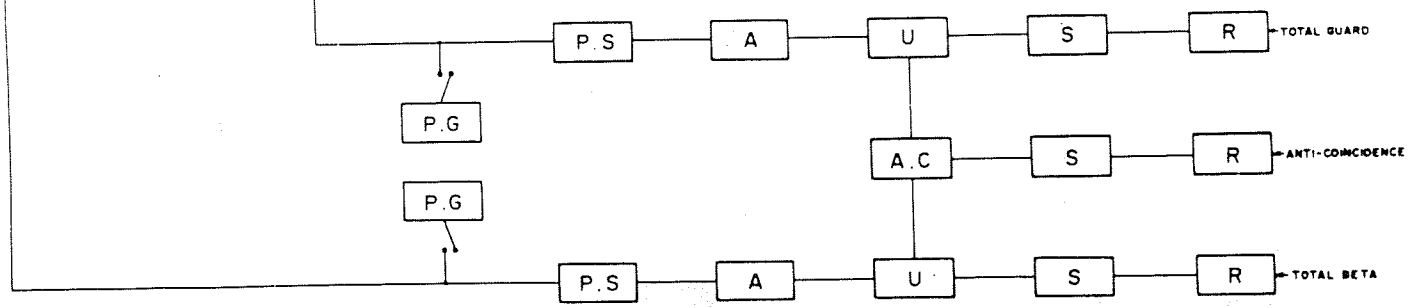

C F – CATHODE FOLLOWER
P S – PULSE SELECTOR
A – AMPLIFIER
P G – PULSE GENERATOR

U – UNIVIBRATOR
A C – ANTICOINCIDENCE LOGIC
S – SCALER, R – REGISTER

The counter is a low background Houtermans-Oeschger type gas proportional counter (Houtermans and Oeschger, 1958; Agrawal et al, 1965) having a total volume of 2.7 litres. The counter is composed of two sensitive volumes which are filled with the same gas but function independently. A cylindrical volume of 1.5 litres is surrounded by an annular zone having a volume of 1.2 litres (Fig. III.4). The two zones are separated by a thin gold plated mylar film of thickness 6 mg. cm^{-2}. Since the maximum energy of the ^{14}C beta radiation is only 156 KeV, corresponding to a half-thickness less than a few mg. cm^{-2}, most of the electrons emanating in either of the zones cannot penetrate to the other zone. However, higher energy-charged particles of an external origin will often penetrate this thin wall, and give rise to pulses in both the counters. Thus a pulse which is produced in the central counting volume and does not occur simultaneously with a pulse in the surrounding envelope, is mostly due to the beta radiation emitted by the radiocarbon sample. Because of this construction, the counter is specially suited for measuring the weak radiation of ^{14}C with a high sensitivity.

A schematic diagram of the metal shielding and the electronics system is shown in Fig. III.4. The counter is successively surrounded by mercury, steel and lead as shown. Such a shielding is commonly adopted in low level counting to cut off the extraneous radiation. The system for the selection of pulses is

shown in Fig. III.4; channels (i) and (iii) register total counts in the central volume and the outer volume of the counter respectively. Channel (ii) registers only counts in the central volume which appear in anti-coincidence with those arising in the outer volume. The difference in the counting rates between the channels (i) and (ii) is a measure of the counts due to the penetrating component of the cosmic radiation (mostly mesons) and charged particles produced in the counter body from any incidental extraneous radiation. This selection system thus results in a large decrease in the background counting rate of the system, due to the elimination of the penetrating component of the cosmic radiation and also of charged particles materializing in the counter wall, without any appreciable loss in the counting efficiency for the radiocarbon radiation emitted in the central volume. A voltage-regulated tube supply was used to provide the required high tension to the counter. Completely transistorised electronics units were used. The units displayed high stability and freedom from pick-up of stray radio-frequency signals.

The counter was always filled with CH_4 to a pressure of 900 mm of Hg, or of 400 mm of Hg in case of a small sample. The counter characteristics were studied without any external source. The operating potentials were fixed from a study of the counting rates with modern and dead carbon samples. Pulses greater than 7 and 12 millivolts coming from the guard and centre counter respectively

were selected.

A number of steps were taken to ensure a high standard of performance. Before measuring the ^{14}C activity of sample, the voltage and sensitivities of electronics were checked by voltmeter and a pulser. Dead and standard (NBS oxalic acid) carbon samples were counted on either side of a set of six or seven samples for which dates were required.

Table III.1 gives the details of the counters used.

III.2.B.3. Calculation of radiocarbon ages

The radiocarbon age (T) of a sample was calculated using the relation:

$$T = \frac{\tau_{\frac{1}{2}}}{\ln 2} \ln \frac{O_n \times 0.95}{S_n} \quad \ldots\ldots \text{III.4.}$$

where O_n and S_n are the net counting rates of the standard NBS oxalic acid and the sample respectively. The relation is, of course, based on:

$$A_T = A_o \exp. \left(\frac{T \times \ln 2}{\tau_{\frac{1}{2}}}\right) \quad \ldots\ldots \text{III.5.}$$

where A_o is the original activity at time T = 0 and A_T is the activity present in the sample having age T. Taking the activity of modern carbon, as internationally accepted at the Groningen Conference (Godwin, 1959), equal to 95% of the net oxalic acid activity A_o is equal to 0.95 O_n/E, where E is the counting efficiency.

Table III.1. Counter details

Particulars	Units	Counter II	Counter III
Material		Stainless steel perspex/ gold mylar	Stainless steel/ perspex/ gold mylar
Sample counter of gold mylar diameter	mm	76	76
Thickness of gold mylar	mg/cm^2	6	6
Beta anode diameter	/um	15	15
G anode diameter	/um	30	30
Anode unshielded length	mm	380	380
Sample beta counter volume	ltr	1.5	1.5
Guard counter volume	ltr	1.2	1.2
Filling pressure at 24.5°C	mm of Hg	400	900
Check voltage	KV	2.794	4.580
Operating voltage	KV	2.916	4.940
Background counting rate=B	cpm	0.9 ± 0.15	1.6 ± 0.15
Net standard counting rate=A_o	cpm	5.3 ± 0.2	11.35 ± 0.2
Figure of merit A_o/B		5.59	8.97
Range in a 40 hrs. counting period in	years	> 31,000	> 35,000

Since A_T is given by S_n/E one gets the age equation III.4 from III.5 where the efficiency E cancels out and need not be known.

Though the counting set-up was operated in an airconditioned room, temperature fluctuations of 1 to 3% occurred. The age calculated using relation (III.4) was corrected for the effects of filling unequal amount of gas in the counter due to the variation in the temperature by an amount:

$$\frac{T\ (t_o - t_s)}{Ln2\ (273+t_s)} \qquad \text{.... III.6.}$$

where t_o and t_s are the filling temperatures for oxalic acid standard and sample respectively.

The error (one standard deviation), T, on a date was calculated using the equation:

$$T = \frac{\tau_{\frac{1}{2}}}{\ln 2}\left[\frac{S_n + 2B}{S_n^2.t} + \frac{O_n + 2B}{O_n^2.t} + 2f^2 + 2c^2 + \left(\frac{T \ln 2}{\tau_{\frac{1}{2}}}\frac{\Delta\tau_{\frac{1}{2}}}{\tau_{\frac{1}{2}}}\right)^2\right]^{\frac{1}{2}} \qquad \text{.... III.7.}$$

This relation takes into account the errors due to counting statistics, fractionation effects in the preparation of CH_4 (f = fractional error in $^{14}C/^{12}C$ ratio arising from fractionation effects), instability of the counting system (c = fractional error arising due to drifts in the electronic system), and

an uncertainty in the value of the radiocarbon half-life (5568 ± 30). B denotes the background counting rate; t is the duration of counting, which is the same for background, oxalic acid standard and the sample to be dated. In the present method we do not expect any isotopic fractionation due to almost total conversion of CO_2 into CH_4 gas, and so the fractionation factor f was taken to be equal to zero.

The value of c has been inferred to be 0.5×10^{-2} from the observed reproducibility of the counting rates of the NBS oxalic acid. The long term variation observed from the oxalic acid standard counting rates is within the expected statistical limits. The error in the dates arising from this variation are probably well covered in the assumed value of c = ± 0.05 for the instability in the electronics.

III.2.C. Dating material and sample collection

We have used the radiocarbon dating method to obtain ages of the palaeosols within the loessic formation. Both soil-organic matter and carbonate fractions of the palaeosols have been dated. Dating these soils will help to place the climatic and environmental events associated with their formation.

Total soil organic matter was dated which can give average ages.

As mentioned in Chapter II, one comes across palaeosols within the thick loessic deposits both on the Himalayan and the Pir Panjal flanks from where samples were collected. The sample sites of the Himalayan side, are Burzahom, Garhi, Olchibagh and Saki Paparian and of the Pir Panjal flank, Puthkhah, Pakharpur and Tsrar Sharif (Fig. II.1).

We have labelled the palaeosols alphabetically for each site (Table III.2; Fig. II.5), following a stratigraphic sequence (top bottomwards) at each section. At this stage it is not possible to stratigraphically correlate the palaeosols of different sites. It is therefore to be clearly noted that, for example, the Palaeosol A of Saki Paparian and Palaeosol A of Olchibagh have per se no implied stratigraphic correlation. One can only correlate them on the basis of ^{14}C dates.

At Burzahom one comes across three Palaeosols (A, B and C; Fig. II.5) within 5-6 m thick loessic deposit overlying the Upper Karewa and below the 5-6 m thick archaeological deposit. Garhi and Burzahom are very close to each other and therefore stratigraphically one expects Palaeosol C of Garhi to correspond to Palaeosol C of Burzahom. Because of steepness of the exposed section, we could only collect Palaeosol C from an accessible slope. At Garhi also one finds three Palaeosols (A, B and C), below the archaeological deposit, within 5-6 m thick deposit of the loess.

At Puthkhah also one finds archaeological debris above the loessic deposit. There were two palaeosols within it. Both Palaeosol A and B were above the Upper Karewa. At Olchibagh and Saki Paparian also one comes across Palaeosol A and B, within the loessic deposit, above the Upper Karewa.

Burzahom, Garhi, Olchibagh, Saki Paparian and Puthkhah are at an altitude of about 1600 m MSL.

At Pakharpura one comes across Palaeosol A and B within an 8 m thick loessic deposit. The loess overlies the gravel bed, the latter is above the Lower Karewa. At Tsrar Sharif also one finds Palaeosols A, B and C within a 6-8 m thick loessic deposit. A gravel bed intervenes between the loess and the Lower Karewa. Pakharpura and Tsrar Sharif both are at an altitude of 2000 m MSL.

From all the above mentioned sites, palaeosol samples were collected for ^{14}C dating.

III.2.D. Results and discussion

The ^{14}C dates on the loess and palaeosol samples are given in Table III.2.

The Burzahom ^{14}C dates are quite consistent in ascribing the (top) Palaeosol A to $\underline{c}$.18,000 $\pm$ 1000 B.P. and the Lower Palaeosols B and C are greater than 31,000 years B.P. As the organic fraction of the samples was small, they could not be counted in high pressure counters.

Table III.2. ^{14}C dates (on $T_{1/2}$=5568 years) of Palaeosols and Loess from different sites in the Kashmir valley

Site	PRL No.	Stratum	Date in B.P. on organic carbon	Date in B.P. on carbonate
Burzahom (Lat. 34° 10' N., Long. 74° 53' E., Alt. 1620 m AMSL)	593	Palaeosol A	18890 + 830 - 750	15700 + 370 - 360
	611	"	N.D.	20190 + 570 - 530
	591	"	N.D.	20340 + 1320 - 1130
	590	"	18460 + 820 - 740	17060 + 350 - 340
	594	"	N.D.	20430 + 920 - 820
	495	"	10320 + 170 - 160	N.D.
	500	Loess A	N.D.	26450 + 890 - 800
	585	Palaeosol B	> 31000	N.D.
	586	Palaeosol C	> 31000	N.D.
Garhi (Lat. 34° 10' N., Long. 74° 53' E., Alt. 1620 m AMSL	592	Palaeosol C	26340 + 2010 - 1610	N.D.

Table III.2 (continued)

Site	PRL No.	Stratum	Date in B.P. on organic carbon	Date in B.P. on carbonate
Olchibagh (Lat. 33° 57' 30" N., Long. 74° 56' E., Alt. 1600 m AMSL)	597	Palaeosol A	N.D.	24960 + 1780 - 1460
	598	Palaeosol B	12560 + 450 - 430	21200 + 630 - 580
Saki Paparian (Lat. 33° 49' N., Long. 75° 7' E., Alt. 1600 m AMSL)	595	Palaeosol A	N.D.	33230 + 2500 - 1900
	596	Palaeosol B	> 31000	> 31000
Puthkhah (Lat. 34° 14' N., Long. 74° 28' E., Alt. 1600 m AMSL)	618	Palaeosol A	18550 + 600 - 550	> 31000
	617	Palaeosol B	25800 + 1100 - 960	28560 + 1560 - 1300
Pakharpur (Lat. 33° 48' N., Long. 74° 47' E., Alt. 2000 m AMSL)	627	Palaeosol A	27630 + 1350 - 1160	N.D.
Tsrar Sharif (Lat. 33° 50' 30" N., Long. 74° 46' E., Alt. 2000 m AMSL)	624	Palaeosol A	> 35000	N.D.
	625	Palaeosol B	> 35000	N.D.
	626	Palaeosol C	> 35000	N.D.

1. N.D. means not determined because of the absence of organic matter or carbonate.

We expected Palaeosol C of Garhi to correspond to Palaeosol C of Burzahom, but the former gave only an age of c.26,000, which was younger than expected. As mentioned before, Palaeosol C was collected with some difficulty from an accessible slope but it appears that humic contamination from the decayed grass of the slope surface made Palaeosol C date younger. Both at Burzahom and Garhi there was a Neolithic deposit on the top dated to c.4500-3500 B.P. (Agrawal and Kusumgar, 1974).

At Puthkhah Palaeosol A dated to c.18,000 B.P. (organic fraction) and Palaeosol B to c.26,000 B.P. (organic fraction). The dates are in conformity with those of Burzahom Palaeosol A, but Puthkhah Palaeosol B seems to be younger than Burzahom B. The Olchibagh dates are a bit anamolous. Palaeosol A did not yield any datable organic matter. Palaeosol B is anamolously younger than Palaeosol A. As Palaeosol B sample did not belong to the same section from which Palaeosol A derived, and also as Palaeosol B did not have any significant loess cover, an admixture with younger debris fallen from the adjacent section cannot be ruled out.

At Saki Paparian the dates are more consistent and both Palaeosols A and B are greater than 31,000 years B.P. and therefore probably correspond with Palaeosols B and C of Burzahom (Fig. II.5) and Palaeosol B is greater than 35,000 years. Pakharpura Palaeosol A is c.28,000 years B.P. while at Tsrar Sharif all the

palaeosols (A, B and C) are greater than 35,000 years B.P.

Discussion: The significance of these dates is threefold. Firstly, we could compare dates based on both organic and inorganic fractions of the palaeosols. The radiocarbon ages of pedogenic carbonates are of course difficult to interpret because of an unknown initial $^{14}C/^{12}C$ ratio in the carbonate and possibility of subsequent contamination with environmental ^{14}C. Except for PRL-598 and 618 (Table III.2), all other dates on both organic and inorganic fractions showed good concordance. Probably this can be taken as an indication that most of the carbonate samples were not subjected to any significant post-depositional chemical exchange and represent the date of formation of the relevant soil.

Secondly, in the geomorphological context of the valley the dates fall in a distinct pattern. The ^{14}C dates from the sites (Burzahom, Garhi, Saki Paparian, Puthkhah) falling in the area of the shrunken Nagum lake (Upper Karewa) do have a distinct top palaeosol, datable to $\leq$.18,000 $\pm$ 1000 B.P., which probably represents the onset of the last deglaciation. We get uncontaminated samples of Palaeosol A mostly where they are preserved under archaeological debris. Exposed palaeosols would be subject to the subsequent soil forming processes as the climatic conditions since the last deglaciation have not changed much. Though the

radiocarbon date, PRL-598, 596 and 617 are on the carbonate fraction of Palaeosol B, yet they appear younger than the dates PRL-597, 595 and 618 on the carbonate fraction of Palaeosol A at Olchibagh, Saki Paparian and Puthkhah. As stratigraphically Palaeosol A overlies Palaeosol B, the anomaly in radiocarbon dates probably indicates introduction of younger carbon.

But the palaeosol dates from the Pir Panjal side suggest that either we have not been able to identify the top palaeosol corresponding to Palaeosol A of Burzahom etc. or that it has eroded away from the sampled sites or else the right locations could not be sampled. Both the Palaeosols A of Pakharpur and Tsarar-Sharif give dates greater than 35,000 B.P. Since loess is deposited by aeolian agencies, the absence of its top in the uplifted portions of the Lower Karewa is enigmatic. One explanation could perhaps be that the wind activity in a confined valley could not lift its silt load beyond a height of 1600 m and therefore the portions of the exposed sediments which were tectonically uplifted above 1600 m did not receive any loessic deposits.

Thirdly, it is clear now that the last deglaciation in the valley goes back to c.18,000 $\pm$ 1000 B.P. which is far beyond the traditional dates of the inception of the Holocene. It is interesting to note that the ^{14}C dated pollen profile from Toshmaidan indicated that the last deglaciation was already in progress at c.15,000 years B.P. at 3120 m altitude.

Deglaciation at an altitude of 1600 m should therefore be still earlier and therefore 18,000 ± 1000 B.P. date for it is consistent with the Toshmaidan evidence (Singh and Agrawal, 1976). Recent work shows that the onset of deglaciation has been globally pushed back, far beyond the Holocene (Mercer, 1972). The report of the Australian Academy of Science (AAS, 1976) says,

> It is established that the last major deglaciation was taking place between 18,000 and 9000 years ago in all investigated parts of the world.

Our evidence from the South Asian context therefore assumes great significance.

III.3. Uranium series dating

For dating the entire Pleistocene epoch no single technique is available as yet. With isotopic enrichment (Grootes, 1977), and accelerator (Muller, et al, 1978; Bennett et al, 1978) techniques one can now go back, at least theoretically, to 100,000 years with the radiocarbon. With isotopes belonging to the uranium series, one can go only as far back as 0.3 m.y. (thorium-230) and 1 m.y. (uranium-234). These methods are applicable for a variety of materials in which uranium is relatively enriched, e.g. carbonates (Ku, 1976; Krishnaswami and Lal, 1978). The application of these methods has contributed significantly towards obtaining chronologies of palaeo-events, in particular of the Late Pleistocene climatic fluctuations (Ku, 1976).

As some of our Late Pleistocene samples were carbonate rich, we have attempted dating them with the $^{230}Th/^{238}U$ and $^{234}U/^{238}U$ methods. Below we discuss the principles and the techniques of these methods.

III.3.A. Principles

Radioactive chronologies are generally based on either (a) the decay of a radioactive nuclide or (b) the build-up (in growth) of a daughter nuclide to attain secular equilibrium with its parent.

Case (a). When a technique is based on the decay of a nuclide with depth in a sediment profile, the basic requirements are: (i) the flux of the radionuclide to the sediment - water interface should remain constant; and (ii) no migration of the radionuclide should occur over the dating interval, i.e. the change in the concentration of the nuclide in the system should be only due to its radioactive decay. If these assumptions are valid, then the activity of the nuclide in the sediment at any depth, from the sediment water interface is given by:

$$A_{(z)} = A_o e^{-\lambda t} \qquad \ldots\ldots \text{III.8.}$$

where A_o is the activity of the nuclide (dpm/g) in a freshly deposited sediment at time t = o, i.e. at the sediment-water interface and its radioactive decay constant.

Case (b). When the chronology relies on the ingrowth of daughter from its parent, then the ratio of the daughter to parent activity at any time 't' is:

$$\frac{A_d}{A_p} = \frac{\lambda_d}{\lambda_d - \lambda_p}\left[1 - e^{(\lambda_p - \lambda_d)t}\right] \quad \ldots\ldots \text{III.9.}$$

where A is the activity, λ the decay constant and the subscripts d and p refer to daughter and parent nuclides respectively. In equation III.9 it is assumed that the activity of the daughter is $A_d = o$, at $t = o$, i.e. the time of formation of the deposit. If $A_d \neq o$ at time $t = 0$, then it is essential to have a precise knowledge of A_d/A_p at the time of formation. In this method also, the validity of the assumption of no-migration in system as required in Case (a) is necessary for both the parent and daughter nuclides. Below we discuss ^{230}Th (Ionium) and $^{234}U/^{238}U$ methods for dating of carbonate fractions of the lake deposits.

^{230}Th, a daughter nuclide of ^{238}U decay series, has been used to date marine corals (Barnes et al, 1956; Tatsumoto and Goldberg, 1958; Blanchard, 1963; Thurber et al, 1965; Veeh, 1966; Broecker and Van Donk, 1970). These carbonates, during their growth, incorporate in their skeleton, the uranium isotopes from the water column with very little ^{230}Th. Therefore, the time dependant growth of ^{230}Th to attain radioactive secular equilibrium, following synchronuous deposition of ^{234}U, can be

used to estimate the age of the sample, if the assumptions mentioned above hold good.

The expected $^{230}Th/^{238}U$ activity ratio in a sample having initial $^{234}U/^{238}U = 1$ and $^{230}Th = 0$ at the time of formation, is given by:

$$\frac{^{230}Th}{^{238}U} = (1-e^{-\lambda_o t}) \quad \text{.... III.10.}$$

In most of the natural water systems, however, the $^{234}U/^{238}U$ activity ratios are more than one due to preferential leaching of ^{234}U during weathering process. In such case the activity ratio would be:

$$\frac{^{230}Th}{^{238}U} = (1-e^{-\lambda_o t}) + (R-1)\frac{\lambda_o}{\lambda_o-\lambda_4}(1-e^{(\lambda_4-\lambda_o)t} \quad \text{.... III.11.}$$

where $R = \frac{^{234}U}{^{238}U}$ initial ratio

The assumptions given above have been shown to be valid for marine corals. Kaufman (1964) and Kaufman and Broecker (1965) have tried to extend the $^{230}Th/^{238}U$ dating technique to lacustrine carbonates using the same assumptions. Their results based on about 50 samples of gastrapods, chara, tufa and marl from lakes Lahontan and Bonneville indicate that in general ^{230}Th ages are in agreement with ^{14}C ages and for samples beyond the ^{14}C range, the ^{230}Th ages are consistent with stratigraphic information.

Unlike the marine corals, however, several of the lacustrine deposits seem to incorporate ^{230}Th in them during their growth, as evidenced by the presence of measurable ^{232}Th in them. Hence a correction for the initial ^{230}Th content would be necessary to get reliable age estimates of the lacustrine carbonates. Kaufman (1964) and Kaufman and Broecker (1965) overcame this problem by estimating the initial or non-radiogenic ^{230}Th content of the samples, using the relation:

$$^{230}Th\ (\text{initial}) = {}^{230}Th\ (\text{observed}) - {}^{230}Th\ (\text{expected}) \quad \ldots\ \text{III.12.}$$

where ^{230}Th (observed) is the measured ^{230}Th content of the sample and ^{230}Th (expected) is the calculated ^{230}Th abundance in samples of known ^{14}C age using recent samples ($<$ 20,000 years in age) they estimated that the initial $^{230}/^{232}Th$ ratio in the lakes Lahontan and Bonneville should be 1.7. This correction involves the assumption that the initial ^{230}Th was incorporated at the time of formation of the carbonate and not at a later date.

Inspite of the uncertainty in the non-radiogenic ^{230}Th correction, the $^{230}Th/^{238}U$ method has proved to be a very useful dating tool for lacustrine carbonate and salt deposit samples upto 300,000 years old where no other dating method is applicable (Broecker, 1965).

The discovery of anomalously high $^{234}U/^{238}U$ activity ratios in natural waters (Cherdyntsev and Chalov, 1955; Cherdynstev et al, 1961; Thurber, 1962, 1963) opened the possibility of using this radioactive disequilibrium between the two uranium isotopes as a dating tool for deposits forming from such waters.

The fractionation or disequilibrium between these uranium isotopes has been attributed to recoil effects during the transformation of ^{238}U to ^{234}U involving alpha and beta particle emission. The recoil energy imparted to the daughter nucleus seem to be large enough to occasionally rupture chemical bonds thereby releasing the ^{234}U atom or leaving it in a metastable lattice position (Starike et al, 1958; Cherdyntsev et al, 1961) or to oxidise it to +6 valence state (Rosholt et al, 1963; Dooly et al, 1966). Because of these effects ^{234}U is more susceptible to leaching compared to ^{238}U from rocks/soil resulting in an excess ^{234}U in natural waters. The extent of $^{234}U/^{238}U$ disequilibrium in the waters seems to depend both on the type of soil/rock being weathered and the chemical composition of water (Thurber, 1963; Bhatt and Krishnaswami, 1969). In addition, a certain fraction of ^{234}U can be formed in the water because of the preferential dissolution of alpha recoil ^{234}U (Kigoshi, 1971).

Any precipitate forming from these waters would have a $^{234}U/^{238}U$ activity ratio same as in water. This excess ^{234}U can

be used as a measure of the age of the system, if (i) the $^{234}U/^{238}U$ ratio at the time of its formation is known and if (ii) the system has remained 'closed' over the dating interval. If these assumptions hold, then the age activity ratio relation is given by:

$$\left[\left(\frac{A^{234}}{A^{238}}\right)_t - 1\right] = \left[\left(\frac{A^{234}}{A^{238}}\right)_o - 1\right] e^{-\lambda_4 t} \quad \ldots\ldots \text{III.13.}$$

where A^{234}/A^{238} is the $^{234}U/^{238}U$ activity ratio, λ_4 is the decay constant of ^{234}U and subscripts t and o refer to time t and zero respectively.

Thurber (1963) and Kaufman (1964) have explored the possibility of using this method to date lacustrine carbonate from fluvial lakes. In these samples, the major problem is to ascertain the $^{234}U/^{238}U$ activity ratios at the time of the carbonate deposition. Based on the analyses of several samples, Kaufman (1964) observed that the $^{234}U/^{238}U$ activity ratios in old samples were too high to be consistent with the assumption that these samples formed with the same $^{234}U/^{238}U$ activity ratio as those observed in recent samples, $\leq$20,000 years age. This variation could be attributed to changes in the $^{234}U/^{238}U$ ratio of lake water, caused by climatic variations, or because the lacustrine carbonates are "open" systems and the present day measured activity ratio are due to secondary effects caused

by groundwater interactions with the carbonates. Because of these uncertainties, the $^{234}U/^{238}U$ dating method has met only with limited success for dating lacustrine carbonates.

III.3.B. Techniques

III.3.B.1. Extraction and radiochemical purification

Several radiochemical procedures for the separation and purification of uranium and thorium exist in literature, compilation of which have been made by Hyde (1960) and Grindler (1962). These procedures have of late been modified and additional steps developed by Amin (1970) and Krishnaswmi and Sarin (1976). In the present work we have followed these improved techniques described briefly for the sake of completeness.

The adopted procedure is summarised in a flow chart (Fig. III.5). The samples were the carbonate phase of the sediments.

All samples were dried at 110°C and finely ground. About 40-60 g of well-mixed material was taken in a beaker with 0.5 M HCl to dissolve the carbonate fraction. The solution was filtered and the residue was rejected. Known activities of ^{234}Th and ^{232}U (1300 counts per minute of ^{234}Th and 8.79 counts per minute of ^{232}U) were added as tracers to the solution. A precipitation

Fig. III.5. Flow chart for extraction of uranium and thorium.

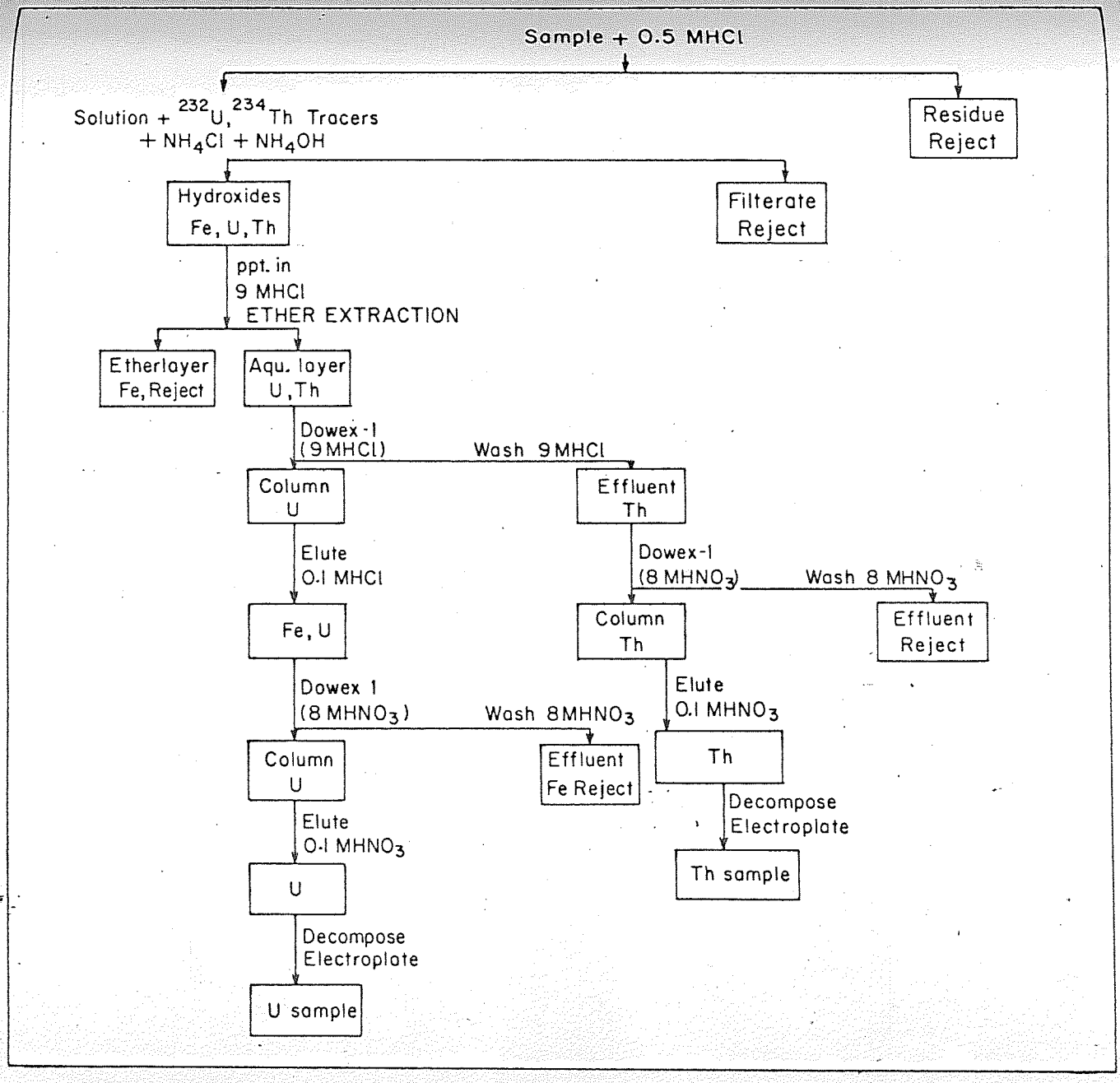
Sample + 0.5 MHCl
Solution + ^{232}U, ^{234}Th Tracers + NH_4Cl + NH_4OH
Residue Reject
Hydroxides Fe, U, Th
Filterate Reject
ppt. in 9 MHCl
ETHER EXTRACTION
Etherlayer Fe, Reject
Aqu. layer U, Th
Dowex-1 (9MHCl)
Wash 9MHCl
Column U
Effluent Th
Elute 0.1 MHCl
Dowex-1 (8 $MHNO_3$)
Wash 8 $MHNO_3$
Fe, U
Column Th
Effluent Reject
Dowex 1 (8 $MHNO_3$)
Wash 8$MHNO_3$
Elute 0.1 $MHNO_3$
Column U
Effluent Fe Reject
Th
Elute 0.1 $MHNO_3$
Decompose Electroplate
Th sample
U
Decompose Electroplate
U sample

of group IIIA was done to scavange uranium and thorium. The iron was removed next by ether extraction. Subsequently, uranium and thorium were separated by ion-exchange methods as shown in Fig. III.5.

The organic matter in the elutes containing uranium and thorium was destroyed by treating with HNO_3. At this stage there should be no visible residue in the beaker. A few drops of 12M HCl were added to the beaker and evaporated to almost dryness. Thorium or uranium was taken up in a mixture of 1 ml of 0.01 M HNO_3, 2 ml of 2 M NH_4Cl (pH-2) and 2 ml of saturated solution of ammonium oxalate (Amin, 1970; Krishnaswami and Sarin, 1976). The solution was transferred to a teflon plating cell and thorium or uranium was plated on a 2.5 cm diameter, 0.025 mm thick platinum disc (the plated area of the disc was 2 cm^2).

Both uranium and thorium were plated at a starting current of 1.0 A. The current increased initially to about 1.4-1.5 A and then decreased to 0.7 A in 30-40 minutes. When the current reached about 0.5 A few drops of ammonia were added to the bath and the anode was removed, washed with water, dried in a flame and counted.

III.3.B.2. Assay of uranium and thorium isotopes

The alpha activities of uranium and thorium isotopes were determined using surface barrier detectors. The beta activity of ^{234}Th tracer was assayed using an end-window G-M counter as described by Amin (1970). The alpha spectrometer assembly consisted of: (i) n-type surface barrier detector (supplied by ORTEC); (ii) one set of charge sensitive low noise preamplifier, main amplifier and post-amplifier (supplied by ECIL); and (iii) a 256 channel nuclear data (ND110) pulse height analyser.

The detector had an active area of 450 mm^2 with a depletion layer of 100 micron and was mounted inside a vacuum chamber which was continuously evacuated by a rotary pump. A trap cooled by liquid nitrogen was provided in between to absorb the condensible gases. A positive bias of 80 volt was applied to the detector. The resolution of the detector (FWHM) at 4.19 MeV (^{238}U) alpha energy was 127 KeV (3%). The counting efficiency of the detector and the stability of the alpha spectrometer was periodically checked by counting the standard NBL (National Brownswick Laboratory) sample. The counting efficiency for detecting alphas in the energy range of 3.6 to 6.9 MeV, which fully covers the energy range of alphas, was determined to be 23 $\pm$ 1%. The background was negligible being less than 20 counts in 2 days. The system displayed high stability over months of counting. Samples were

counted for a period of about 48 hours and statistical errors of ± 1% on the measurements of ^{238}U, ^{234}U and less than 2% for ^{232}Th, ^{230}Th isotopes could be obtained.

Generally a 20 channel envelope (covering a total energy range of 300 eV) was selected to compute the number of counts under each isotope peak. No corrections for blank and background were made since the sum effect of these contributions did not amount to >0.1% of the total counts occurring in individual envelopes.

From the spectral peak area, the absolute disintegration rate D(dpm) for each isotope (^{238}U, ^{234}U, ^{232}Th, ^{230}Th) was calculated using the formula:

$$D = \frac{C_o \times 100}{E_c} \qquad \text{.... III.14.}$$

where C_o was the count rate per minute, E_c was the counting efficiency in percentage.

The chemical efficiency in the case of thorium samples was determined by counting the high energy beta of ^{234}Pa (E_{max} = 2.31 MeV), a short lived daughter of ^{234}Th. The beta activity of ^{234}Th tracer was analysed using an end-window, gas flow (98.7% helium and 1.3% butane mixture gas type) G-M counter. It had a gold mylar window of 6 mg/cm^2 to absorb both alpha particles as well as the low energy beta of ^{234}Th (E_{max} = 0.19 MeV).

The tracer ^{232}U was calibrated by depositing a known solution of the tracer and counting on the alpha spectrometer.

The growth of ^{230}Th towards the radioactive equilibrium with parent ^{238}U in a carbonate sample (assumed to be a closed system) is given by the relation (Broecker, 1963). From equation III.11, one can calculate the age.

The re-establishment of radioactive equilibrium between ^{238}U and ^{234}U in a closed system is given by the relationship (Cherdynastsev et al, 1963), equation III.13.

The uranium series age can be calculated by the following two methods, (i) based on the measured $^{230}Th/^{238}U$ ratio and $^{234}U/^{238}U$ by using equation III.11 and III.13 respectively.

III.3.C. Sample collection

For dating the Upper Karewa formation, two sites were sampled. Carbonate samples were collected from Burzahom and Hatwari from below the loess on the Himalayan side. The samples were collected at 5 to 10 m intervals.

III.3.D. Results and discussion

The results for uranium and thorium isotope measurements are presented in Table III.3.

Table III.3. Concentrations of uranium and thorium isotopes in the Burzahom and Hatwari carbonate samples

S. No.	% of carbonate	^{230}Th dpm/g	^{232}Th dpm/g	$^{230}Th/^{232}Th$	^{238}U dpm/g	$^{230}Th/^{238}U$	$^{234}U/^{238}U$
BRZ/79/4	52.12	0.235 ± 0.004	0.216 ± 0.004	1.088 ± 0.02	0.438 ± 0.002	0.536 ± 0.007	1.072 ± 0.01
BRZ/79/2 20 m.b.s.	47.03	0.134 ± 0.003	0.164 ± 0.003	0.814 ± 0.02	0.254 ± 0.002	0.524 ± 0.008	1.154 ± 0.01
BRZ/79/3 30 m.b.s.	65.75	0.472 ± 0.007	0.417 ± 0.007	1.13 ± 0.02	0.556 ± 0.002	0.944 ± 0.014	1.072 ± 0.15
HTW/79/1 10 m.b.s.	6.14	0.309 ± 0.006	0.491 ± 0.007	0.629 ± 0.01	0.592 ± 0.002	0.522 ± 0.009	1.095 ± 0.01
HTW/79/2 20 m.b.s.	12.08	0.163 ± 0.005	0.201 ± 0.006	0.811 ± 0.02	0.235 ± 0.002	0.693 ± 0.009	1.20 ± 0.01
HTW/79/3 30 m.b.s.	12.60	0.246 ± 0.007	0.396 ± 0.01	0.621 ± 0.01	0.159 ± 0.002	0.772 ± 0.019	1.175 ± 0.01

m.b.s. = meter below surface

The Burzahom samples have carbonate content of about 50 to 60% while the samples from Hatwari contain about 6 to 12% only.

^{238}U concentration is of the order of 0.1 to 0.6 dpm/g which is too little for dating the carbonate fraction.

^{230}Th concentrations do not show any systematic decrease with respect to depth.

The ratio of $^{230}Th/^{232}Th$ is only 1.008 for the sample BRZ/79/4 and 1.13 for BRZ/79/3. Other samples show ^{232}Th concentration more than ^{230}Th. Possibly 0.5 m HCl treatment dissolves clay fraction also.

There is no systematic variation of $^{234}U/^{238}U$ ratio with depth.

From the available data it appears that U-series dating method has not worked for dating the carbonate fractions of the Upper Karewa.

CHAPTER IV

IV. DEPOSITIONAL REMANENT MAGNETIZATION AND STRATIGRAPHY OF THE KAREWAS

IV.1. Introduction

IV.2. Principles of Palaeomagnetism

- IV.2.A. Origin of Palaeomagnetism
- IV.2.B. Reliability of the record of magnetization
- IV.2.C. A criterion for stability of NRM in the sedimentary rocks

IV.3. Measurement techniques

IV.4. Sampling procedure and collection of samples

IV.5. Results

IV.6. Magneto stratigraphic correlations : discussion

IV.1. Introduction

The magnetic polarity reversal sequence observed in the ocean sediment profiles and their correlation with the reversal record of the continental rocks provides an age index extending far beyond the Pleistocene epoch. The significance of the study of the palaeomagnetic reversal sequences lies in providing absolute chronologies for the ocean sediments (Opdyke, 1972) which have been intercompared with extrapolated dates obtained on volcanic rocks by radioactive dating methods. The Cenozoic chronology has been founded on biostratigraphy : the terrestrial system is based on specific events of mammalian evolution, and the marine system is based on molluscan or foraminiferral faunal events. The correlation of continental and marine strata is difficult because their mutually exclusive environments of deposition preclude the frequent interdigitation of diagnostic fauna and flora. As a consequence, the resolution within and between the continental and marine records has reached its practical limits with the conventional biostratigraphic correlation techniques. The recent development of the magnetic polarity stratigraphy as an accurate chronological correlation tool (Opdyke, 1972) has now made it possible to correlate strata even from mutually exclusive depositional environments. The success of remanent magnetic studies in defining the stratigraphy of pelagic sediments has shown the way for its use on other sediment types,

especially terrestrial sedimentary formations, like lake and river sediment deposits.

Magnetic polarity stratigraphy has been extensively used for sequences of volcanic rocks (Roche, 1950, 1951; Hospers, 1954 and many others), but its use in terrestrial sedimentary deposits has been rather restricted. The Russian workers were among the first to use the technique on the Pliocene and Quaternary sections of Western Turkmenia (Kharmov, 1958). A number of investigators have worked on terrestrial sediments like Griffiths (1955), Bucha et al (1969), Van Montfrans and Hospers (1969), Johnson et al (1975), Keller et al (1977). The present study tries to extend this type of work to the Kashmir valley, especially to the Karewas.

IV.2. Principles of Palaeomagnetism

Generally rocks show magnetic properties. One such property is the tendency of a rock specimen to behave as a magnet, with a north and a south pole and a magnetic axis. This magnetisation is a naturally occurring property and is referred to as fossil magnetism, or natural remanent magnetism, which is abbreviated as NRM. Fossil magnetism is impressed when the rock is formed, its axis being along the direction of the earth's magnetic field at the time. As a result, rocks serve as fossil compasses useful

for determining the direction of the ancient geomagnetic (palaeomagnetic) field. The intensity and the ancient direction of the field can be determined by employing suitable techniques which will be discussed later.

IV.2.A. Origin of Palaeomagnetism

Most rock-forming minerals do not contribute to fossil magnetism and are referred to as the non-magnetic minerals. The fossil magnetism is due to the iron oxides and sulphides present as accessory minerals which generally constitute no more than a small percentage of the total rock. They are referred to as the magnetic minerals.

The fossil magnetism has been used for determining the direction of the ancient geomagnetic field. The mechanism by which the fossil magnetism is acquired depends on the mode of formation and the subsequent history of a rock. It may be acquired on cooling from high temperatures when it is called thermoremanent magnetism (TRM), or during the formation of iron minerals at low temperatures, when it is referred to a chemical remanent magnetism (CRM). NRM of a sedimentary deposit is generally considered to be caused by the statistical alignment of the ferromagnetic mineral grains along the direction of the ambient magnetic field during their sedimentation and this remanent magnetization in bulk is called the detrital or

depositional remanent magnetization (DRM). A great deal of palaeomagnetic investigations on NRM of sedimentary rocks has been made in the last decade. As mentioned, the procedure depends on the ability of the sediments to record and preserve the geomagnetic imprint at the time of deposition. The lake sediments can acquire a remanent magnetization in the direction of the ambient field by two different mechanisms. First, they can acquire a chemical magnetic remanence (CRM). This happens when the magnetic grains in the sediments grow through a critical size known as the blocking volume. At this time, the remanent magnetization is parallel to the ambient field and remains fixed in this direction even if the field direction changes or the grains increase further in size.

The second type of remanence is detrital remanence magnetization (DRM). In DRM, the magnetic grains within the sediment which already have a remanent magnetization rotate to align themselves parallel to the ambient field direction. Originally it was thought that this mechanism operated when the sediment fell through water, but it has now been shown that this alignment occurs after deposition.

It is also possible for the fine grained particles to rotate and align themselves to the ambient field direction in water filled interstices of unconsolidated sediments. This specific type of remanence is called post-depositional remanence (PDRM).

The magnetization acquired by the above means is referred to as the primary magnetization and any magnetization acquired after consolidation, or due to new chemical changes is termed as the secondary component. The secondary component of magnetism can be removed by using alternating current field demagnetization on the samples.

IV.2.B. Reliability of the record of magnetization

In palaeomagnetic studies the directions of natural remanent magnetization (NRM) fall into two distinct groups, opposite in direction to each other. Even after correcting for the unstable components, one finds that the mean directions of the groups are, within experimental errors, found to be 180^{o} apart. In both igneous and sedimentary rocks one finds both normal and reversed polarity almost in equal proportion.

For the reversals, the following two alternative explanations have been suggested:

(1) The geomagnetic field may have periodically reversed itself;

(2) Some rocks may have acquired a spontaneous magnetization in a direction opposite to that of the applied field, known as self-reversed magnetization.

Several possible mechanisms for self-reversal have been suggested, but experiments carried out in the laboratory may not be able to simulate nature, because in nature geological time scales are involved. If the observed reversals of magnetization arose from field reversals, then certainly the following effects should be recognizable:

(a) The same polarity should occur in rocks of the same age irrespective of the rock type in all regions, if field has remained the same during the formation of the beds. Positive and negative zones should occur in stratigraphic succession so that boundaries between the zones of opposite polarities are parallel to the time planes and do not cut across them.

(b) In between the opposite polarities, transitional direction of magnetization should occur at least in some cases. Because of the fragmentary nature of the record, the transitional levels may not be discernible in all cases. In favourable circumstances traverses through the same stratigraphic levels at different localities should show comparable direction changes.

(c) There should not be any difference in chemical, mineralogical, or physical properties of the magnetic minerals in positive and negatively polarized rocks.

(d) The polarities in igneous bodies should be the same as those in their respective baked contact rocks.

(e) The laboratory tests for self-reversal mechanisms should prove negative when due account is taken of the uncertainty of such tests.

Only in the Haruna rock (Nagata, 1952) spontaneous self-reversal of total TRM occurred by cooling the natural rock. In the Asio and Sokoto rocks, a partial TRM component is self-reversed, but the total TRM is parallel to the field. In the Allard lake specimens and the carboniferous pyrrohotite shale, specific heat treatments are necessary to induce self-reversal. Out of the many thousands of TRM experiments on natural rocks, the Haruna dacite is the only established case of spontaneous self-reversal. The demonstrated cases of self-reversal properties in rocks occur in minerals of the ilmenite-hematite series and in pyrrhotite. No self-reversals have ever been found in magnetite, titanomagnetite or hematite, which are the minerals responsible for the fossil magnetism of the most igneous rocks and sediments.

The results from the extensive palaeomagnetic study show that the Recent and Late Pleistocene rocks are negatively magnetized in the same sense as the present field. The geomagnetic polarity stratigraphy is available for the last 5.0 m.y. on marine sediments based on K-Ar ages, with revised K-Ar decay constant (McDougall, 1978).

One therefore feels fairly secure in using the palaeomagnetic polarity data for magnetostratigraphic and chronological correlations.

IV.2.C. A criterion for stability of NRM in the sedimentary rocks

The natural remanent magnetisation (NRM) of a rock is composed of (a) the primary magnetisation acquired by the rock-mass at the time of formation and (b) the secondary components of magnetization acquired subsequent to formation. There are few natural processes like influence of the geomagnetic field, weathering, heating due to physical contact with an igneous body, thunder bolt etc., responsible for the secondary magnetization. The secondary component could be strong enough in some cases to distort the original magnetic polarity condition (Radhakrishnamurthy and Misra, 1966). So one is likely to encounter inconsistencies in magnetic directions among samples from a site in spite of all the precautions taken during sampling.

The known laboratory stability tests, like thermal and alternating current field demagnetization techniques, can be used easily in the case of igneous rocks, but they are quite difficult and cumbersome to use in the case of weakly magnetic sedimentary rocks (Radhakrishnamurthy and Sahastrabudhe, 1965).

The field tests for sedimentary rocks suggested by Graham (1949) and Everitt and Clegg (1962) require special in situ conditions and hence have limited applicability. The technique suggested by Radhakrishnamurthy and Misra (1966) can be used for igneous as well as sedimentary rocks and possess an added advantage in that it allows one to do away with the cumbersome demagnetization work.

A useful parameter, first introduced by Koenisberger (1938), is the ratio of intensity of the natural remanent magnetization (J_n) to that induced (J_i) in a field of the order of the earth's field (0.5Oe).

A simplified Koenisberger ratio, referred to here as Q_n, can be defined as:

$$Q_n = \frac{J_n}{J_i} \qquad \ldots\ \text{IV.1.}$$

According to Nagata (1953), the Q_n values for the igneous rocks vary from about 1 to 175, being around 10 in most of the effusive rocks. Though not explicitly mentioned in literature, it is a common belief that, as pointed out by Radhakrishnamurthy et al (1968) (Radhakrishnamurthy, 1970; Amin et al, 1972), high Q_n means a high remanence per unit volume of magnetic material of the rocks, i.e. a large fraction of single domain or pseudo-single domain particles, hence high stability, on the other hand, a low value of Q_n indicates the opposite, i.e. a large

fraction of multidomain or paramagnetic particles.

As a general rule Q_n ratios greater than 0.5 indicate favourable magnetic properties (in the present context) and those less than 0.5 do not. The available data on susceptibility of sediments in weak fields is rather scanty, chiefly because of the measurement of the magnetization induced in low fields has been quite difficult. But now we have a technique of measuring Q_n of sediments (Likhite and Radhakrishnamurthy, 1965).

The specimens having Q_n values of about 1 or less do not show any improvement on cleaning (Radhakrishnamurthy and Misra, 1966). So the value of Q_n can be taken as a significant criterion for cleaning studies. Here the measurement of J_i does not involve any damage to the specimen or to its NRM and it is possible to do it for all the specimens. The value of Q_n can be used as a general and significant criterion for assessing the magnetic stability of the various rock types, particularly the weakly-magnetic sedimentary rocks (Radhakrishnamurthy and Misra, 1966; Amin et al, 1972). Here AC cleaning process was not attempted because of the large size of the samples and also because our interest is on the indication of reversals and not on precise A and D of the samples.

IV.3. Measurement techniques

In all the cases orientations of the samples collected are recorded. Hence the direction and Q_n value (the ratio of natural magnetic moment to the induced magnetic moment in a field of 0.50e) for all samples could be measured. Both are measured for the same sample. The details of the measurements are described below.

The induced magnetic moment in a field of 0.50e was measured using a sensitive susceptibility apparatus developed by Likhite and Radhakrishnamurthy (1965).

The apparatus is an improved version of the one designed by Bruckshaw and Robertson (1948). It consists of a pair of Helmholtz coils at the centre of which is placed a double coil. A uniform field is provided by feeding current in Helmholtz coils through high quality power amplifier and audio-frequency oscillator combination. The double coil can be balanced to a very high degree at any frequency upto 200 C.P.S. by means of an extra winding connected through a potentiometer. The specimen which is placed inside the double coil behaves like an alternating dipole under the influence of energizing field and induces a differential emf in the coil. The signal is amplified and read on a meter.

Measurements of magnetic moment and direction of natural remanent magnetization in the specimens were made using a high sensitivity astatic magnetometer (Blackett, 1952). The magnetometer consists of two almost identical Alcomax IV bar magnets, 2 mm x 2 mm x 3 mm, mounted in an antiparallel direction at two ends of an aluminium beam. The beam carries a mirror at the centre and is suspended with a quartz or phosphor bronze fibre. To achieve good astatization two additional small trimmer magnets made of viccalloy were mounted on the beam, at right angles to each other. The whole system behaves as a non-magnetic one when a uniform magnetic field is applied. The specimen is mounted on a turn-table under the magnetic system which is housed at the centre of the three pairs of Helmoltz's coils carrying suitable currents to neutralize the earth's field. Magnetic direction and intensity were calculated from the measured value of components X, Y, Z of the magnetic vector. Declination (A), inclination (D), remanent intensity (J_n) and the induced intensity (J_i) in the specimen are given by:

$$A = \tan^{-1} \frac{Y}{X} \qquad \text{.... IV.2.}$$

$$D = \tan^{-1} \frac{Z}{[X^2 + Y^2]^{\frac{1}{2}}} \qquad \text{.... IV.2.}$$

$$J_n = \frac{\sigma [X^2 + Y^2 + Z^2]^{\frac{1}{2}}}{M} \qquad \text{.... IV.3.}$$

$$J_i = \frac{\sigma' d}{M} \qquad \text{.... IV.4.}$$

$$Q_n = \frac{J_n}{J_i} \qquad \text{.... IV.5.}$$

where A and D are expressed in degrees, J_n and J_i in emu, σ and σ' are the instrumental constants of the magnetometer and the susceptibility apparatus respectively. M denotes the mass of specimen in grams which could not be measured since the sample is fixed in the holder with plaster of Paris. But as we are interested only in the value of A, D and Q_n to determine the stable magnetic component of the specimen, value of M is not essential. d is the deflection due to the specimen.

IV.4. Sampling procedure and collection of sample

To collect oriented sediment samples, plastic sample holders were used (Fig. IV.1). Cylinders of the sediment were carved out (after removing the weathered portion) on the horizontal strata and collected in the plastic holders by fixing them with Plaster of Paris (analar grade $CaSO_4$). The top and the north directions were marked on the sample holder. Two spirit levels at right angles to each other were used to ensure the horizontality of the plain. Clinometric magnetic compass was used for aligning one of the sides of the holder parallel to north-south direction. Once the plaster dried, the sample was removed by cutting at the base. Plaster of Paris was poured again to fix the bottom portion of the sample also in position in the holder.

Fig. IV.1. Schematic section and plan of palaeomagnetic plastic sample holder.

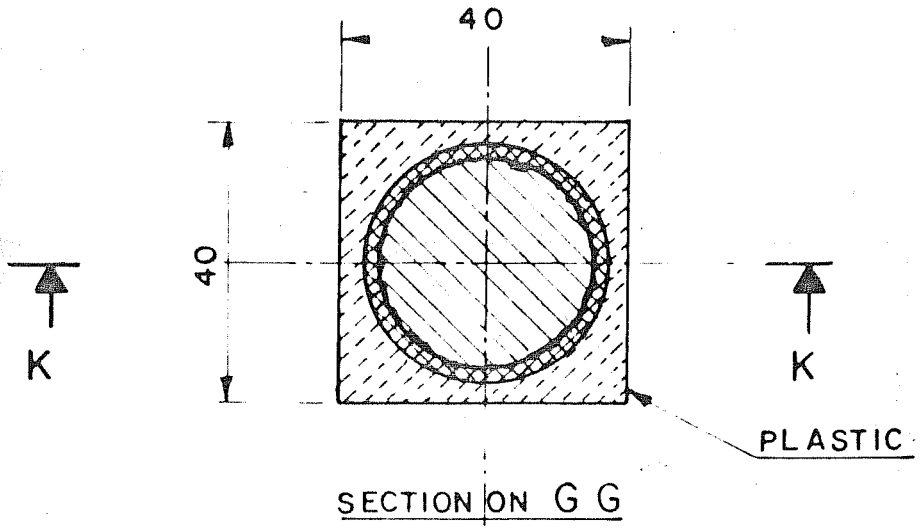

SECTION ON G G

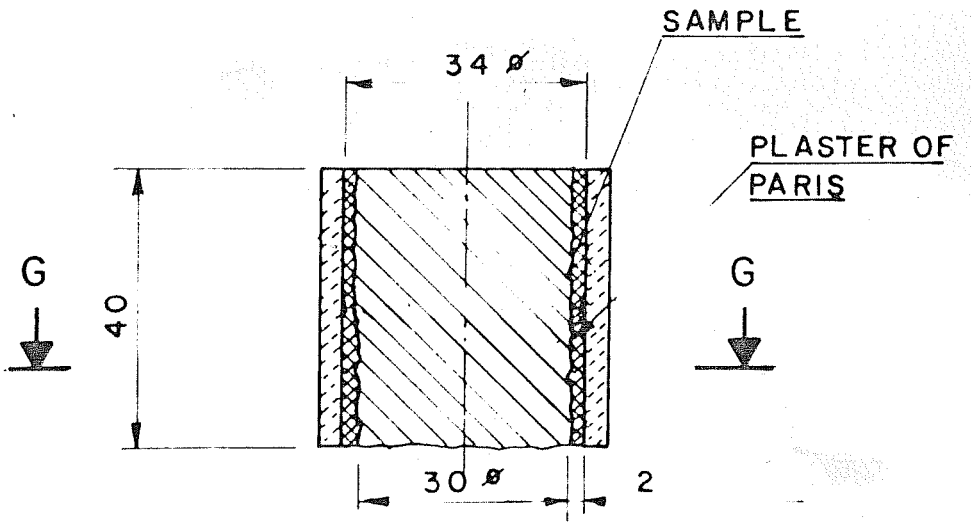

SECTION ON K K

ALL DIMENSIONS ARE IN M.M.

Samples for magnetostratigraphy were collected from both the Himalayan and Pir Panjal sides of the Kashmir valley. Care was taken to choose only those Karewa sections where maximum thickness was available and which were located in a clear stratigraphic context. In the case of the Upper Karewa, we have collected samples from all the clay strata of the sections approximately at one meter interval, thus ensuring that we do not miss any magnetic events.

Samples of Upper Karewa formation were collected from three sites: Olchibagh, Saki Paparian and Puthkhah (Fig. II.1). For the Lower Karewa formation a total of three sites namely Hirpur, Aripanthan and Pakharpura were sampled (Fig. II.1). Hirpur and Aripanthan sites were sampled to cover the entire deposit while from Pakharpura only one sample was collected below Gravel 3.

All the three sites of Upper Karewa formation (Nagum Lake) Olchibagh, Saki Paparian and Puthkhah have a loessic deposit.

Olchibagh has a total thickness of about 30 m of lacustrine sediments of the Upper Karewa, and at Saki Paparian about 44 m. Nearly 80 palaeomagnetic samples were collected from these sites. At Saki Paparian the Upper Karewa sediments are separated from the top of the tilted beds of Lower Karewa by a thin gravel sheet.

Fig. IV.2. Schematic sections of Saki Paparian (S-1, S-2, S-3) and Olchibagh (O) with magnetic sample locations and their polarity.

EPOCH AGE (m.y.)
0
Normal
BRUNHES
0.72
S-1
S-2
S-2
0
LOESS
LAMINATED MEMBER
UPPER KAREWA

Puthkhah has a total thickness of about 20 m. Both Saki Paparian and Olchibagh sites are on the Himalayan side, while Puthkhah falls on the Pir Panjal side.

As discussed in Chapter II, the maximum exposure of Lower Karewa formation is on the southwest on the Pir Panjal side of the valley i.e. along the Rembiara River near Hirpur. The Rembiara River cuts through the Lower Karewa deposits and has exposed a complete section of Lower Karewa between Dubjan, Hirpur and Shopian. There are large exposures available on the two banks of Rembiara which allows one to understand the stratigraphy. The occurrence of three gravels serves as stratigraphic markers and has been used for palaeomagnetic sampling. The Hirpur section was sampled at broad intervals to enable us to cover the complete sequence. A total of 40 magnetic samples was collected from this section, between Gravel 1 to Gravel 3. The Lower Karewa formation has been divided into Hirpur- A, B, C, D, E and I, II, and III sub-sections. Hirpur-A consists of Basal Conglomerate of 200 m thickness. Hirpur-B, C, D, E and the lower half of I consist of alternate deposits of laminated members of clay, silt and sand with occasional lignite beds in between. Hirpur sections I and II comprise Gravel-2, overlain by laminated members of clay, silt and sand, the latter continues upto Hirpur III.

Fig. IV.3. Stereographic projections of magnetic polarity measurements from the Upper Karewa sites of Olchibagh, Puthkhah and Saki Paparian.

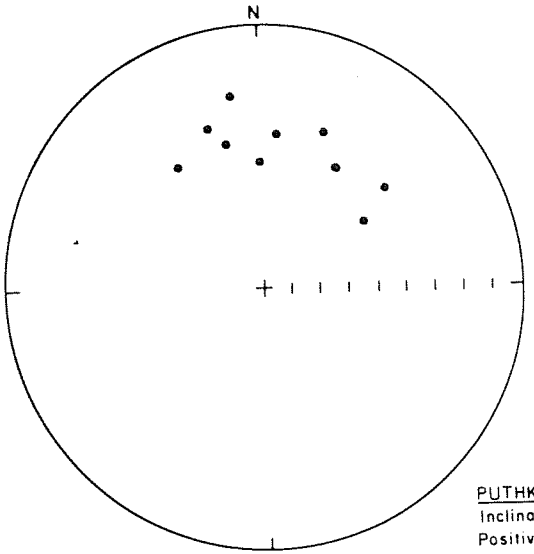

PUTHKHAH
Inclination
Positive ●

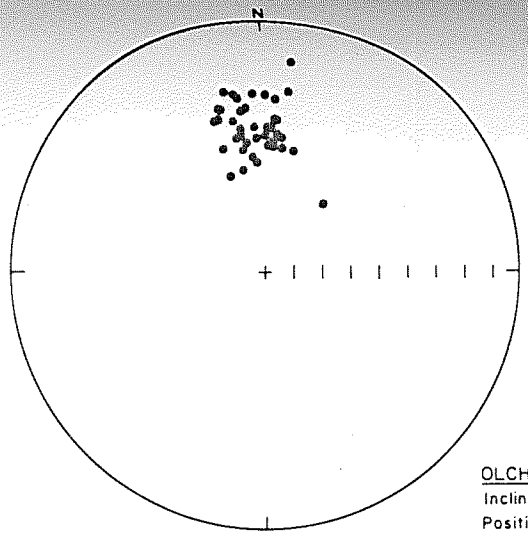

OLCHIBAGH
Inclination
Positive ●

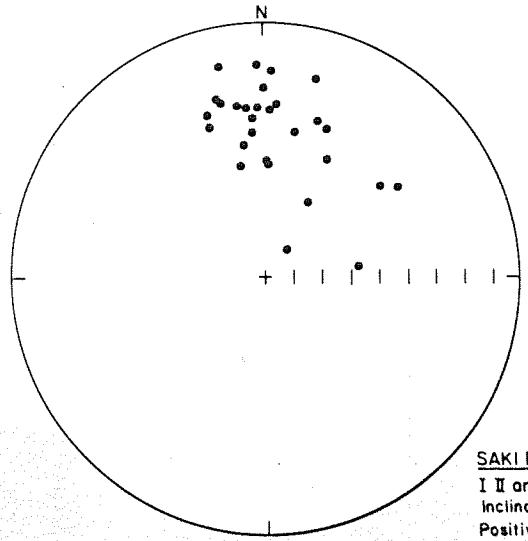

SAKI PAPARIAN
I II and III
Inclination
Positive ●

At Ari Panthan, another Lower Karewa formation site, which was sampled, the laminated members of clay, silt and sand sandwich the middle gravel (Gravel 2).

From Pakharpura, only one sample was collected. The section has the following sequence, from top bottomwards:

Loess at the top; 3 m thick deposit of Gravel 3; 100 m deposit of laminated members of alternating clay, silt and sand; 8-10 m of sand; and at the bottom a 1 m thick deposit of clay. The sample was collected from clay deposit exposed at the bottom of the section.

IV.5. Results

The results of determinations of magnetic moments and Q_n values (J_n/J_i) in the samples collected from the Loess, the Upper Karewa (Olchibagh, Saki Paparian and Puthkhah) and the Lower Karewa (Hirpur, Ari Panthan and Pakharpura) are presented in Tables IV.1 to IV.6 and Fig. IV.2 to IV.6.

The total remanent magnetic moment in Olchibagh samples varies from a minimum value of 14.86×10^{-5} emu to a maximum value of 76.94×10^{-5} emu and induced magnetic moment around $(30 \pm 10) \times 10^{-5}$ emu. Most of the values of the samples show Q_n values around 2 ± 1, thus indicating stability of the magnetic components. Declination and inclination of all samples showed positive polarity site (Table IV.1; Fig. IV.2, 3).

Saki Paparian (Upper Karewa) site also shows normality in the whole of the section (Table IV.2; Fig. IV.2, 3) with total remanent magnetic moment variation from 35 x 10^{-5} emu to 110 x 10^{-5} emu. And all samples show total induced magnetic moment ranging from 11 x 10^{-5} to 97 x 10^{-5} emu, with Q_n value $\geqslant 1$ (near 1 or more than 1).

Puthkhah (Upper Karewa) site showed normal polarity (Table IV.3; Fig. IV.3). Total remanent magnetic moment variation is from 6 x 10^{-5} emu to 155 x 10^{-5} emu while total induced magnetic moment is around 35 x 10^{-5} emu uniformly through out the section except PI/3 samples show Q_n ratio $\geqslant 1$.

All the Upper Karewa sites show normal polarity and high Q_n i.e., around 1 or higher than 1, which is the main criterion for a reliable measurement of magnetic direction (polarity) as suggested by Radhakrishnamurthy and Misra (1966) and Amin et al (1972).

At Ari Panthan (Lower Karewa) samples above Gravel-2 show normal polarity (Table IV·4; Fig. IV.5). The total remanent magnetic moment is very low ranging from 6 x 10^{-5} to 21 x 10^{-5} emu, though total induced magnetic moment, which is indicative of the magnetic material, lies between 30 x 10^{-5} emu to 50 x 10^{-5} emu. Except for two samples AI/7, AI/6 all other samples show very low Q_n value viz., less than one, rendering the measurements unreliable (Radhakrishnamurthy and Misra, 1966; Amin et al, 1972). The section below Gravel 2, the inclination shows reverse (-ve) direction in Sample A/5, and Sample AI/2 shows reverse declination with + 7 inclination; the Q_n is very low (Table IV.4).

Table IV.5 gives the direction of polarity and magnetic moment of remanent and an induced magnetization of the Hirpur samples.

Hirpur III shows reverse polarity (Fig. IV- 4,5) in HIII/2 and HIII/1 samples, with Q_n values 2.28 and 1.16. Sample HIII/6 shows an indication of reverse polarity but has a very low Q_n value; HIII/5 shows reverse polarity in only inclination, but has normal 17^{o} declination.

Hirpur Sections II and I show normal polarity in all samples where Q_n value is high, i.e. more than 0.5 (Fig. IV- 4, 5).

Hirpur sections E and D also show normal polarity (Fig. IV- 4, 5). In Section E, Sample HE/2 and HE/1 both show low Q_n value viz., less than 0.5. In Section D, two samples show high Q_n value while another two samples show low Q_n viz., less than 0.5 (Table IV.5).

Hirpur Section C and B show reverse polarity in samples HC/3 and HC/1. HC/2 shows normal polarity (Fig. IV.4, 5). HC/3 has Q_n value of 0.74, while the other two samples have Q_n value less than 0.5.

Fig. IV.4. A composite section of the Hirpur sub-sections showing magnetic sampling locations and polarity reversals.

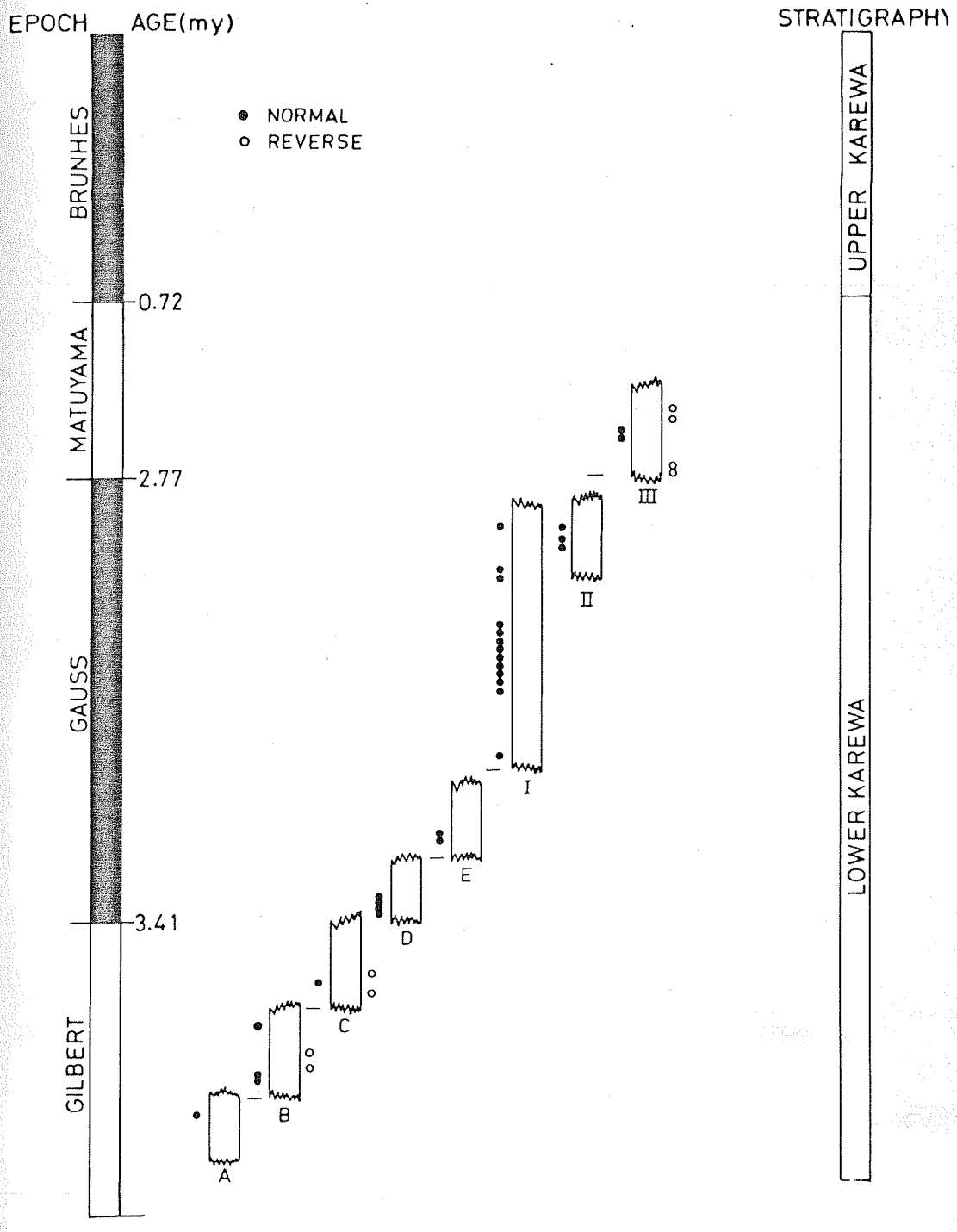
EPOCH
AGE(my)
STRATIGRAPHY
NORMAL
REVERSE
BRUNHES
MATUYAMA
GAUSS
GILBERT
0.72
2.77
3.41
UPPER KAREWA
LOWER KAREWA
A
B
C
D
E
I
II
III

Fig. IV.5. Stereographic projections of the polarity measurements of the Hirpur and Ari Panthan sections.

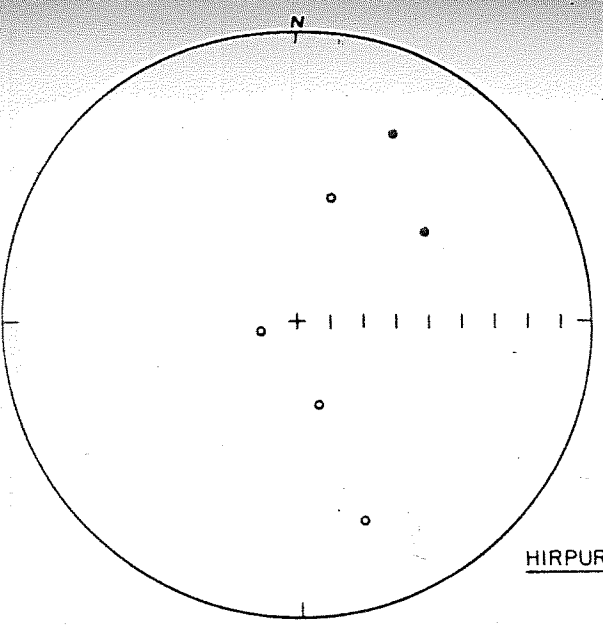

HIRPUR III

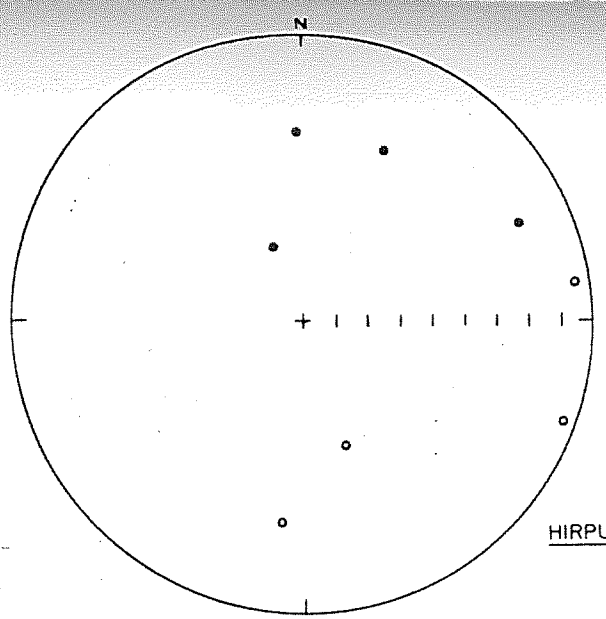

HIRPUR B & C

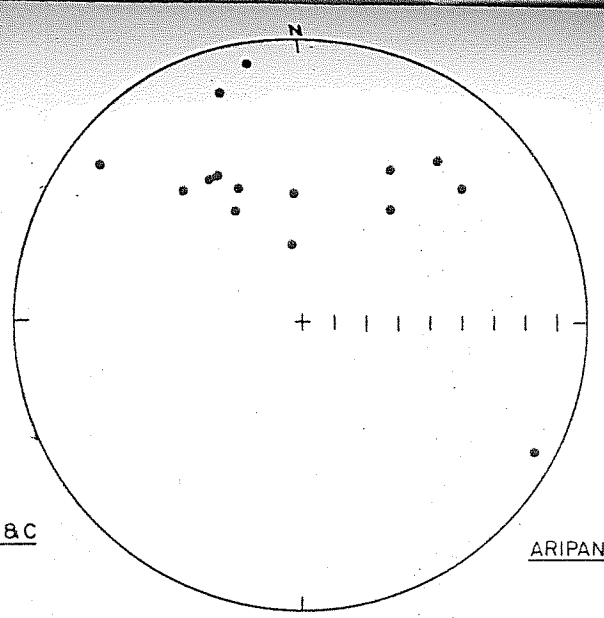

ARIPANTHAN

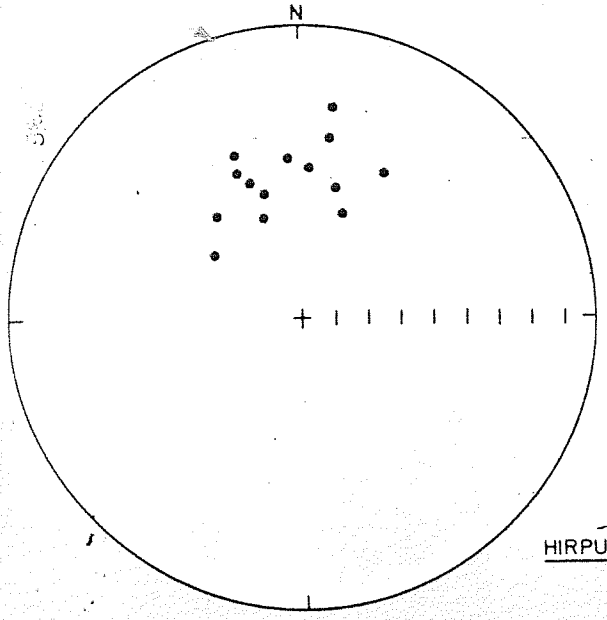

HIRPUR I & II

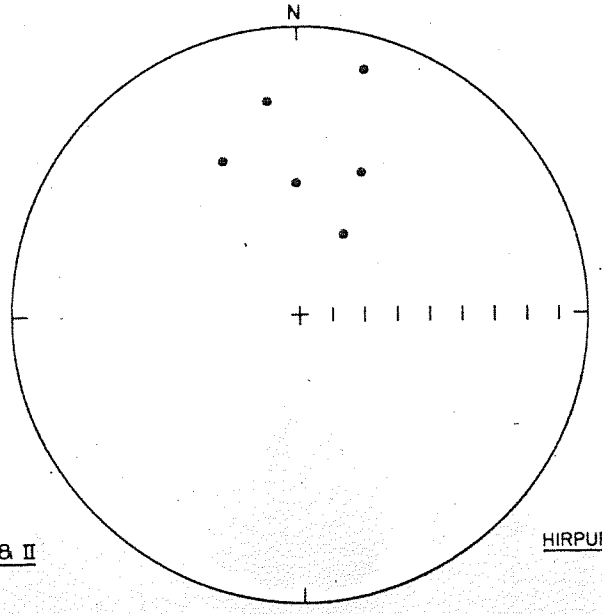

HIRPUR D & E

Inclination

Positive •

Negative ○

IV.6. Magnetostratigraphic correlation: discussion

On the Himalayan side, lying unconformably below the loess are the Upper Karewa sediments. These are horizontally bedded lacustrine and glacio-fluvial sediments.

Due to tectonic uplifts described in Chapter II, the lower loessic deposit of the Pir Panjal side is coeval with the lacustrine Upper Karewas of the Himalayan flank.

The total sequence of the loess and Upper Karewa formations on the Himalayan side shows a clear normal polarity and high Q_n values in all the samples collected from Olchibagh, Saki Paparian and Puthkhah.

The Upper Karewa and the loess represent a normal epoch, i.e. Brunhes normal epoch. The loess capping Upper Karewa has also been dated by radiocarbon method.

The section Hirpur III, lies between Gravel 2 and 3, covering a total thickness of about 30 m and shows a reverse magnetic polarity with high Q_n value.

The Hirpur Section B shows a reverse polarity in Samples HB/3 and HB/2, with Q_n value 2.41 and 0.41 respectively. Other samples show normal polarity, only HB/4 shows a Q_n value of 0.85, while other samples have Q_n values less than 0.5, i.e. 0.47, 0.29 and 0.42 for samples HB/2, HB/1 and HB/1a respectively.

Fig. IV.6. The composite section of the total Karewa column showing correlation between litho-, bio-, and magneto -stratigraphies. Position of Pleistocene fossils is approximately marked.

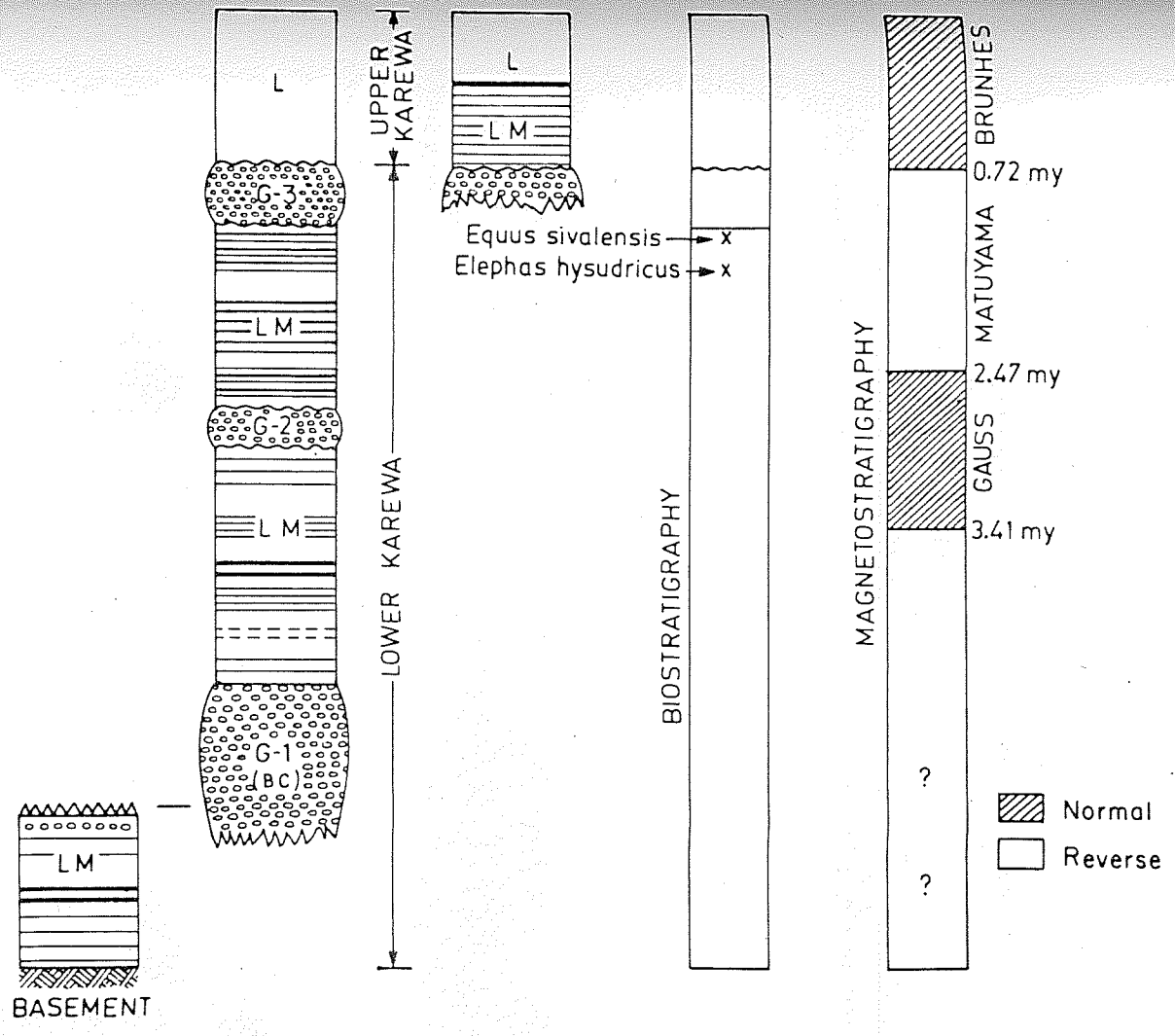

L = Loess, LM = Laminated member, G = Gravel, BC = Basal conglomerate

The Sample HA/1 from Section A shows normal polarity and has a Q_n value less than 0.5, i.e. 0.47. Pakharpura, another Lower Karewa site, shows a reverse polarity with 0.56 Q_n value.

Almost all the samples from the Upper Karewa and the Lower Karewa show induced magnetic moment in the range of 30×10^{-5} emu to 50×10^{-5} emu, while remanent magnetic moment in the Lower Karewa shows some variations.

The section Hirpur II, I, E and D all show normal polarity and thus may be representing the normal Gauss epoch (Fig. IV.4).

The Hirpur B and C sections have a good indication of reverse polarity in samples. This can probably be identified as the reverse Gilbert epoch (Fig. IV- 4, 6). This probably includes Hirpur A also.

Though detailed stratified faunal evidence is not available (Table II.10), the occurrence of at least two Pleistocene forms Equus sivalennis (Tiwari and Kachroo, 1979) and Elephas hysudricus (de Terra and Paterson, 1939) has been reported below Gravel-3 on Section III (Fig. IV- 4, 6). This reversal epoch may thus represent the Matuyama epoch. The normal epoch below this, covering sections Hirpur II, I, E and D, might thus represent the next epoch, Gauss normal (Fig. IV- 4, 6). The sections labelled Hirpur B and C, where again there is a good indication of a reversed polarity, might thus represent the Gilbert epoch (Fig. IV.6).

Thus by ensuring a thorough sampling of some of the best preserved complete sections, we could cover the total sediment profile. To make sure that we are starting with an intact top, we ^{14}C dated the top of the loess and the overlying archaeological deposit. The bottom of the lake is provided by the basal rocks. Pleistocene fossils helped us in defining the placement of the Matuyama epoch. We could thus work out with ^{14}C dates and fossils as absolute dating markers, a complete magnetostratigraphy of the Karewa sediment profile which covers Brunhes, Matuyama, Gauss and Gilbert epochs thus indicating that the lake was probably formed around 5 m.y. Of course, the absolute time interpretations of these magnetic polarity events depend upon the present understanding of the sedimentary profile and its completeness.

Table IV.1. Measurements of remanent magnetization in Olchibagh samples

Key: N.S. Not Sampled

Horizon	Thickness in m	S. No.	Declination (Deg.)	Inclination (Deg.)	J_n ($\times 10^{-5}$) emu	J_i ($\times 10^{-5}$) emu	Q_n
Top							
Loess	8.0	N.S.	-	-	-	-	-
Thick band of sand and clay	2.0	O/39	8	+ 27	18.29	15.7	1.16
		O/38	356	+ 52	17.82	16.4	1.09
Yellow clay	1.0	O/37	341	+ 45	67.30	30.7	2.19
Silty clay bands	1.5	O/36	4	+ 30	55.29	19.9	2.78
Silty clay sands	1.0	O/35	2	+ 40	33.06	24.9	1.33
Laminated silty clay band with yellow clay	1.0	O/34	3	+ 47	70.85	25.7	2.76
Sand	1.0	N.S.	-	-	-	-	-
Yellow clay	0.5	O/33	331	+ 35	27.20	20.7	1.31
Sandy grey clay silt	1.5	N.S.	-	-	-	-	-
Sand bed	0.2	N.S.	-	-	-	-	-

Table IV.1 (continued)

Horizon	Thickness in m	S. No.	Declination (Deg.)	Inclination (Deg.)	J_n ($\times 10^{-5}$) emu	J_i ($\times 10^{-5}$) emu	Q_n
Grey silt	1.0	O/32	344	+ 31	14.86	17.8	0.84
		O/31	353	+ 33	54.36	21.0	2.59
Yellow silt	1.2	N.S.	-	-	-	-	-
Yellow clay	0.2	O/30	14	+ 47	76.94	27.8	2.8
Yellow clay, silty sand, alternate bands of grey sand	5.0	O/29	340	+ 55	26.58	22.1	1.55
		O/28	356	+ 44	44.98	27.8	1.55
		O/27	1	+ 40	189.29	47.1	4.02
		O/26	350	+ 42	48.12	37.8	1.27
		O/25	4	+ 30	40.7	27.8	1.46
		O/24	0	+ 43	141.16	33.5	4.21
Grey laminated silt	0.5	O/23	8	+ 16	36.06	24.2	1.51
		O/22	5	+ 37	34.74	29.3	1.19
		O/21	0	+ 29	29.727	19.9	1.49
Yellow clay	0.5	O/20	356	+ 28	189.0	47.1	4.01
Sand	0.2	N.S.	-	-	-	-	-
Yellow clay	0.1	O/19	348	+ 37	118.29	36.4	3.25
Yellow clay	0.1	O/18	351	+ 29	96.71	31.4	3.08
Sand	0.2	N.S.	-	-	-	-	-
Ash coloured clay	1.0	O/17	4	+ 37	77.13	44.3	2.24
		O/16	5	+ 42	128.93	36.4	3.54

Table IV.1 (continued)

Horizon	Thickness in m	S. No.	Declination (Deg.)	Inclination (Deg.)	J_n ($\times 10^{-5}$) emu	J_i ($\times 10^{-5}$) emu	Q_n
Compacted grey clay	1.0	N.S.	-	-	-	-	-
Constructed break	4.0	N.S.	-	-	-	-	-
Hard compacted clay bands	1.0	O/15	350	+ 28	32.88	26.4	1.25
		O/14	356	+ 52	67.56	26.4	2.56
Sandy clay band	1.0	O/13	350	+ 40	130.54	30.7	4.25
		O/12	7	+ 43	87.03	29.3	2.97
		O/11	8	+ 47	147.97	46.4	3.19
Pale to grey clay	5.0	O/10	350	+ 47	157.31	34.3	4.59
		O/9	347	+ 26	114.3	25.7	4.45
		O/8	352	+ 45	106.11	32.8	3.23
		O/7	348	+ 54	175.93	35.8	4.65
		O/6	356	+ 40	61.95	22.8	2.38
		O/5	351	+ 34	21.25	23.6	0.91
		O/4	42	+ 59	6.48	19.9	0.33
		O/3	348	+ 43	50.62	25.7	1.97
		O/2	4	+ 45	272.1	87.8	3.09
		O/1	355	+ 50	186.65	56.0	3.33

Table IV.2. Measurements of remanent magnetization in Saki Paparian samples

Key: N.S. = Not Sampled

Horizon	Thickness in m	S. No.	Declination (Deg.)	Inclination (Deg.)	$J_n (x10^{-5})$ emu	$J_i (x10^{-5})$ emu	Q_n
Saki Paparian III							
Loess	1.0	S/15	350	+ 26	44.76	47.1	0.95
Palaeosol	0.2	N.S.	-	-	-	-	-
Loess	4.0	N.S.	-	-	-	-	-
Kankar	0.2	N.S.	-	-	-	-	-
Loess	1.5	S/14	2	+ 50	35.8	31.4	1.14
Palaeosol	0.2	N.S.	-	-	-	-	-
Loess	3.5	N.S.	-	-	-	-	-
Laminated silt deposit	2.0	N.S.	-	-	-	-	-
Marl	0.1	S/13	354	+ 30	53.47	29.27	1.36
Yellow laminated clay	22.0	S/12	355	+ 39	68.07	28.56	2.38
		S/11	15	+ 18	58.75	23.56	2.48
		S/10	348	+ 50	95.36	31.4	3.04
		S/9	35	+ 29	55.84	35.7	1.56
		S/8	56	+ 33	50.84	24.9	2.04
		S/7	85	+ 41	73.58	21.42	3.44

Table IV.2 (continued)

Horizon	Thick-ness in m	S. No.	Decli-nation (Deg.)	Incli-nation (Deg.)	J_n ($\times 10^{-5}$) emu	J_i ($\times 10^{-5}$) emu	Q_n
Yellow laminated clay	22.0	S/6	358	+ 30	8.41	17.8	0.40
		S/5	1	+ 66	55.62	23.56	2.36
		S/4	4	+ 29	110.15	32.8	3.36
		S/3	5	+170	37.35	22.8	1.64
		S/2	30	+ 60	30.2	11.4	2.65
		S/1	48	+ 52	25.9	18.5	1.35
Saki Paparian II							
Yellow laminated clay	23.0	S/15	28	+ 43	94.3	37.8	2.50
		S/14	340	+ 34	56.7	58.5	1.0
		S/13	351	+ 43	82.3	97.8	0.8
		S/12	12	+ 38	62.5	67.8	0.9
		S/10	241	+ 30	196.7	54.9	3.6
		S/9	0	+ 23	92.1	62.8	1.46
		S/8	2	+ 32	120.5	47.1	2.6
		S/7	358	+ 30	80.0	46.4	1.7
		S/6	23	+ 33	65.3	39.3	1.66
		S/5	40	+ 47	81.5	27.1	2.2
		S/4	348	+ 14	108.8	48.5	2.2
		S/3	19	+ 32	19.1	24.9	0.8
		S/2	52	+ 38	43.1	27.8	1.6
		S/1	356	+ 34	29.8	26.4	1.1
Saki Paparian Ia							
Laminated clay	3.5	N.S.	-	-	-	-	-
Coarse sand and small pebbles	0.5	N.S.	-	-	-	-	-

Table IV-3 (continued)

Horizon	Thick-ness in m	S. No.	Decli-nation (Deg.)	Incli-nation (Deg.)	J_n ($\times 10^{-5}$) emu	J_i ($\times 10^{-5}$) emu	Q_n
Laminated clay	2.0	N.S.	-	-	-	-	-
Laminated clay	1.0	S/10	35	+28	58.5	17.1	3.4
Laminated clay	2.0	N.S.	-	-	-	-	-
Laminated clay	1.0	S/9	42	+28	53.7	23.5	2.9
Hard rock	1.0	N.S.	-	-	-	-	-
Cross bedded sand	1.0	N.S.	-	-	-	-	-
Pebbly clay-sand	0.5	N.S.	-	-	-	-	-
Saki Paparian I							
Constructed break							
Rock	0.5	N.S.	-	-	-	-	-
Cross bedded sand	1.0	N.S.	-	-	-	-	-

Table IV.2 (continued)

Horizon	Thickness in m	S. No.	Declination (Deg.)	Inclination (Deg.)	J_n ($\times 10^{-5}$) emu	J_i ($\times 10^{-5}$) emu	Q_n
Alternate bands of clay and blue sand	2.0	S/6	3	+ 28	223.3	132.0	1.7
		S/5	3	+ 40	136.1	64.9	2.1
Laminated silty clay	2.0	S/4	6	+ 30	195.8	52.1	3.8
		S/3	5	+ 38	127.6	74.9	1.7
Laminated green silt	3.5	S/8	1	+ 32			
		S/7	6	+ 36			
Laminated light brown clay	2.5	S/2	287	+ 37	97	37.0	2.6
		S/1	4	+ 48	148.3	74.9	1.8

Table IV.3. Measurement of remanent magnetization in Puthkhah samples

Key: N.S. = Not Sampled

Horizon	Thickness in m	S. No.	Declination (Deg.)	Inclination (Deg.)	J_n ($\times 10^{-5}$) emu	J_i ($\times 10^{-5}$) emu	Q_n
Hill top							
Loess	4.0	N.S.	-	-	-	-	-
Dark brown sand	0.5	N.S.	-	-	-	-	-
Yellow grey alternating lamination	1.0	PI/8	7	+ 37	68.34	41.5	1.65
Bluish grey clay	0.5	PI/7	326	+ 40	29.46	35.5	0.83
		PI/6	342	+ 33	30.07	35.5	0.85
Greenish sand	1.0	N.S.	-	-	-	-	-
Slope wash	1.0	N.S.	-	-	-	-	-
Laminated clay and sand	0.5	PI/5	347	+ 40	34.07	40.0	0.85
Yellow and dark brown clay and sand	2.0	N.S.	-	-	-	-	-
Sand clay and silt	0.5	PI/4	352	+ 24	24.34	37.5	0.65
		PI/4a	1	+ 47	155.3	49.5	3.14

Table IV.3 (continued)

Horizon	Thick-ness in m	S. No.	Decli-nation (Deg.)	Incli-nation (Deg.)	J_n ($\times 10^{-5}$) emu	J_i ($\times 10^{-5}$) emu	Q_n
Laminated clay with fine sand layer	2.0	PI/3	59	+ 48	6.36	31.0	0.21
Brown silty clay with yellowish patches and marly bands	2.0	PI/2	24	+ 32	76.13	40.5	1.9
Laminated silty clay	2.0	N.S.	-	-	-	-	-
Greenish brown clay	1.0	PI/1 PI/1a	53 339	+ 35 + 41	15.75 26.04	28.0 29.0	0.56 0.90

Table IV.4. Measurements of remanent magnetization in Ari Panthan samples

Key: N.S. = Not Sampled

Horizon	Thickness in m	S. No.	Declination (Deg.)	Inclination (Deg.)	J_n ($\times 10^{-5}$) emu	J_i ($\times 10^{-5}$) emu	Q_n
Greenish yellow silty clay unexposed	1.0	AI/14	317	+ 35	21.57	39.0	0.55
Greenish clay and silt with brown patches unexposed	3.0	AI/13	334	+ 44	13.52	38.0	0.36
Greenish clay with brown patches	2.0	AI/12	328	+ 50	3.96	41.0	0.09
Greenish brown sand	2.0	N.S.	-	-	-	-	-
Dark brown clay	2.0	N.S.	-	-	-	-	-
Greenish brown sand	2.0	N.S.	-	-	-	-	-
Greenish clay with brown patches	2.0	AI/11	340	+ 14	12.14	40.5	0.29
Unexposed	1.0	N.S.	-	-	-	-	-
Reddish clay	1.0	N.S.	-	-	-	-	-
Brown clay	1.0	N.S.	-	-	-	-	-

Table IV.4 (continued)

Key: N.S. = Not Sampled

Horizon	Thickness in m	S. No.	Declination (Deg.)	Inclination (Deg.)	J_n ($\times 10^{-5}$) emu	J_i ($\times 10^{-5}$) emu	Q_n
Unexposed	1.0	N.S.	-	-	-	-	-
Brown clay	1.0	N.S.	-	-	-	-	-
Yellowish green clay	1.0	AI/10	30	+ 35	16.32	41.0	0.39
Greenish clay	1.0	N.S.	-	-	-	-	-
Greenish sand	1.0	N.S.	-	-	-	-	-
Yellowish green clay	1.5	AI/9	40	+ 24	11.83	37.5	0.32
Unexposed	1.5	N.S.	-	-	-	-	-
Greenish clay with brown patches	2.0	N.S.	-	-	-	-	-
Brown clay and silt	1.5	N.S.	-	-	-	-	-
Greenish clay with brown patches	2.5	AI/8	329	+ 37	6.59	35.0	0.19
Dark brown clay	2.5	AI/7	326	+ 36	145.63	107.5	1.35
Unexposed	2.5	N.S.	-	-	-	-	-
Gravel layer with clay	2.5	N.S.	-	-	-	-	-

Table IV.4 (continued)

Horizon	Thick-ness in m	S. No.	Decli-nation (Deg.)	Incli-nation (Deg.)	J_n ($\times 10^{-5}$) emu	J_i ($\times 10^{-5}$) emu	Q_n
Greenish clay	2.0	AI/6	356	+ 50	100.8	51.4	1.98
		AI/6a	50	+ 25	10.13	37.0	0.27
Grey clay with red patches	2.0	AI/4	38	+ 45	22.54	39.5	0.57
		AI/5	307	- 10	21.06	47.5	0.44
Sand	0.2	N.S.	-	-	-	-	-
Greenish clay	1.0	AI/3	351	+ 66	7.36	40.0	0.18
Clay	2.0	AI/1	348	+ 7	31.33	44.5	0.70
		AI/2	119	+ 7	3.06	40.5	0.07
Clay	0.2	N.S.	-	-	-	-	-
Sand	1.0	N.S.	-	-	-	-	-

Table IV.5. Measurements of remanent magnetization in Hirpur samples

Key: NS. = Not Sampled

Horizon	Thickness in m	S. No.	Declination (Deg.)	Inclination (Deg.)	J_n ($\times 10^{-5}$) emu	J_i ($\times 10^{-5}$) emu	Q_n
Hirpur-III							
Slope wash	10.0	N.S.	-	-	-	-	-
Clay	1.0	H-III/6	255	- 78	16.04	37	-
Sand	1.2	N.S.	-	-	-	-	-
Laminated clay	0.5	H-III/5	17	- 51	8.0	30	0.27
	0.5	H-III/4	55	+ 43	12.95	36	0.36
	3.0	N.S.	-	-	-	-	-
	0.5	H-III/3	28	+ 26	15.29	41	0.37
Sand and clay	7.0	N.S.	-	-	-	-	-
Clay	1.0	H-III/2	162	- 36	121.0	53	2.28
Sand	1.5	N.S.	-	-	-	-	-
Purple clay	1.0	H-III/1	168	- 64	49.9	43	1.16
Hirpur-II							
Top							
Sand	5.0	N.S.	-	-	-	-	-
Clay	1.0	H-II/3	339	+ 57	24.9	39	0.64

Table IV.5 (continued)

Horizon	Thickness in m	S. No.	Declination (Deg.)	Inclination (Deg.)	J_n ($\times 10^{-5}$) emu	J_i ($\times 10^{-5}$) emu	Q_n
Sand	1.0	N.S.	-	-	-	-	-
Clay	3.0	N.S.	-	-	-	-	-
Sand	1.5	N.S.	-	-	-	-	-
Clay	1.0	H-II/2	344	+ 50	27.2	44	0.62
Clay	1.0	H-II/1	356	+ 41	283.0	74	3.82
Sand	4.0	N.S.	-	-	-	-	-
Clay	2.5	N.S.	-	-	-	-	-
Gravel	5.0	N.S.	-	-	-	-	-
River bed							
Hirpur-I							
Green sand with thick brown band	4.0	N.S.	-	-	-	-	-
Clay	2.0	H-I/12	306	+ 58	290.0	48.5	5.97
		H-I/12a	324	+ 48	51.29	66.0	0.78
Greenish sand with pebble line	5.0	N.S.	-	-	-	-	-

Table IV.5 (continued)

Horizon	Thickness in m	S. No.	Declination (Deg.)	Inclination (Deg.)	J_n ($\times 10^{-5}$) emu	J_i ($\times 10^{-5}$) emu	Q_n
Gravel sand lenses	8.0	N.S.	-	-	-	-	-
Purple clay	1.2	H-I/11	298	+ 31	154.2	53.5	2.88
		H-I/11a	336	+ 44	509.0	84.5	6.02
Green sand with brown bands	2.0	N.S.	-	-	-	-	-
Purple clay	1.0	H-I/10	317	+ 36	120.0	33.0	3.64
Clay with sand band	3.0	N.S.	-	-	-	-	-
Greenish sand	3.0	N.S.	-	-	-	-	-
Purple laminated clay	1.5	N.S.	-	-	-	-	-
Clay bands	3.0	N.S.	-	-	-	-	-
Clay bands slope wash	3.0	"					
Brownish sand	1.0	"					
Clay with sand bands	2.5	"					
Banded brown sand	3.0	"					
Clay	0.2	H-I/9	338	+ 26	120.9	56.0	2.16

Table IV.5 (continued)

Horizon	Thickness in m	S. No.	Declination (Deg.)	Inclination (Deg.)	J_n ($\times 10^{-5}$ emu)	J_i ($\times 10^{-5}$ emu)	Q_n
Sand	0.2	H-I/8	339	+ 46	59.21	44.0	1.35
Sand	0.5	N.S.	-	-	-	-	-
Clay	0.2	H-I/7	30	+ 39	231.0	66.0	3.5
Sand	0.3	N.S.	-	-	-	-	-
Purple clay	0.5	H-I/6	9	+ 34	57.3	46.0	1.25
Sand	0.2	N.S.	-	-	-	-	-
Brown and purple banded clay	0.7	H-I/5	3	+ 44	26.1	38.0	0.69
Purple clay	1.0	N.S.	-	-	-	-	-
Sand	0.5	N.S.	-	-	-	-	-
Purple clay	0.5	N.S.	-	-	-	-	-
Sand brown band	0.5	N.S.	-	-	-	-	-
Brownish clay	0.5	H-I/4	322	+ 56	186.4	54.0	3.45
Sand	0.5	N.S.	-	-	-	-	-
Purple clay	1.0	N.S.	-	-	-	-	-

Table IV.5 (continued)

Horizon	Thickness in m	S. No.	Declination (Deg.)	Inclination (Deg.)	J_n ($\times 10^{-5}$) emu	J_i ($\times 10^{-5}$) emu	Q_n
Greenish sand with brown band	1.0	N.S.	-	-	-	-	-
Dark clay	1.0	H-I/3	337	+ 42	41.87	43.0	0.97
Greenish sand	1.0	N.S.	-	-	-	-	-
Clay	0.5	H-I/2	15	+ 49	153.0	56.0	2.73
Banded shale with clay lines	3.0	N.S.	-	-	-	-	-
Clay	0.5	H-I/1	321	+ 49	22.7	37.0	0.61
Carbonaceous band	0.5	N.S.	-	-	-	-	-
Shale with clay laminations	2.0	N.S.	-	-	-	-	-
Dark clay	0.5	N.S.	-	-	-	-	-
Clay	1.0	N.S.	-	-	-	-	-
Shale	1.0	N.S.	-	-	-	-	-
Clay	1.0	N.S.	-	-	-	-	-
Sandy shale	1.0	N.S.	-	-	-	-	-
Clay	1.0	N.S.	-	-	-	-	-

Table IV.5 (continued)

Horizon	Thickness in m	S. No.	Declination (Deg.)	Inclination (Deg.)	J_n ($\times 10^{-5}$) emu	J_i ($\times 10^{-5}$) emu	Q_n
Shale	0.5	N.S.	-	-	-	-	-
Dark grey clay	2.5	N.S.	-	-	-	-	-
Yellow shale	2.0	N.S.	-	-	-	-	-
Hirpur-E							
Grey clay	1.0	N.S.	-	-	-	-	-
Shale	1.0	N.S.	-	-	-	-	-
Clay	3.0	N.S.	-	-	-	-	-
Sand	1.0	N.S.	-	-	-	-	-
Grey clay with sand beds	0.5	N.S.	-	-	-	-	-
Brownish clay sand	3.0	N.S.	-	-	-	-	-
Sand	3.0	N.S.	-	-	-	-	-
Sandy grey clay	7.0	N.S.	-	-	-	-	-
Brownish sand/ bluish clay	3.0	N.S.	-	-	-	-	-
Grey clay band	1.5	H-E/2	352	+ 23	7.8	32.0	0.24
Grey clay band	1.0	H-E/1	334	+ 37	11.19	36.0	0.31
River bed unexposed							

Table IV.5 (continued)

Horizon	Thickness in m	S. No.	Declimation (Deg.)	Inclination (Deg.)	J_n (x10^{-5}) emu	J_i (x10^{-5}) emu	Q_n
Hirpur-D							
Greenish sand deposit	10.0	N.S.	-	-	-	-	-
Greenish clay band	1.0	H-D/4	28	+ 62	211.6	44.0	4.81
Greenish clay band	1.0	H-D/3	359	+ 49	97.7	38.0	2.57
Blackish lignitic band	1.0	N.S.	-	-	-	-	-
Lignite band	2.0	N.S.	-	-	-	-	-
Yellowish clay bands	2.0	H-D/2	24	+ 42	17.6	46.0	0.38
Greyish clay band	1.0	H-D/1	15	+ 11	17.4	39.0	0.45
River bed unexposed							
Hirpur-C							
Yellowish silt	2.0	N.S.	-	-	-	-	-
Loosely fixed conglomerate	5.0	N.S.	-	-	-	-	-

Table IV.5 (continued)

Horizon	Thickness in m	S. No.	Declination (Deg.)	Inclination (Deg.)	J_n ($\times 10^{-5}$) emu	J_i ($\times 10^{-5}$) emu	Q_n
Sandy clay	7.0	N.S.	-	-	-	-	-
Greyish clay band	5.0	HC/1	162	- 50	31.02	42.0	0.74
		HC/2	66	+ 17	12.08	41.0	0.29
Thick deposit of clay	4.0	HC/1	82	- 5	9.26	42.0	0.22
River bed							
Hirpur-B							
Brownish clay	2.0	N.S.	-	-	-	-	-
Yellowish clay	2.0	N.S.	-	-	-	-	-
Sand	4.0	N.S.	-	-	-	-	-
Yellowish clay	1.0	HB/4	358	+ 32	39.11	46.0	0.85
Greenish clay	1.0	HB/3	187	- 28	99.01	41.0	2.41
Yellowish clay	1.0	N.S.	-	-	-	-	-
Sand	2.0	N.S.	-	-	-	-	-
Yellowish clay	3.0	N.S.	-	-	-	-	-
Sand	3.0	N.S.	-	-	-	-	-
Greenish clay	1.0	HB/2	111	- 4	24.16	51.0	0.47

Table IV.5 (continued)

Horizon	Thickness in m	S. No.	Declination (Deg.)	Inclination (Deg.)	J_n ($\times 10^{-5}$) emu	J_i ($\times 10^{-5}$) emu	Q_n
Greenish clay	1.0	HB/1	337	+ 66	13.88	48.0	0.29
		HB/1a	26	+ 32	16.8	40.0	0.42
Slope wash	7.0	N.S.	-	-	-	-	-
Hirpur-A							
Basal Conglomerate	3.0	HA/1	350	+ 57	13.01	30.0	0.47

Table IV.6. Measurement of remanent magnetization in Pakharpura samples

Horizon	Thickness in m	S. No.	Declination (Deg.)	Inclination (Deg.)	J_n (x10^{-5}) emu	J_i (x10^{-5}) emu	Q_n
Sand	10.0	N.S.	-	-	-	-	-
Clay	2.0	PK/1	206	- 4	20.12	36.0	0.56

CHAPTER V

V. DATING OF PALAEOCLIMATIC EVENTS

V.1. Introduction

V.2. Global climatic change

V.2.A. Quaternary climatic fluctuations

V.3. Palaeoclimatic cycles in the Kashmir valley

V.1. Introduction

The main aim of this thesis is to employ physical techniques for dating the sedimentary profile of the Karewas in the Kashmir basin. We have been able to give a broad chronological framework for the various lithozones of the Karewa stratigraphy (Fig. IV.6). Since our chronology is tied down to the well-defined lithostratigraphic units, it is hoped that this work would provide the chronological framework to future workers investigating some of these sections.

In this chapter, we would like to use our chronological framework to date the palaeoclimatic sequence in the Kashmir basin. We would, however, like to emphasize here that this work is not aimed at offering any palaeoclimatic interpretation of the sedimentary profile. We will only make use of the available climatic data both for Kashmir and the world. The main aim of this chapter is to show the potential of building up a detailed palaeoclimatic curve in Kashmir with the help of the time-frames provided by us.

V.2. Global climatic change

There is clear evidence of the climatic fluctuations the earth has gone through. Various estimates suggest ice ages coming every 250 m.y. From the middle of the Tertiary the

evidence of progressive cooling of the earth is now better documented. Floral remains from Antarctica show that it had a deciduous type of vegetation before the ice-sheets developed there. But by 7 m.y. the great ice-sheets of Antarctica (Fig. V.1) had come into existence destroying all vegetation (Lamb, 1977). From Argentina also there is evidence of glaciations around 3.6 m.y. and between 2.1 and 1 m.y. There was no glaciation there between 3.6 and 2.1 m.y. (Fleck et al, 1972). But the most intense and severe glaciations were witnessed by the earth only during the Quaternary period.

Several efforts have been made to define the Plio-Pleistocene boundary all over the world. The XVIII International Geological Congress agreed that the base of the Calabrian in Italy, defined by the appearance of foraminifera Anomalina baltica and mollusk Arctica islandica should be taken as the boundary between Pliocene and Pleistocene. In the sea-cores, extinction of Discoasteridae and Globorotalia menardii (dextral) and appearance of Globorotalia tuncatulinoides etc. around 1.9 m.y. marks the Plio-Pleistocene boundary (Ericson et al, 1964). In the magnetic polarity scale, the Olduvai event marks the Plio-Pleistocene boundary.

Climatic curves have also been constructed from the percentage of coarse particles (fragments of foraminifera greater than 180 $/^{u}$ diam) and $^{18}O/^{16}O$ variation on some foraminiferal species (like

Table V.1. *Names of the principal warm and cold climate stages recognized in Quaternary deposits in different regions of the northern hemisphere and their probable correspondence (after Lamb, 1977)*

Notes: Youngest stages at top of table
Interglacial periods are underlined

		North America Central Sector	Britain	North European plain	European Russia	Alps
HOLOCENE	Post-glacial		Flandrian	Flandrian		
PLEISTOCENE	Upper	Wisconsin	Devensian	Weichsel	Valdai	Wurm
		Sangamon	Ipswich	Eem	Mikulino	Riss-Wurm
		Illinois	Wolstonian (or Gipping)	Saale	Moskva Oldintsovo Dniepr	Riss
	Middle	Yarmouth	Hoxne	Holstein	Likhvin	Mindel-Riss
		Kansan	Anglian (Lowestoft)	Elster		Mindel
		Afton	Cromer	Cromer	Morozov	Gunz-Mindel
			Beeston Paston			
	Lower	Nebraskan	Baventian	Menap	Odessa	Gunz
			Antian	Waal		Donau-Gunz
			Thurne	Eburon		Donau
			L dham	Tegel (Tiglian)		Biber-Donau
			Walton	Bruggen		Biber
				Pre-Tiglian		
				Amstel		

Globeriginoides sacculifera) from the sea-cores (Emiliani, 1961; Shackleton and Opdyke, 1976). Such curves show some ten glacial maxima during the last million years. Hays et al (1976) made a power spectrum analyses of such climatic curves of the last 500,000 years and discovered fluctuations of 100,000 years, 40,000 years and 20,000 years lengths, thus lending support to Milankovitche's (1930) theory of glaciation. He attributed the glacial-interglacial periods to changes in insolation arising due to the earth's orbital vagaries (Milankovitch, 1930). Ample experimental proof for global scale climatic geophysical changes has recently been acquired (Hays et al, 1976; Bhandari, 1977; Somayajulu, 1977). There are many theories attempting to explain climatic changes attributing them to fluctuations in solar radiation (Simpson, 1957); volcanic dust (Budyko, 1969); instability of polar-ice caps (Brooks, 1949); polar wandering (Ewing and Donn, 1956) etc., to name only a few, into which we will not go here. Here we will only delineate the global climatic curve and try to evaluate the Kashmir basin evidence in that light.

IV.2.A. Quaternary climatic fluctuations

The four-fold sequence of Alpine glaciation, comprising Gunz, Mindel, Riss and Wurm was considered more or less a universal sequence of Pleistocene glaciations, though the names

Fig. V.1. Global climatic correlations for the last 100 million years based on a variety of global data. A marked cooling during the Pliocene is clearly indicated (after Lamb, 1977).

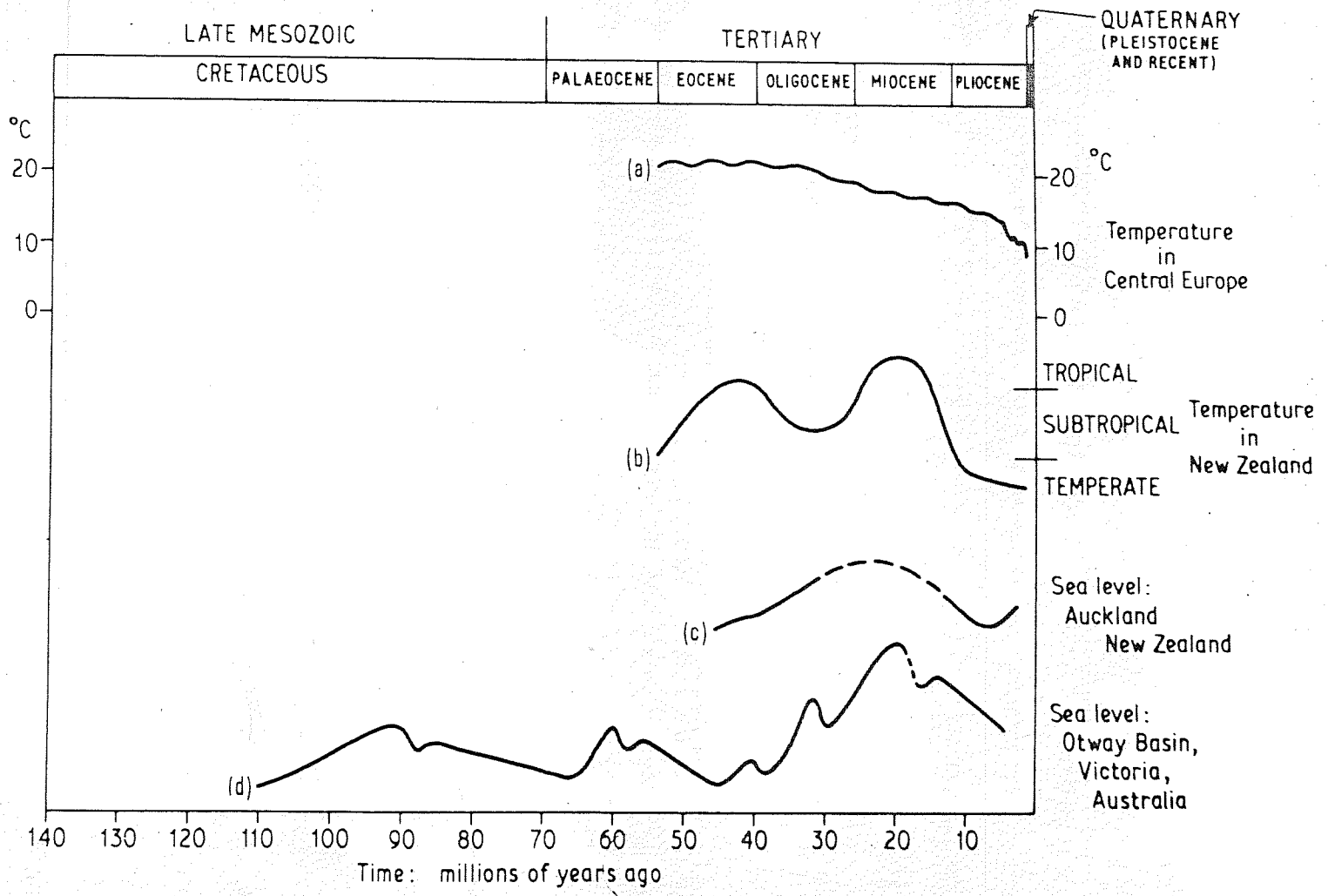
LATE MESOZOIC
CRETACEOUS
TERTIARY
PALAEOCENE
EOCENE
OLIGOCENE
MIOCENE
PLIOCENE
QUATERNARY
(PLEISTOCENE AND RECENT)
°C
20
10
0
(a)
°C
20
10
0
Temperature in Central Europe
TROPICAL
SUBTROPICAL
TEMPERATE
(b)
Temperature in New Zealand
(c)
Sea level: Auckland New Zealand
(d)
Sea level: Otway Basin, Victoria, Australia
140 130 120 110 100 90 80 70 60 50 40 30 20 10
Time: millions of years ago

for these events in various continents varied. As there is no unanimity about the correlation of regional and global schemes, the regional sequences continue to be used, creating quite a bit of confusion. We give here Lamb's (1977) tentative scheme of correlation (Table V.1) of glacial and interglacial events. But subsequent work showed that there are more glacial stages. For example, glacial maxima during Wurm and Riss have been identified as Wurm -I, -II and -III, Riss -I, and -II (Table V.2).

Recently Shackleton and Opdyke (1973) have used Emiliani's curve to mark the various climatic stages during the last million years (Fig. V.2). This is based on studies of the Pacific core (V28-238) in which oxygen isotopic variations in Globeriginoides sacculifera have been interpreted as indicators of climatic change. In this core, which covers 0.87 m.y., they have identified 11 cold and 12 warm fluctuations. Cold phases are even numbered and warm ones odd. These stages have been correlated with the revised Atlantic and Caribbean time sequence (Table, V.2), following Emiliani and Geiss (1957). But as one goes back in time the uncertainties of correlation increase.

For the last 100,000 years the climatic record is on firmer grounds. Fig. V.3 depicts the global climatic variations based upon a variety of data. Multiple evidence from Greenland ice cores, Gulf of Mexico, Southern France, North America, summarized

Fig. V.2. Climatic oscillations during the last 870,000 years based on oxygen isotopic measurements of marine foraminifera from the sea core V28-238 (after Emiliani, 1961; Shackleton and Opdyke, 1976).

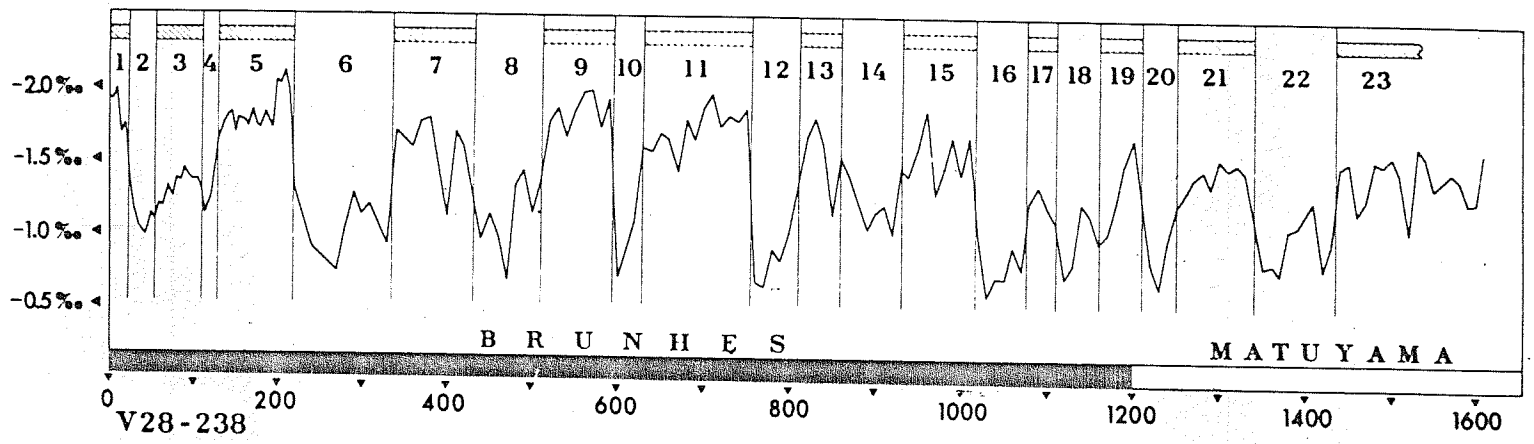

DEPTH IN CORE, cm

Fig. V.3. Climatic record of average temperatures over the last 100,000 years derived from various indicators.

(a) Northern Greenlands: Oxygen-18 variations at Camp Century (77° N., 56° W.) (after Dansgaard et al, 1970).

(b) Central Europe: Mean air temperatures in July, from evidence of the flora, fauna and soil mollusca (after Gross, 1958).

(c) Netherlands: Mean air temperatures in July, from evidence of flora and soil formations (after van der Hammen et al, 1967.

(d) Mean sea surface temperature in the tropical Atlantic (all year) from $^{18}O/^{16}O$ ratio in the remains of planktonic foraminifera in the ocean bed deposits (after Emiliani, 1961).

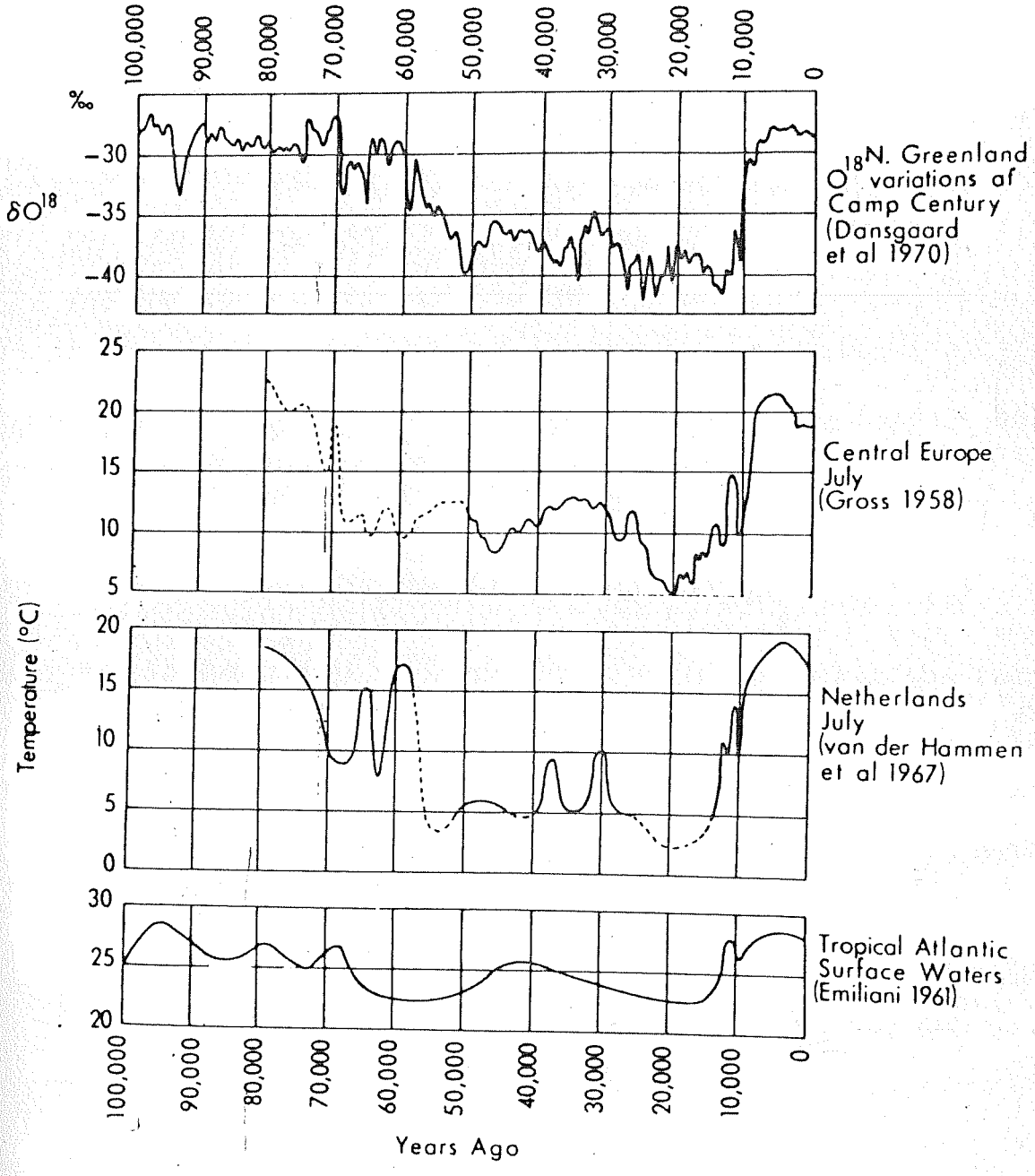
100,000
90,000
80,000
70,000
60,000
50,000
40,000
30,000
20,000
10,000
0
‰
−30
−35
−40
δO18
O18N. Greenland variations of Camp Century (Dansgaard et al 1970)
25
20
15
10
5
Central Europe July (Gross 1958)
Temperature (°C)
20
15
10
5
0
Netherlands July (van der Hammen et al 1967)
30
25
20
Tropical Atlantic Surface Waters (Emiliani 1961)
Years Ago

by Lamb (1977) indicates the end of a warm phase around 90,000 years B.P. and the sudden onset of a cold phase. There was a warm period following this phase and before the main Wurm/Wisconsin ice age which starts at c.70,000 years B.P. Despite a warm interstadial, the glacial ice sheets continued to grow till they attained a maximum around 45,000 years B.P. The glacial maximum seems to be at c.20,000 years B.P. Though the record of the glacial maxima and even interglacial periods are better preserved, the intervening interstadials leave only an ambiguous record.

V.3. Palaeoclimatic cycles in the Kashmir valley

As explained in Chapter II, we tried to put the faunal and floral evidence, reported so far, in our lithostratigraphic scheme. As de Terra and Paterson (1939) did not probably go beyond Hirpur, they could not report on the significance of the complete Hirpur section, nor could they tie up the other sections to the key section of Hirpur. Moreover, their correlation of different sections is based on lignite layers and not on litho-markers. As pointed out by Bhatt (1979), lignite layers are likely to form on the peripheral shallow ponds and not in the main lakes and therefore are very unreliable markers for correlation. Within these constraints we would try to draw inferences from the palaeontological and sedimentological evidence and see how

they fit in our chronological framework.

Floral evidence: de Terra and Paterson (1939) described a detailed list of plant remains from Lithozone 4, Vishnu Mittre (1974) described a vegetation sequence by assuming a glacial-interglacial scheme of his own and superimposed it on de Terra and Paterson's (1939) lithological scheme. It is, however, obvious that there is a clear succession of plants, thus showing climatic fluctuations.

de Terra's Lithozone 1, on the basis of Laradura section, can perhaps be equated with our pre-Boulder Conglomerate zone. It had an oak-deodar-alder forest type vegetation marking a warm, temperate, wet climate. This will fall in Pliocene period or Gilbert's magnetic polarity epoch.

The first cooling follows Lithozone 1, and should therefore be marked mainly by the Boulder Conglomerate. Unfortunately it has been interpreted differently by different workers. But if it represents a glacial outwash, it must represent a massive glaciation. The blue pine vegetation associated with it indicates glacial conditions. It is interesting to note that Pliocene represents a period of general cooling and fall in sea-levels (Fig. 14.9 in Lamb, 1977). In our magnetic dating (Fig. IV.6) this Boulder Conglomerate is appreciably older than 3.4 m.y.

As mentioned earlier, there is evidence from Argentina of a pre-3.6 m.y. glaciation. Thus the Boulder Conglomerate (Gravel 1; Fig. IV.6) may be the first dated evidence of a Pliocene glaciation in the Asian continent.

Above this, presumably in de Terra's Lithozone 3, warmer conditions prevailed, followed again by a cold oscillation. de Terra and Paterson's Lithozone 3-4 was marked by the destruction of blue pines; only grasses (Artemesia and Chenopodiaceae) grew. According to our chronology this cold phase should still be in the Pliocene, though not in its terminal phase.

The last warm phase, before the onset of the Pleistocene glaciation, is marked by de Terra's Lithozone 4. The palaeobotanical evidence would suggest a mixed dense oak-deciduous-broad-leaves forest with some spruce and deodar.

Matuyama epoch would cover most of de Terra's Lithozone 5, but botanical evidence is hardly available for the main Pleistocene glacials and interglacials. As explained above (Fig. V.2), even between Matuyama (partial) and Brunhes, there were 12 cold climatic phases recorded in the sea-cores. The Plio-Pleistocene boundary should be located somewhere between the Gravels-2 and -3 (Fig. IV.6) in the section.

Table V. 2. Identification of the northern hemisphere glaciations on the northern continents with Emiliani's numbered stages found in deep sea sediments (after Lamb, 1977)

Stage number	Alpine glaciation
2	Wurm II and III
4	Wurm I
6	Riss or Riss II
8	?
10	Mindel
12	?
14	Gunz

Tentatively one can place two major glacial maxima, in our section, between the loess and the upper part of the laminated member underlying it. Thus G-3 (Fig. IV.6) may represent a major Pleistocene glacial maximum (stage 10 of Emiliani, or Mindel in the Alpine sequence). The rest of the glacial maxima and intervening interglacials and interstadials are represented by the loess (loess plus lacustrine sediments on the Himalayan side) covered by the Brunhes magnetic epoch (greater than 700,000 years B.P.; Fig. IV.6).

There are three palaeosols representing warmer periods exposed on the Himalayan side. The topmost is radiocarbon dated to 18,000 ± 1000 years B.P. and the lower two are older than 32,000 years B.P., but presumed to be younger than 100,000 years B.P. This 18,000 years B.P. palaeosol should represent the last deglaciation, though minor ephemeral colder phases even after this cannot be ruled out. It is supported by the radiocarbon dated pollen sequence of Toshmaidan (Singh, 1963; Singh and Agrawal, 1975) which shows that the onset of warmer conditions at 3000 m sites was already on at c.15,000 B.P., followed by a cold and warm phase.

The loess on the Pir Panjal side is far thicker than the Himalayan flank and possibly has many more palaeosols. As our field work on the palaeosols and loess of Pir Panjal side was

limited, and very little has been done by previous workers, it will be premature to hazard any guess at this stage regarding their age.

It is therefore obvious that the Karewa sediment profile contains a unique climatic record of a series of climatic oscillations, comprised of glacials, interglacials and interstadials, thus the number of glaciations definitely exceeds four. The evidence seems to indicate a Pliocene glaciation, as also several climatic oscillations during the Pleistocene.

This study thus provides a broad time-frame within which these climatic oscillations can be arranged.

CHAPTER VI

CONCLUSIONS

Following are the major conclusions which could be drawn from the present study:

(1) The topmost palaeosol in the loessic deposit is dated to c.18,000 ± 1000 B.P. and marks the last deglaciation in the Kashmir valley (Fig. II.5).

(2) The Upper Karewa sediment falls within the Brunhes magnetic normal epoch, younger than 0.72 m.y. (Fig. IV.2, 6).

(3) The Plio-Pleistocene boundary lies between the Gravels -2 and -3 (Fig. IV.6).

(4) There are good indications that the topmost section of the Lower Karewa falls within the Matuyama (0.72-2.47 m.y.) and the middle section probably the Gauss (2.47-3.41 m.y.), and lower section within the Gilbert magnetic epochs (Fig. IV.6).

(5) With the help of the chronology built by this work and the available palaeontological and sediment logical data, one can broadly delineate the climatic fluctuations, as outlined in Chapter V. The probability of an extensive early Pliocene glaciation has also been pointed out.

BIBLIOGRAPHY

Agrawal, D.P., Datta, P.S., Kusumgar, Sheela, Mehrotra, N.C., Nautiyal, V., Pant, R.K. and Shali, S.L. 1978. Preliminary sedimentological studies on the Quaternary deposits of Kashmir. Himalayan Geology 9 (in press).

Agrawal, D.P. and Kusumgar, Sheela 1974. Prehistoric Chronology and Radiocarbon Dating in India. Munshiram Manoharlal, Delhi.

Agrawal, D.P., Kusumgar, Sheela and Lal, D. 1965. The measurement of radiocarbon activity and some determination of ages of archaeological samples. Current Science 34, 394-397.

Agrawal, D.P. and Pande, B.M. (eds.) 1977. Ecology and Archaeology of Western India. Concept Publishing Company, Delhi.

Amin, B.S. 1970. Dating of ocean sediments by radioactive methods. M.Sc. Thesis, University of Bombay.

Amin, B.S., Likhite, S.D., Radhakrishnamurthy C. and Somayajulu, B.L.K. 1972. Susceptibility, Stratigraphy and Palaeomagnetism of some deep Pacific Ocean Cores. Deep Sea Research 19, 249-252.

Anderson, E.C., Arnold, J.R. and Libby, W.F. 1949. Age determination by radiocarbon content: world wide assay of natural radiocarbon. Science 109, 207-208.

Australian Academy of Science 1976. Report of a Climatic Committee. Report No. 21, Canberra.

Badam, G.L. 1968. Note on the occurrence of fossil vertebrates in Karewas of Kashmir. Bulletin of Punjab University No. 5 19(3-4), 453-455.

Badam, G.L. 1972. Additional mammalian fossils in the Karewas of Kashmir. Current Science 41, 529-530.

Badam, G.L. 1979. Pleistocene Fauna of India. Deccan College, Poona.

Barnes, J.W., Lang, E.J., Potratz, H.A. 1956. Ratio of ionium to uranium in coral limestone. Science 124, 175-176.

Bennett, C.L., Beukens, R.P., Clover, M.R., Elmore, D., Gove, H.E., Kilius, L., Litherland, A.E. and Purser, K.H. 1978. Radiocarbon dating with electrostatic accelerators: dating of milligram samples. Science 201, 345-346.

Bhandari, N. 1977. Astrophysical causes of climatic changes. In Agrawal, D.P. and Pande, B.M., 21-27.

Bhat, S.G. and Krishnaswami, S. 1969. Isotopes of U and Ra in Indian rivers. Proceedings of Indian Academy of Sciences 70A, 1-17.

Bhatia, S.B. 1968. Pleistocene ostracodes from the Upper Karewas of Kashmir, India. Micropaleontology 14(4), 465-483.

Bhatia, S.B. 1974. Some Pleistocene molluscs from Kashmir, India. Himalayan Geology 4, 371-395.

Bhatt, D.K. 1975. On the Quaternary geology of the Kashmir valley with special reference to stratigraphy and sedimentation in recent geological studies in the Himalayas. Geological Survey of India Miscellaneous Publications 24, 188-203.

Bhatt, D.K. 1976. Stratigraphical status of the Karewa group of Kashmir, India. Himalayan Geology 6, 197-208.

Bhatt, D.K. 1979. Kashmir valley. Neogene/Quaternary boundary Conference, Chandigarh Guide Book, 34-48.

Bhatt, D.K. and Chatterji, A.K. 1976. An appraisal of field observations on the geology of the Plio-Pleistocene Karewa group and more recent Quaternary deposits of Kashmir valley In Srinivasan, M.S. (ed.), 11-21.

Blackett, P.M.S. 1952. A negative experiment relating to magnetism and the earth's rotation. Phil. Trans. Roy. Soc. London Ser. A. 245, 309-370.

Blanchard, R.L. 1963. Uranium series Disequilibrium in Age Determination of Marine Calcium Carbonates. Ph.D. Thesis, Washington University.

Broecker, W.S. 1965. Isotope geochemistry and Pleistocene climatic record. In Wright, H.E. Jr., and Grey, D.G. (eds.).

Broecker, W.S. and Thurber, D.L. 1965. Uranium-series dating of coral and oolites from Bahaman and Florida Key limestone. Science 149, 58-60.

Broecker, W.S. and Van Donk, J. 1970. Insolation, ice volumes and ^{18}O record in deep sea cores. Review of Geophysics and Space Physics 8, 169-198.

Brooks, C.E.P. 1949. Climate Through the Ages, Benn, London, 2nd edition.

Bruckshaw, J.M. and Robertson, E.I. 1948. The measurement of magnetic properties of rocks. Journal of Sci. Inst. 25, 444-446.

Bucha, V. 1970. Influence of the earth's magnetic field on radiocarbon dating. In Olsson I.U. (ed.), 501-511.

Bucha, V., Horacek, J., Koci, A. and Kukla, J. 1969. Palaeomagnetische messungen in dem Lossen. In Demek, J., and Kukla J. (eds.), 123-131.

Budyko, M.I. 1969. The effect of solar radiation variations on the climate of the Earth. Tellus 21, 611-619.

Chatterjee, A.K. and Bhatt, D.K. 1969. Geological Survey of India Progress Report for 1968-69, unpublished.

Cherdyntsev, V.V., Chalov, P.I. 1955. Ob. izotopnom Sostave radio elementov-V privodynykh obyektakh V Sviazi S Voprosami geokronologii. In Trudy III Sessil komissi Opredelenyu Absolyutnogo Yozrastu, Moscow 175-233.

Cherdyntsev, V.V., Oriov, D.P., Isabaev, E.A., Ivanov, V.I. 1961. Isotopic composition of uranium in minerals, Geochemistry 10, 927-936.

Damon, P.E., Long, A. and Wallick, E.J. 1972. Dendrochronologic calibration of the carbon-14 time scale. In Rafter T.A. and Grant-Tylor, T. (eds.), 44-59.

Damon, P.E., Long, A. and Wallick, E.J. 1973. On the magnitude of the 11-year radiocarbon cycle. Earth and Planetary Science Letters 20, 300-306.

Dansgaard, W., Johnson, S.J., Clausen, H.B. and Langway, C.C. 1971. Climatic record revealed by the Camp Century ice-core. In Turekian, K.K. (ed.), 37-56.

Demek, J. and Kukla, J. (eds.) 1969. Periglanzialzone, Loess and Paleolithikum der Tschechoslowakei. Tschechoslovakisch Akademie der Wissenschaften Geographisches Institut, Brono.

de Terra, H. 1935. Geological studies in the northwest Himalaya between the Kashmir and Indus valleys. Connecticut Academy Arts and Science Memoirs 8, part 1.

de Terra and Paterson, T.T. 1939. Studies on the Ice Age in India and Associated Human Cultures. Carnegie Institute, Washington Publication No. 493.

Dooley, J.R., Granger, H.C., Rosholt, J.N. 1966. Uranium-234 fractionation in the sandstone type uranium deposits of the Ambrosia Lake, District New Mexico. Economic Geology 61, 1362-1382.

Embleton, C. and King, C.A.M. 1969. Glacial and Periglacial Geomorphology. Edward Arnold, Edinburgh.

Emiliani, C. 1961. Cenozoic climatic changes as indicated by the stratigraphy and chronology of deep sea cores. Globerigina ooze facies. Annals of New York Academy of Science 95(1), 521-536.

Emiliani, C. and Geiss, J. 1957. On glaciations and their causes. Geol. Rundschau 46(2), 576-601.

Ericson, D.B., Ewing, M. and Wollin, G. 1964. The Pleistocene epoch in deep sea sediments. Science 146, 729-732.

Everitt, C.W.F. and Clegg, J.A. 1962. A field test of palaeomagnetic stability. Geophysics Journal R.A.S. 6(3), 312-319.

Ewing, M. and Donn, W.L. 1956. A theory of ice ages. Science 123, 1061-1066.

Fairhall, A.W., Schell, W.R. and Takashima, Y. 1961. Apparatus for methane synthesis for radiocarbon dating. Review of Scientific Instruments 32, 323-325.

Farooqi, I.A. and Desai, R.N. 1974. Stratigraphy of Karewa, Kashmir, India. Journal of the Geological Society of India 15(3), 299-305.

Ferguson, C.W. 1970. Dendrochronology of bristlecone pine, Pinus aristata. In Olsson, I.U. (ed.), 237-259.

Fleck, R.J., Mercer, J.H., Nairn, A.E.M. and Peterson, D.N. 1972. Chronology of the late Pliocene and early events in southern Argentina. Earth and Planetary Science Letters 16, 15-22.

Fleischer, R.L. and Raabe, O.G. 1978. Recoiling alpha-emitting nuclei: mechanisms for uranium-series disequilibrium. Geochimica et Cosmochimica Acta 1, 973-978.

Flint, R.F. and Deevey, E.S. 1961. Editorial statement. Radiocarbon 3.

Godwin-Austen, H.H. 1859. On the lacustrine or Karewa deposits of Kashmir. Quaternary Journal, Geological Society, London 15(1), 221-229.

Godwin-Austen, H.H. 1864. Geological Notes on parts of the North-western Himalayas. Quaternary Journal, Geological Society, London, 20, 383-388.

Godwin, H. 1959. Carbon-dating Conference at Groningen. Nature 184, 1365-1366.

Godwin, H. 1962. Half-life of Radiocarbon. Nature 195, 984.

Graham, J.W. 1949. The stability and significance of magnetism in sedimentary rocks. Journal of Geophysical Research 54, 131-167.

Griffiths, D.M. 1955. Remanent magnetization of varved clays from Sweden. Royal Astron. Soc. Monthly Notices, Geophys. Abs. Supp. 7, 103-114.

Grindler, J.E. 1962. The Radiochemistry of Uranium. USA E.C. Report No. NAS-NS-3050.

Grootes, P.M. 1977. Thermal Diffusion Isotopic Enrichment and Radiocarbon Dating beyond 50,000 Years B.P., Ph.D. Thesis, Rijisuniversiteit, Groningen.

Gross, H. 1958. Die bisherige Ergebnisse von ^{14}C-Messungen und palaolithischen Untersuchungen fur die Gilederung und chronologie des Jungpleistozans in Mitteleuropa and den Nachbargebieten. Eiszeit und Gegenwart 9, 155-187.

Gustavsson, J.E. and Hogberg, S.A.C. 1972. Uranium/thorium dating of Quaternary carbonates. Boreas 1, 247-274.

Hammen, T., Maarleveld, V.D., Vogel, G.C. and Zagwijn, W.H. 1967. Stratigraphy, climatic succession and radiocarbon dating of last glacial in the Netherlands. Geologie en Mijnbouw 46, 79-95.

Haring, A., de Vries, A.E. and de Vries, H. 1958. Radiocarbon dating upto 70,000 years by isotopic enrichment. Science 128, 472-473.

Hays, J.D., Imbrie, J. and Shackleton, N.J. 1976. Variation in the earth's orbit: pacemaker of the ice ages. Science 194, 1121-1132.

Hospers, J. 1954. Summary of studies in rock magnetism. Journal of Geomagnetism and Geoelectricity 6, 172-175.

Houtermans, F.G. and Oeschger, H. 1958. Proportional zahlrchr zur messung schwacher aktivitaten weicher strahlung. Helvetica Physics Acta 31, 117-126.

Hyde, E.K. 1960. The Radiochemistry of Thorium. U.S.A.E.C. Nuclear Science Service Report No. NAS-NS-3004.

Irving, E. 1964. Palaeomagnetism and its application to Geological and Geophysical problems. John wiley and Sons, New York.

Iyengar, M.O.P. and Subramanyan, R. 1943. Fossil diatoms from the Karewa beds of Kashmir. Proc. National Academy of Science, India 13, Sec. B., 225-237.

Johnson, N.D., Opdyke, N.D. and Lindsay, E.H. 1975. Magnetic polarity stratigraphy of Pliocene/Pleistocene terrestrial deposits and vertebrate fauna, San Pedro valley, Arizona. Geological Society of America Bulletin 86, 5.

Kaufman, A. 1964. ^{230}Th-^{234}U Dating of Carbonates from Lakes Lahontan and Bonneville. Ph.D. Thesis, Columbia University.

Kaufman, A. and Broecker, W.S. 1965. Comparison of ^{230}Th and ^{14}C ages for carbonate materials from Lake Lahontan and Bonneville. Journal of Geophysical Research 70, 4039-4054.

Keller, H.M., Tahirkheli, R.A.K., Mirza, M.A., Johnson, G.D., Johnson, N.M. and Opdyke, N.D. 1977. Magnetic polarity stratigraphy of the Upper Siwalik deposits, Pabbi Hills, Pakistan. Earth and Planetary Science Letters 36, 187-201.

Khramov, A.N. 1960. Palaeomagnetism and Stratigraphic Correlation. English translation by Lojkine, A.T., Australian National University, Canberra.

Kigoshi, K. 1971. Alpha-recoil thorium 234: dissolution into water and the uranium-234/uranium-238 disequilibrium in nature. Science 173, 47-48.

Koenigsterger, J.G. 1938. Natural residual magnetism of eruptive rocks. Part 1 and II, Terrestrial Magnetic Atmosphere 43, 119-127 and 299-320.

Koppen, W. and Geiger, R. 1930. Handbuch der Klimatologie, I. Teil A, Borntraeger, Berlin.

Krishnaswami, S. and Lal, D. 1978. Radionuclide Limnochronology in Lakes, their Chemistry, Geology and Physics (ed.) Lerman, A., Spinger, Vexlag, 153-177.

Krishnaswami, S. and Sarin, M.M. 1976. The simultaneous determination of Th, Pu, Ra isotopes, ^{210}Pb, ^{55}Fe, ^{32}Si and ^{14}C in marine suspended phases. Analytica Chemica Acta 83, 143-156.

Krishnaswamy, V.D. 1947. Stone Age in India. Ancient India 3, 11-57.

Kukla, J. 1970. Correlation between loesses and deep-sea sediments. Geologiska Foreningens i stockholm Forhandlingar 92, 148-180.

Kusumgar, Sheela, Agrawal, D.P. and Krishnamurthy, R.V. 1979. Studies on the loess deposits of the Kashmir valley and ^{14}C dating. 10th International Radiocarbon Conference, Bern (in press).

Kusumgar, S., Lal, D. and Sharma, V.K. 1963. Radiocarbon dating: techniques. Proceedings of Indian Academy of Science 58, 125-141.

Ku, Teh-Lung, 1976. The uranium-series methods of age determination. Annual Review of Earth and Planetary Science 4, 347-379.

Lal, D. and Peters, B. 1962. Cosmic ray produced isotopes and their application to problems in geophysics. Progress in Elementary Particle and Cosmic Ray Physics 6, 1-72.

Lamb, H.H. 1977. Climate: Present: Past and Future 2, Methuen and Co., London.

Lerman, JC., Mook, W.G. and Vogel, J.C. 1970. ^{14}C in tree rings from different localities. In Olsson, I.U. (ed.). 275-301.

Libby, W.F. 1955. Radiocarbon Dating. University of Chicago Press, Chicago, 2nd edition.

Libby, W.F. 1970. Radiocarbon dating. Philosophical Transaction of Royal Society 269A, 1-10.

Likhite, S.D. and Radhakrishnamurthy, C. 1965. An apparatus for the determination of susceptibility of rocks in low field at different frequencies. Bulletin of NGRI 3, 1-8.

Lingenfelter, R.E. and Ramaty, R. 1970. Astrophysical and Geophysical variations in C-14 production. In Olsson I.U. (ed.), 514-537.

Lydekker, R. 1878. Note on the geology of Kashmir, Kishtwar and Pangi. Rec. Geol. Surv. Ind. 11, 30-36.

Lydekker, R. 1883. The geology of Kashmir and Chamba territories and the British district of Khagam. Mem. Geological Survey of India 22, 1-344.

Malota, F. 1962. Eine Erweiterung der Methode fur Altersbestimmungen durch Anreicherung des C^{14}-Isotops im Trennrohr, Thesis, Munnich.

McDougall, I. 1978. Revision of the geomagnetic polarity time scale for the last 5 m.y. In Fourth International Conference on Geochrnology, Cosmochronology, Isotope Geology (ed.) Zartman, R.E., 287-289.

McKelvey, V.E., Everhart, D.L., Garreis, R.M. 1955. Origin of uranium deposits. In Economic Geology, 464-533 (ed.) Beteman, A.M., Penn Lancaster Press, Lancaster.

Mercer, J.H. 1972. The lower boundary of the Holocene. Quaternary Research 2, 15-24.

Michael, H.N. and Ralph, E.K. 1972. Discussion of radiocarbon dates obtained from precisely dated sequoia and bristle-cone pine samples. In Rafter, T.A. and Grant-Taylor, T. (eds.) 28-43.

Middlemiss, C.S. 1911. Section on the Pir Panjal range and Sind valley. Geological Survey of India 41, Pt. 2, 115-144.

Middlemiss, C.S. 1924. Lignite coal field in the Karewa formations of the Kashmir valley. Geological Survey of India Rec. 55, 241-253.

Milankovitch, M. 1930. Mathematische Klimalehre und astronomische Theorie der Klimaschroankungen. In Koppen, W. and Geiger, T. (eds.).

Muller, R.A., Stephenson, E.J. and Mast, T.S. 1978. Radio-isotope dating with an accelerator: a blind measurement. Science 201, 347-348.

Nagata, T. 1952. Reverse thermo-remanent magnetism. Nature 169, 704.

Nagata, T. 1953. Rock Magnetism. Maruzen, Tokyo.

Nair, P.K.K. 1960. Palynological investigations of the Quaternary (Karewa) of Kashmir. Journal Scientific and Industrial Research 19C(6), 145-154.

Olsson, I.U. (ed.) 1970. Radiocarbon Variations and Absolute Chronology. John Wiley, New York.

Opdyke, N.D. 1972. Palaeomagnetism of deep sea-cores. Review of Geophysics and Space Physics 10(1), 213-249.

Pant, R.K., Agrawal, D.P. and Krishnamurthy, R.V. 1978. Scanning electron microscope and other studies on the Karewa beds of Kashmir, India. In Scanning Electron Microscopy in the Study of Sediments (ed.) Whalley, W.B., Geo Abstracts, Norwich.

Radhakrishnamurthy, C. 1970. Laboratory studies for ascertaining the suitability of rocks for palaeomagnetism. In Palaeogeophysics, Runcorn, S.K. (ed.), Academic Press, 235-241.

Radhakrishnamurthy, C., Likhite, S.D., Amin, B.S. and Somayajulu, B.L.K. 1968. Magnetic susceptibility stratigraphy in ocean sediment cores. Earth and Planetary Science Letters 4, 464-468.

Radhakrishnamurthy, C. and Misra, D.C. 1966. A criterion for stability of NRM in the sedimentary rocks. Bulletin of NGRI 4, No. 3, 103-108.

Radhakrishnamurthy, C. and Sahstrabudhe, P.W. 1965. Instruments and techniques for the study of magnetic stability in rocks. Journal of I.G.U. (India) 2(1), 5-16.

Rafter, T.A. and Grant Taylor, T. 1972. Proceedings of the 8th International Conference on Radiocarbon Dating, October 1972, Lower Hutt City, New Zealand.

Rao, A.R. and Awasthi, P. 1962. Diatoms from the Pleistocene of Kashmir (India) - Part 1, Centric Diatoms, Palaeobotanist 11 (1 & 2), 82-91.

Roche, A. 1950. Sur les caracteres magnetiques du systeme eruptif de Gergovie. C.R. Academy of Science, Paris 230, 113-115.

Roche, A. 1951. Sur les inversion de iaimantion remanents des roches volcaniques dans les monts d'Auvergne. C.R. Academy of Science, Paris 233, 1132-1134.

Rosholt, J.N., Doe, B.R., Tatsumoto, M. 1966. Evolution of the isotopic composition of uranium and thorium in soil profiles. Geological Society of American Bulletin 77, 987-1003.

Rosholt, J.N., Shields, W.R., Garner, E.L. 1963. Isotopic fractionation of uranium in sandstone. Science 139, 224-226.

Roy, D.K. 1975. Stratigraphy and palaeontology of the Karewa group of Kashmir. In Geological Survey of India Miscellaneous Publications No. 24, 204-221.

Sastri, V.V. and Pant, S.C. 1959. Survey of coastal areas for collecting specimens of beach rocks, miliolite, etc. for studying the changes of sea-level, Geological Survey of India (unpublished report).

Shackleton, N.J. and Opdyke, N.D. 1973. Oxygen isotope and palaeomagnetic stratigraphy of equatorial Pacific core V28-238: oxygen isotope temperatures and ice volumes on a 10^5 years and 10^6 years scale. Quaternary Research 3, 39-55.

Shackleton, N.J. and Opdyke, N.D. 1976. Oxygen isotope and palaeomagnetic stratigraphy of Pacific core V28-239, Late Pliocene to Latest Pleistocene. Geological Society of American Memoir 145 ed. Hays, J.D. and Cline, R.M., 449-464.

Simpson, G.C. 1957. World temperature during the Pleistocene. Quaternary Journal of Royal Meteorological Society 85, 332-349.

Singh, G. 1963. A preliminary survey of the post-glacial vegetational history of Kashmir valley. Palaeobotanist 12(1), 73-108.

Singh, G. and Agrawal, D.P. 1976. Radiocarbon evidence for deglaciation in northwestern Himalaya, India. Nature 206, 232.

Somayajulu, B.L.K. 1977. Palaeoclimates: old and new ideas. In Agrawal, D.P. and Pande, B.P. (eds.), 5-16.

Somayajulu, B.L.K., Radhakrishnamurthy, C. and Walsh, T.J. 1978. Susceptibility as a tool for studying magnetic stratigraphy of marine sediments. Proceedings of Indian Academy of Science 87(A), 201-213.

Srinivasan, M.S. (ed.) 1976. Proceedings of the VI Indian colloquium on Micropaleontology and stratigraphy, B.H.U., Varanasi.

Starik, I.E., Kolyadin, L.B. 1958. The occurrence of uranium in ocean water. Geochemistry 3, 245-256.

Stuiver, M. 1970. Long-term C-14 variations. In Olsson, I.U. (ed.), 197-213.

Suess, H.E. 1970. Bristlecone-pine calibration of the radiocarbon timescale 5200 B.C. to the present. In Olsson, I.U. (ed.), 303-311.

Tatsumoto, M. and Goldberg, E.D., 1959. Some aspects of the marine geochemistry of uranium. Geochemica Cosmochimica Acta 17, 201-208.

Tewari, B.S. and Kachroo, R.K. 1979. On the occurrence of Equus sivalensis from Karewas of Shupiyan, Kashmir valley. In Recent Researches in Geology 3, 468-475, Hindustan Publishing Corporation, Delhi.

Thurber, D.L. 1962. Anomalous $^{234}U/^{238}U$ in nature. Journal of Geophysical Research 67, 4518-4520.

Thurber, D.L. 1963. Anomalous $^{234}U/^{238}U$ and Investigations of the Potential of ^{234}U for Pleistocene Chronology. Ph.D. Thesis, Columbia University, New York.

Thurber, D.L., Broecker, W.S., Blanchard, R.L., Potratz, H.A. 1965. Uranium series ages of Pacific atoll coral. Science 149, 55-58.

Tripathi, C. 1971. Quaternary deposits of the Indian subcontinent. Rec. Geological Survey of India 98(2), Pt. 2, 144-174.

Tripathi, C. and Chandra, P.R. 1962. Detailed examination of the Karewas of Kashmir for the remains of early man. Geological Survey of India Report (unpublished).

Tripathi, C., and Chandra, P.R. 1972. Fossil from Karewa around Nichahom, Kashmir. Miscellaneous Publication, Geological Survey of India 15, 261-267.

Turekian, K.K. (ed.) 1969. The Late Cenozoic Glacial Ages. Yale University Press, New Haven.

Van Montfrans, H.M. and Hospers, J. 1969. A preliminary report on the stratigraphical position of the Matuyama-Brunhes geomagnetic field reversal in the Quaternary sediments of the Netherlands, Geologie en. Mijnbouw, 48, 565-572.

Veeh, H.H. 1966. $^{230}Th/^{238}U$ ages of Pleistocene high sea level stands. Journal of Geophysical Research 71, 3379-3386.

Vishnu-Mittre 1964. On the Plio-Pleistocene boundary in north-west India. Palaeobotanist 12, No. 3, 270-276.

Vishnu-Mittre, 1974. Quaternary vegetation in northern region. Aspects and appraisal of Indian Palaeobotany, 657-664.

Vishnu-Mittre, Singh, G. and Saxena, K.M.S. 1962. Pollen analytical investigations of the Lower Karewa. Palaeobotanist 11, No. 182, 92-95.

Vogel, J.C. and Zagwijn, W.H. 1967. Groningen radiocarbon dates VI, Radiocarbon 9, 63.

Wadia, D.N. 1941. Pleistocene Ice Age deposits of Kashmir. Proceedings of National Institute of Science, India 7(1), 19-59.

Wadia, D.N. 1948. The transitional passage of Pliocene into the Pleistocene in the north-western sub-Himalayas. International Geological Congress Session, XVIII, Report 11, 43-48.

Wadia, D.N. 1961. Geology of India. MacMillan & Co., London.

Wodehouse, R.P. and de Terra, H. 1935. The Pleistocene pollen of Kashmir. Connecticut Academy of Arts and Science Mem. 9, part 1.

Wright, H.E., Jr. and Grey, D.G. (eds.) 1965. The Quaternary of the United States. Princeton University Press, Princeton.

Young, A.E.C. and Fairhall, A.W. 1972. Variation of natural radiocarbon during the last 11 millennia and geophysical mechanisms for producing them. In (eds.) Rafter, T.A. and Grant-Taylor, T.